DOCTORAL THESIS

Co-gasification of Biomass and Oil Shale in a CO_2 Atmosphere

Mari Sinisalu

TALLINNA TEHNIKAÜLIKOOL
TALLINN UNIVERSITY OF TECHNOLOGY
TALLINN 2026

TALLINN UNIVERSITY OF TECHNOLOGY
DOCTORAL THESIS
77/2026

Co-gasification of Biomass and Oil Shale in a CO_2 Atmosphere

MARI SINISALU

TAL TECH PRESS

TALLINN UNIVERSITY OF TECHNOLOGY
School of Engineering
Department of Energy Technology
This dissertation was accepted for the defence of the degree 30/10/2026

Supervisor: Professor Alar Konist
School of Engineering
Tallinn University of Technology
Tallinn, Estonia

Co-supervisor: Professor Oliver Järvik
School of Engineering
Tallinn University of Technology
Tallinn, Estonia

Opponents: Professor Antonio Soria-Verdugo
Department of Thermal and Fluids Engineering
University Carlos III of Madrid
Madrid, Spain

Professor Edward John Anthony
Department of Chemical and Biological Engineering
University of Ottawa
Ottawa, Canada

Defence of the thesis: 11/12/2026, Tallinn

Declaration:
Hereby I declare that this doctoral thesis, my original investigation and achievement, submitted for the doctoral degree at Tallinn University of Technology has not been submitted for doctoral or equivalent academic degree.

Mari Sinisalu

---
signature

European Union
European Regional
Development Fund

Investing
in your future

Copyright: Mari Sinisalu, 2026
ISSN 2585-6898 (paperback)
ISBN 978-9916-80-589-3 (paperback)
ISSN 2585-6901 (PDF)
ISBN 978-9916-80-588-6 (PDF)
https://doi.org/10.23658/taltech.77/2026
Printed by Koopia Niini & Rauam

Sinisalu, M. (2026). *Co-gasification of Biomass and Oil Shale in a CO2 Atmosphere* [TalTech Press]. https://doi.org/10.23658/taltech.77/2026

TALLINNA TEHNIKAÜLIKOOL
DOKTORITÖÖ
77/2026

Biomassi ja põlevkivi koosgaasistamine CO_2 keskkonnas

MARI SINISALU

TAL TECH
KIRJASTUS

Contents

List of Publications 7
Author's Contribution to the Publications 8
Introduction 9
Research Objectives 10
Novelty 11
Methodology 12
Research Contribution and Dissemination 13
Abbreviations and Terms 15
1 Literature Review 16
1.1 Biomass as Gasification Feedstock 16
1.2 Oil Shale as Gasification Feedstock 16
1.3 Gasification Fundamentals 17
1.3.1 CO_2 Gasification 18
1.3.2 Reactions 19
1.3.3 Catalysts and Additives 20
1.3.4 Co-gasification 22
2 Experimental 27
2.1 Materials 27
2.2 Methods 27
2.2.1 Fuel Compositional Analysis 27
2.2.2 General Experimental Considerations 28
2.2.3 Fixed-bed Reactor and Gas Chromatography 28
2.2.4 TGA–MS 30
2.2.5 Surface Area 30
2.2.6 Synergistic Behavior Investigation 30
3 Results and Discussion 32
3.1 Feedstock Characterization 32
3.2 Thermal Decomposition Behavior and TGA–MS Analysis 34
3.3 Producer Gas Composition 38
3.3.1 Relationships between Feedstock Properties and Producer Gas Concentration 39
3.4 Co-gasification and Synergy Quantification 40
3.4.1 Uncertainty Evaluation 41
3.5 Solid Residue Characteristics 42
3.6 Factors Influencing Synergistic Behaviour 44
4 Conclusions 47
List of Figures 49
List of Tables 50
References 51
Acknowledgements 64
Abstract 65
Lühikokkuvõte 67

Appendix 1 (Publications) 69
Appendix 2 123
Curriculum vitae 125
Elulookirjeldus 126

List of Publications

The list of author's publications, based on which the thesis has been prepared:

I Järvik, O., **Sulg, M**., Cascante Cirici, P., Eldermann, M., Konist, A., Gusca, J., & Siirde, A. (2020). Co-Pyrolysis and Co-Gasification of Biomass and Oil Shale. *Environmental and Climate Technologies*, *24*(1), 624–637. https://doi.org/10.2478/rtuect-2020-0038

II **Sulg, M.**, Konist, A., & Järvik, O. (2021). Characterization of different wood species as potential feedstocks for gasification. *Agronomy Research*, *19*(1), 276–299. https://doi.org/10.15159/AR.21.005

III **Sinisalu, M.**, Järvik, O., Mets, B., & Konist, A. (2024). Co-gasification of biomass and oil shale under CO_2 atmosphere: Comparative analysis of fixed-bed reactor, gas chromatography and thermogravimetric analysis coupled with mass spectroscopy (TGA–MS). *Bioresource Technology*, *393*. https://doi.org/10.1016/j.biortech.2023.130086

Author's Contribution to the Publications

Contribution to the papers in this thesis are:

Paper I – Conceptualizing the study in co-operation with co-authors; literature review; interpretation of findings; manuscript preparation

Paper II – Conceptualizing the study with co-authors; planning and coordinating the experimental work; conducting experimental analyses; supervising laboratory activities; collecting, validating and interpreting experimental data; preparing figures and tables; drafting, writing and revising the manuscript

Paper III – Conceptualizing the study and developing the methodology in collaboration with co-authors; designing experiments; setting up apparatus; conducting the experiments; processing, analyzing and interpreting the data; preparing figures and tables; drafting, writing and revising of manuscript

Introduction

Estonia has set ambitious climate targets, aiming for climate neutrality by 2050 and an interim emissions reduction goal for 2035 [1]. Achieving these targets while maintaining energy security and system flexibility requires highly efficient utilization of locally available energy resources, particularly biomass and oil shale. Biomass is a renewable source of carbon. For Estonia, oil shale remains an important domestic energy resource with established infrastructure. Therefore, the development of efficient thermochemical conversion pathways for both biomass and oil shale feedstocks is of considerable interest.

Biomass-based energy systems can reduce fossil fuel usage and support climate neutrality if biomass is sustainably sourced and managed. In Estonia, the contribution of bioenergy, a key source of district and household heating and derived mainly from domestic forestry biomass, has grown from 14% to 24% of the total energy supply between 2010 and 2022 [1]. As a widely available renewable resource, biomass is expected to remain an important component of the future energy system of the country.

Estonia's energy system has historically relied on domestic oil shale, which has contributed to energy security but is also associated with high carbon intensity. Oil shale is an important and complex natural resource. Energy, shale oil, and various chemical products can be derived from oil shale. Maximizing its value requires the full and integrated utilization of all its components, including organic matter, mineral fraction, and by-products. Oil shale pyrolysis has been extensively studied, with a primary focus on shale oil production and upgrading [2]-[4]. Estonia has a history of oil shale gasification; however, its industrial production has declined several decades ago because of economic competition with imported natural gas [5]. Despite limited industrial application, research into oil shale gasification continues in the country, particularly for meeting climate targets, developing modern gasification technologies, and resource valorization [6].

Biomass and oil shale have different chemical and mineral compositions. Biomass composition is inherently heterogeneous and varies with species, anatomical fraction, and growing conditions [7], which may highly influence gasification behavior and interaction effects. Some key characteristics influencing gasification include elemental composition, heating value, volatile matter, and ash composition [8]. Alkali and alkaline earth metals (AAEMs) such as K and Ca are known to act as catalysts in char gasification and tar conversion reactions, while high silica and ash contents may inhibit reactivity [9], [10]. Therefore, understanding the physicochemical characteristics of regionally available biomass feedstocks is essential for interpreting gasification performance and potential interaction effects.

Estonian oil shale is characterized by a high mineral content, especially carbonate minerals such as $CaCO_3$ and $CaMg(CO_3)_2$, which decompose between 600 and 900 °C to form CaO and MgO [11]. These oxides may influence char–CO_2 reactions during gasification. In coal and biomass co-gasification, inorganic constituents, particularly AAEMs in biomass, have been reported to promote gasification of coal-derived char and alter the product distribution [12]-[16]. The catalytic effects of such inorganic species are particularly relevant when CO_2 or H_2O is used as the gasifying agent [16]. However, reported interaction effects in co-gasification studies are often inconsistent and strongly dependent on feedstock composition and operating conditions [16].

In Estonia, thermochemical gasification remains largely at the research and development stage, with no large-scale industrial deployment of biomass gasification to date, despite its potential for syngas production and higher-value energy and chemical applications [17]. Co-gasification of biomass with coal, plastics, and waste materials has been extensively investigated because of its potential to improve conversion efficiency and product quality [18]-[20]. Oil shale is a promising feedstock for co-processing with biomass owing to its high mineral content and distinct composition from those of conventional fossil fuels [20], [21]. Previous studies on the co-combustion and co-pyrolysis of biomass and oil shale in Estonia have demonstrated that combining feedstocks with contrasting organic and mineral compositions can influence the conversion behavior [22]-[24]. Co-gasification therefore represents an opportunity to combine the renewable carbon content of biomass with the mineral-rich features of oil shale, potentially enhancing char conversion and producer gas composition. However, it remains unclear whether beneficial interactions occur during biomass and oil shale co-gasification and what factors influence their occurrence and extent.

Use of CO_2 as a gasifying agent is of particular interest. CO_2 gasification enables the production of CO-rich producer gas through char–CO_2 reactions, thereby providing a potential pathway for CO_2 utilization [25], [26]. In addition, the gasification behavior in a CO_2 atmosphere is strongly influenced by feedstock composition and mineral matter [16], [27]-[29], making it a suitable medium for investigating interaction effects between biomass and oil shale. These characteristics make CO_2 gasification both scientifically relevant and a promising pathway for integrating carbon utilization with thermochemical conversion [26].

To address these gaps, this study combines comprehensive chemical characterization of woody biomass species grown in Estonia with controlled laboratory-scale co-gasification experiments under a CO_2 atmosphere. A multimethod approach, comprising thermogravimetric analysis coupled with mass spectrometry (TGA–MS), fixed-bed gasification, gas chromatography, and surface area analysis, was applied to evaluate the effects of oil shale addition on the producer gas composition, synergistic behavior, and solid residue properties.

By integrating physicochemical characterization with experimental gasification results, this research investigates how feedstock composition influences gasification behavior under CO_2 and whether mineral-rich oil shale can improve biomass conversion through synergistic effects. The findings contribute to advancing the understanding of biomass and oil shale interaction mechanisms and support the development of targeted thermochemical conversion strategies for both renewable and mineral-rich feedstocks.

Research Objectives

Alongside biomass, oil shale is a key component of Estonia's energy landscape. Therefore, their co-combustion is gaining increasing acceptance in the country. However, alternative thermochemical pathways, such as gasification, remain underdeveloped. In particular, biomass and oil shale interactions during CO_2 co-gasification remain insufficiently understood, including the influence of feedstock properties and mineral composition on gasification behavior. Therefore, investigating their co-gasification under a CO_2 atmosphere is both scientifically relevant and strategically important.

The scope of this work is limited to laboratory-scale CO_2 co-gasification of Estonian woody biomass and kukersite oil shale, with particular emphasis on feedstock-dependent interaction effects, producer gas composition, and solid residue behavior.

This study had three objectives. The first was to establish a conceptual and methodological foundation for the co-processing of biomass and oil shale (**Paper I**). This involved reviewing existing literature on co-gasification and co-pyrolysis, conducting preliminary experiments, and defining experimental conditions for subsequent investigations. Specifically, this involved:

- identifying knowledge gaps in biomass and oil shale co-gasification;
- characterizing thermal decomposition behavior relevant for co-gasification;
- establishing a methodological framework for subsequent co-gasification studies; and
- defining the initial experimental conditions reactor configuration.

The second objective was to characterize the woody biomass grown in Estonia and evaluate its suitability for thermochemical conversions (**Paper II**). Specifically, this objective focused on:

- performing comprehensive proximate, ultimate, and elemental analyses of 19 woody species, with separate treatment for wood and bark;
- application of chemometric methods for identifying patterns, clustering, and relationships between feedstock properties;
- evaluating how species-specific characteristics may influence gasification behavior; and
- providing a regional compositional baseline for feedstock selection and interpretation of co-gasification experiments.

The third and primary research objective was to experimentally evaluate whether the co-gasification of biomass and Estonian kukersite oil shale under a CO_2 atmosphere deviated from the linear additive behavior and to investigate the potential role of feedstock composition and mineral-related interactions in the observed behavior (**Paper III**). Specifically, this objective included:

- quantifying gaseous and solid products to evaluate gas composition and residue yield;
- comparing the results obtained from a fixed-bed reactor along with gas chromatography and TGA–MS;
- investigating feedstock-dependent behavior in biomass blends containing 10–30 wt% oil shale; and
- evaluating whether oil shale addition resulted in additive, synergistic, or inhibitory effects during co-gasification.

Novelty

This work provides the first systematic experimental investigation of biomass and Estonian oil shale co-gasification under CO_2 conditions, combining comprehensive feedstock characterization with complementary thermochemical analyses. Although biomass and coal co-gasification has been extensively studied, interactions between biomass and kukersite oil shale under CO_2 gasification have received little experimental attention. By combining thermogravimetric and fixed-bed experiments, this study

demonstrates that interaction effects observed during fixed-bed gasification are not apparent from thermogravimetric mass-loss behavior alone. This demonstrates the importance of the experimental environment in evaluating feedstock interactions.

Additionally, this work establishes a comprehensive compositional dataset for woody species grown in Estonia, covering 19 species, with wood and bark fractions characterized separately. The integration of physicochemical characterization with chemometric analysis provides a compositional basis for evaluating biomass variability and interpreting feedstock-dependent gasification behavior.

A key finding of this thesis is that the effect of oil shale addition is strongly feedstock-dependent rather than universal. Positive nonadditive effect on CO formation was observed for bark-based blends, whereas wood-based blends showed mainly additive or inhibitory behavior. Pine bark provided the strongest combined evidence of enhanced gasification, with increased CO formation accompanied by a lower-than-additive residue yield. Together with the compositional differences between the feedstocks, these results provide evidence that biomass properties play an important role in determining the interaction with oil shale during CO_2 gasification.

The mechanistic interpretation further links the observed behavior to carbon availability and mineral-mediated effects involving inherent biomass AAEMs and oil shale-derived mineral species. Although their individual contributions and the specific catalytic pathways could not be distinguished experimentally, the results provide a mechanistic framework and identify targeted approaches for further verification of these mechanisms.

Finally, the study demonstrates the value of integrating feedstock characterization, TGA–MS, fixed-bed gasification, gas analysis, solid residue characterization, and additive modeling with uncertainty analysis to identify and interpret nonadditive behavior in chemically dissimilar feedstocks.

Methodology

The methodological framework of this thesis was designed to address the defined research objectives through a combination of feedstock characterization and controlled thermochemical experiments conducted at different scales.

Feedstock characterization

Standardized laboratory procedures were applied to characterize all feedstocks, including woody species grown in Estonia and kukersite oil shale (**Paper II, Paper III**). Proximate and ultimate analyses and elemental composition were determined using validated methods. This comprehensive characterization afforded consistent baseline data and enabled the interpretation of feedstock-dependent behavior in subsequent co-gasification experiments.

Drop-in batch and fixed-bed reactor gasification

Two reactor configurations were employed to address different experimental objectives. The preliminary study utilized a preheated drop-in batch reactor to achieve high heating rates and investigate devolatilization behavior under rapid thermal conditions, providing information on the initial thermal decomposition of the feedstocks (**Paper I**).

Subsequent co-gasification experiments were conducted in a laboratory-scale fixed-bed reactor (**Paper III**), which provides controlled heating and extended gas–solid

contact. Gasification was performed under a CO_2 atmosphere to promote char–CO_2 reactions and to evaluate potential synergistic effects between biomass and oil shale. Experimental parameters such as temperature, heating rate, residence time, particle size, and blending ratio were selected based on previous studies and relevant literature.

Producer gas composition was quantified by gas chromatography, while solid residues were characterized using BET (Brunauer–Emmett–Teller) surface area analysis (**Paper III**).

Gasification performance was evaluated using a linear additive model applied to gas composition and residue yields to identify potential nonadditive interaction effects between biomass and oil shale (**Paper III**).

TGA–MS experiments

TGA–MS was used to investigate thermal decomposition and gas evolution under controlled microscale conditions (**Paper I, Paper III**). The heating program and gas atmosphere were aligned with fixed-bed experiments to facilitate the comparison. TGA–MS enabled detailed evaluation of mass-loss behavior and qualitative assessment of gas evolution trends, providing insights into the thermal behavior and potential interaction effects between feedstocks.

These methodologies allowed a systematic comparison of feedstock-dependent behavior across scales and supported the investigation of potential interaction effects during biomass and oil shale co-gasification under a CO_2 atmosphere.

Research Contribution and Dissemination

This thesis contributes to the understanding of thermochemical conversion processes by investigating biomass and oil shale co-gasification under a CO_2 atmosphere and integrating compositional analysis with the experimental evaluation of interaction effects.

First, this work provides **a comprehensive compositional baseline for Estonian woody biomass**. A total of 19 woody species grown in Estonia were systematically characterized, including separate analyses of wood and bark. Proximate and ultimate analyses and mineral and trace-metal composition were combined with chemometric methods to identify correlations relevant to gasification behavior. This dataset provides a regional reference dataset for feedstock selection and future thermochemical conversion studies.

Second, the study provides **a systematic experimental evaluation of biomass and oil shale co-gasification in a CO_2 atmosphere**. By combining TGA–MS and fixed-bed experiments, it demonstrates that synergistic interactions can be clearly observed under fixed-bed conditions, although they remain largely absent during TGA.

Third, **the study demonstrates that synergistic behavior is governed by feedstock composition, not by oil shale addition alone**. Enhanced CO formation was observed only for bark samples with elevated AAEMs and fixed carbon contents, which indicates that the catalytic influence of oil shale depends on the intrinsic properties of the biomass. These findings further demonstrate that the gasification behavior cannot be explained by individual feedstock properties alone; instead, it arises from the combined influence of mineral composition, fixed carbon, and interactions between biomass and oil shale during gasification.

Finally, this thesis applies **a systematic methodology combining linear additive modeling with uncertainty analysis** to distinguish additive, synergistic, and inhibitory behaviors during co-gasification with chemically dissimilar feedstock mixtures.

The results of this work have been disseminated through three peer-reviewed journal articles, ensuring scientific validation and contributing to the broader research community in thermochemical conversion and sustainable energy systems.

Abbreviations and Terms

A	Ash
AAEMs	Alkali and alkali earth metallic species
BET	Brunauer–Emmett–Teller
BirchB	Birch (*Betula pendula*) bark
BirchW	Birch (*Betula pendula*) wood
BM	Biomass
db	Dry basis
FC	Fixed carbon
FTIR	Fourier transformation infrared
GC	Gas chromatography
GCV	Gross calorific value
ICP-MS	Inductively coupled plasma mass spectrometry
IPA	Isopropanol
m/z	Mass-to-charge ratio
MS	Mass spectrometry
OS	Oil shale
PineB	Pine (*Pinus sylvestris)* bark
PineW	Pine (*Pinus sylvestris) wood*
ppm	Parts per million
SSA	Specific surface area
t	Time, s
T	Temperature, °C
TGA	Thermogravimetric analysis
TIC	Total inorganic carbon
VM	Volatile matter
VOC	Volatile organic compounds
W	Moisture
WD-XRF	Wavelength dispersive X-ray fluorescence spectrometry
wt%	Weight percent
%db	Mass percentage on dry basis

1 Literature Review

1.1 Biomass as Gasification Feedstock

BM (biomass) is a renewable feedstock that can be climate-neutral if sustainably sourced, as the CO_2 released during conversion is offset by carbon uptake during plant growth [30]. It can produce syngas, bio-oil, biochar, heat, and hydrogen through thermochemical conversion [31]. Furthermore, integrating BM gasification with carbon-capture technologies may allow low-carbon hydrogen production and improved carbon utilization [32].

BM includes herbaceous plants, agricultural residues, aquatic plants, animal and human wastes, refuse-derived fuel, and other organic wastes [33]. The present study focuses on woody lignocellulosic BM because of its abundance, established utilization pathways, and relevance to the Estonian energy sector.

Estonia is among the most forested countries in the European Union, with forests covering 51.8% of its land area in 2024 [34]. Forestry BM contributed 23% of the national energy supply in 2022 and is a primary fuel for both district and household heating [1].

Lignocellulosic BM consists mainly of cellulose (40–44 wt%), hemicellulose (20–30 wt%), and lignin (18–35 wt%), whose relative proportions govern the thermochemical conversion behavior of the BM [31], [35]. Hemicellulose decomposes at relatively low temperatures, promoting the early release of volatiles, followed by the main decomposition of cellulose, while lignin decomposes gradually over a broader temperature range and contributes more strongly to char formation [26], [31], [35]. These differences influence gas yield, tar formation, and char reactivity during gasification.

BM is characterized by a high volatile matter and hydrogen content, which are responsible for its high reactivity during thermochemical conversion [36]. However, its high moisture and oxygen contents reduce its energy density and increase the heat demand, while alkali, halogens, and trace elements may cause operational problems such as corrosion, slagging, and fouling [36], [37].

Mineral matter plays a key role in BM gasification. Concentrations of ash-forming elements vary with BM type, growth conditions, and plant fraction (e.g., bark, wood, and foliage) [38]. AAEMs, particularly Ca and K, catalyze char gasification [9]. Their catalytic activity depends on their chemical forms, which typically occur as water-soluble salts, calcium compounds, and ions bound to functional groups within the BM structure [29]. In contrast, silica and alumina may suppress gasification reactivity by immobilizing AAEMs through the formation of stable silicate and aluminosilicate compounds [9], [39], [40].

1.2 Oil Shale as Gasification Feedstock

OS (oil shale) has attracted considerable interest as an energy and chemical resource [41], [42]. In Estonia, it remains an important source of domestic energy, although the country aims to reduce its use for energy production and adopt low-carbon technologies [1], [43]. For now, however, the country aims to focus on improving OS utilization and valorization.

Dictyonema argillite and kukersite are the two main OS types found in Estonia. Kukersite is more commonly used because of its higher organic matter and lower sulfur concentration [44]. It is a calcium-rich, low-grade sedimentary rock characterized by high

ash content and complex mineral composition [45]. Its organic matter, kerogen (~30%), occurs in layers of varying thickness within the mineral matrix and is classified as Type I–II kerogen (H/C = 1.26; O/C = 0.09), reflecting its algal origin and high oil-generating potential [11], [46]. As a result, pyrolysis has become the dominant conversion route, and both research and industrial utilization have traditionally focused on shale oil production.

The inorganic fraction of kukersite is dominated by carbonate minerals (~41%) and sandy-clay components (~26%) [11]. These carbonates, primarily calcite ($CaCO_3$) and dolomite ($CaMg(CO_3)_2$), decompose at 600–900 °C to form CaO and MgO [11], [47]. The resulting CaO is particularly relevant for gasification, as it may promote char–CO_2 reactions under suitable conditions [48]. In addition, OS minerals and trace metals influence thermal conversion behavior and product quality [20].

Compared with higher-rank coals dominated by stable aromatic structures, OS contains a greater proportion of saturated aliphatic hydrocarbons with long straight-chain alkanes [21]. Consequently, its thermal conversion is more complex than that of coal, because of the strong association between organic matter and the mineral matrix [49].

Although technically feasible, OS gasification has received less attention than pyrolysis owing to its high ash content, low volatile yield, and complex organic–mineral interactions, which reduce process efficiency and increase operational complexity [46]. Nevertheless, OS gasification has historical precedent in Estonia, where gas produced in chamber furnaces was used as a household fuel until the 1970s, before being replaced by imported natural gas [5].

The high mineral content of OS may also promote thermochemical conversion. Tang et al. [50] showed that although a higher ash content decreases the reactivity, elevated K_2O and CaO concentrations enhance pyrolysis and CO_2 gasification. Similarly, minerals in OS semicoke have been reported to exhibit catalytic activity [5]. These findings suggest that OS minerals can greatly influence thermochemical conversion behavior, particularly in blended systems.

1.3 Gasification Fundamentals

Gasification is a thermochemical process in which solid carbonaceous feedstock is transformed into combustible gas through reaction with a gasifying agent at elevated temperatures (typically 800–1000 °C) [51]. In BM conversion, gasification follows drying and pyrolysis and occurs under controlled oxidizing conditions that are insufficient for complete combustion. The process redistributes chemical energy from the solid matrix into gaseous intermediates suitable for combustion or chemical synthesis [31].

Pyrolysis is the initial stage of gasification, during which BM decomposes into char, tar, and gases in the absence of oxidizing agents [16], [31], [52]. The distribution of pyrolysis products is influenced by the reaction temperature and heating rate, with fast pyrolysis favoring bio-oil formation and slow pyrolysis promoting biochar production [53]. Pyrolysis gas mainly consists of H_2, CO_2, CO, CH_4, C_2H_6, and C_2H_4, along with trace amounts of heavier organic vapors and water vapor [35], [54]. Pyrolysis char retains oxygen-containing functional groups and residual organic structures that influence its subsequent reactivity [31].

Gasification technologies are commonly classified according to the reactor type (e.g., bubbling or circulating fluidized beds, fixed-bed, updraft, or downdraft), operating pressure (atmospheric or pressurized), gasifying agent (air, steam, CO_2 or mixtures such

as O_2-enriched air, CO_2-steam, O_2-steam, and O_2-CO_2), and gas-cleaning method (wet, hot filtration, or catalytic) [55]. Consequently, gasification behavior and product composition are governed by multiple interacting parameters, including fuel composition, temperature, pressure, gasifying agent, reactor design, and catalysts [56], [57]. Heat and mass transfer also play an important role, particularly in BM systems with low thermal conductivity, where particle size affects conversion behavior and product distribution [39], [58], [59]. Temperature is a key parameter, with higher values favoring endothermic reactions and promoting tar cracking [21], [60]-[62].

The gasifying agent strongly influences producer gas composition. Air gasification typically yields 5–25 vol% H_2, whereas steam gasification may produce 20–60 vol% H_2 due to enhanced water-gas and water-gas shift reactions [63]. In contrast, CO_2 gasification promotes the Boudouard reaction, increasing CO concentration while lowering the H_2/CO ratio [56], [64]. BM gasification produces gas consisting mainly of CO, H_2, CH_4, H_2O, CO_2, light hydrocarbons, tar, and ash particles [53], [65], [66]. Syngas consists primarily of H_2 and CO.

Producer gas also contains contaminants, including ash and char particles, sulfur and chlorine compounds, trace metals, and condensable hydrocarbons (tar) [37]. Tar is a major technical challenge in gasification systems, because it fouls downstream equipment and deactivates reforming catalysts. Tar yield depends on temperature, pressure, gasifying medium, equivalence ratio, residence time, and gasifier design [31]. Operating temperatures above 800 °C, longer residence time, and catalysts reduce tar formation through enhanced thermal cracking and reforming reactions [31], [67], [68].

Char yield depends mainly on ash, lignin, and extractives contents [69]. During gasification, approximately 70–80 wt% of BM is volatilized, leaving a reactive char residue [70]. BM char is generally more reactive than coal char because of its less-ordered carbon structure, higher surface area, and catalytic influence of AAEMs.

Char reactivity depends on pore accessibility, the density of active sites, surface area, mineral dispersion, structural evolution during gasification, and operating conditions, such as temperature, CO_2 partial pressure, and catalyst presence [71], [72]. For example, demineralized char exhibits low reactivity despite a measurable surface area, whereas the presence of catalytic species such as K and Fe significantly enhances both active-site availability and gasification rate [73].

1.3.1 CO_2 Gasification

In recent years, increasing research attention has been directed toward CO_2 as a gasifying agent because it enables CO_2 utilization, production of CO-rich syngas, avoidance of nitrogen dilution, and integration with carbon-capture strategies [26], [56], [64], [72], [74]-[77]. Compared with steam gasification, CO_2 gasification is less corrosive and enables dry reforming pathways that enhance VOC cracking and reduce tar formation [78]. In addition, recirculation of process-derived CO_2 streams supports the development of more resource-efficient and circular thermochemical conversion systems [79]. However, CO_2 gasification generally requires higher temperatures and longer residence times than steam or oxygen-assisted gasification [66]. Compared with steam gasification, CO_2 gasification produces CO-rich gas with a high CO/H_2 ratio, which makes it more suitable as a fuel rather than a raw precursor for the synthesis of industrial products, H_2 production, or Fischer–Tropsch synthesis without an additional water-gas shift step [66]. To overcome this limitation, CO_2 is often combined with steam to improve H_2 yield and adjust syngas composition [56], [77].

Consequently, air- and oxygen-based gasification processes are more widely applied, as they afford higher reaction rates with simpler thermal management systems [56], [66]. From a carbon management perspective, CO_2 gasification may be particularly attractive when a suitable CO_2 source is readily available, as the extraction, separation, capture, or production of CO_2 can otherwise increase process costs compared with air gasification [56].

CO_2 gasification is an allothermal process in which heat is supplied externally rather than generated by partial fuel oxidation [37], [56]. Unlike O_2, CO_2 is a relatively weak oxidizing agent and reacts with char through an endothermic Boudouard reaction. This reaction requires elevated temperatures and is strongly influenced by char structure, mineral composition, surface reaction kinetics, and gas-phase diffusion [47], [66], [80]. CO_2 gasification can generate a highly microporous and amorphous char structure that enhances CO_2 diffusion and access to reactive sites, thereby promoting char conversion [64], [66], [81]. However, steam gasification generally produces chars with higher specific surface areas because of the stronger pore-developing effect of steam [64]. Furthermore, CO_2 gasification is sensitive to catalytic effects from the feedstock mineral matter [16], [27], [28]. In particular, AAEMs, especially Ca and K, promote char–CO_2 gasification by enhancing CO formation and char reactivity at elevated temperatures [29].

Below approximately 600 °C, CO_2 behaves similarly to N_2, whereas at higher temperatures, it participates in gasification reactions and alters the producer gas composition [77]. Accordingly, studies comparing CO_2 and N_2 atmospheres have reported higher production of CO, CH_4, alkanes, and hydrocarbon gases in the presence of CO_2 [82], suggesting that CO_2 participation in gasification and reforming reactions can significantly affect product distribution.

Studies on CO_2 gasification of OS remain limited, with most co-processing research focusing on co-pyrolysis rather than gasification. Previous studies indicate that OS exhibits similar pyrolysis behavior under N_2 and CO_2 at lower temperatures, which suggests that CO_2 acts largely as an inert medium during devolatilization [79], [83]. Above 800 °C, however, CO_2 becomes reactive through the Boudouard reaction, thereby enhancing char gasification [47], although higher activation energy may be required than that needed under N_2 [83]. Tang et al. [50] further showed that CO_2 reduced the activation energy and enhanced the decomposition of alkali-rich OS compared to that achieved with N_2, highlighting the importance of mineral composition for CO_2 gasification. These findings suggest that CO_2 gasification is particularly sensitive to mineral-mediated effects and may amplify interactions between BM-derived AAEMs and carbonate-rich OS minerals.

1.3.2 Reactions

The principal reactions involved in BM and OS co-gasification are summarized in Table 1. Pyrolysis initiates the process by decomposing the feedstock into char, tar, and gaseous products under heating [31].

Table 1. Main reactions in the BM and OS gasification process [31], [84], [85]

Reaction name	Reaction equation	ΔH at 25 °C (kJ/mol)	
Pyrolysis	$C_nH_mO_p + Heat = \sum_{liquid} C_aH_bO_c + \sum_{gas} C_xH_yO_z + \sum_{solid} C$	>0	*(1)*
Boudouard reaction	$C + CO_2 \leftrightarrow 2CO$	+172	*(2)*

Reaction name	Reaction equation	ΔH at 25 °C (kJ/mol)	
Water-gas reaction	$C + H_2O \leftrightarrow CO + H_2$	+131	*(3)*
Hydrogasification	$C + 2H_2 \leftrightarrow CH_4$	-74.8	*(4)*
Water-gas shift reaction	$CO + H_2O \leftrightarrow CO_2 + H_2$	-41.2	*(5)*
Methanation	$2CO + 2H_2 \leftrightarrow CH_4 + CO_2$ $CO + 3H_2 \leftrightarrow CH_4 + H_2O$	-247 -206	*(6)* *(7)*
Dry tar reforming	$Tar\ (C_xH_y) + xCO_2 \rightarrow 2xCO + (\frac{y}{2})H_2$	+980~+3112	*(8)*
Tar cracking	$C_xH_yO_z + CO_2 \leftrightarrow CH_4 + H_2 + H_2O + C_nH_m$	>0	*(9)*
Carbonate decomposition	$CaCO_3 \leftrightarrow CaO + CO_2$ $MgCO_3 \leftrightarrow MgO + CO_2$	+178.1 +117.3	*(10)* *(11)*

In CO_2 gasification, the Boudouard reaction is the dominant gasification reaction. Owing to its high activation energy, the char–CO_2 reaction proceeds slowly below ~1000 K (727 °C), and it is generally considered the rate-limiting step [31], [66], [72], [74], [86]. Its rate depends on temperature, surface heterogeneity, and the relative partial pressures of CO_2 and CO [87]. The reaction proceeds via the formation of surface C–O complexes, which subsequently decompose to release CO and regenerate active carbon sites [62], [74], [87].

During gasification, the feedstock undergoes drying (<200 °C), devolatilization (200–600 °C), and char gasification (>700 °C) [88]. During devolatilization, volatiles may undergo reforming reactions (the reverse of Reaction 6) [74]. Increasing the temperature enhances the reaction rate according to Arrhenius kinetics, while simultaneously shifting the reaction equilibrium toward CO formation in accordance with Le Chatelier's principle [31], favoring endothermic reactions such as Boudouard and dry reforming, while suppressing exothermic reactions such as methanation [52], [89].

In addition to the Boudouard reaction, secondary reactions may occur depending on process conditions (Reactions 3–9) [31], [84]. Under CO_2 gasification, dry reforming and catalytic cracking contribute to tar reduction and syngas formation, particularly in the presence of Ca- or alkali-based catalysts [31], [55], [90], [91]. Thermal cracking requires temperatures above 1000 °C [31], [91].

The decomposition of dolomite and calcite is described by Reactions 10 and 11. At elevated temperatures, carbonation of CaO and MgO becomes thermodynamically less favorable, shifting the equilibrium toward carbonate decomposition [92], [93], although carbonate stability remains strongly dependent on CO_2 partial pressure [94], [95].

Gas–solid reactions occur at active sites on the char surface, where AAEMs enhance the catalytic activity by increasing the availability of reactive sites [62], [96], [97]. Consequently, gasification reactivity depends more strongly on the concentration of active carbon sites and the dispersion of catalytic species than on the total surface area [98]. The interaction of CO_2 with char is commonly described by the oxygen exchange mechanism, in which CO_2 forms oxygenated surface complexes that subsequently decompose to release CO [99], [100]. AAEMs enhance catalytic gasification by facilitating oxygen transfer to active carbon sites through a redox cycle [101], [102].

1.3.3 Catalysts and Additives

Although catalysts are not essential for BM gasification, they are still widely employed to enhance tar reforming, methane conversion, and overall syngas quality [31], [32]. Effective gasification catalysts must exhibit high activity, resistance to carbon deposition

and sintering, mechanical stability, and economic feasibility. Nevertheless, the use of conventional catalysts in BM gasification is often limited by their cost and tendency to deactivate. Consequently, naturally occurring BM minerals and low-cost additives are attracting increasing attention as alternative catalytic materials for improving gasification performance and syngas composition.

Natural mineral catalysts such as dolomite and olivine have been extensively studied for BM gasification. Dolomite [($CaMg(CO_3)_2$], after calcination, typically consists of 30%–35% CaO, 15%–21% MgO, and 40%–41% CO_2 [31], [90], [103]. It begins to decompose at approximately 700 °C in a CO_2 atmosphere [94]; however, its effective catalytic activity is typically observed only above approximately 800 °C [31], [90], [103]. Calcination considerably increases the catalytic activity of dolomite by transforming the carbonate phases into more active CaO and MgO phases [104], which enhance tar reforming, promote dry reforming with CO_2, and reduce tar yield at high temperatures [31], [55]. Although dolomite gradually deactivates because of carbon deposition, its low cost makes it an attractive catalyst for BM gasification.

Olivine [$(Mg,Fe)_2SiO_4$] exhibits catalytic performance comparable to that of calcined dolomite [31]. The catalytic activity of Ca-based materials strongly depends on intimate contact between Ca species and the carbon matrix, with organically associated Ca exhibiting enhanced char–gas interactions [105]. CaO has been shown to increase CO yield during CO_2 gasification [93] by promoting CO_2 chemisorption and facilitating C–CO_2 and C–H_2O reactions [48], [105]. In addition, CaO may function as an in situ CO_2 sorbent, increasing the heating value of producer gas [39]. Besides natural minerals, Ni-based catalysts are also highly effective for tar reforming and dry reforming, enhancing CO generation. However, their practical application is limited by carbon deposition and particle agglomeration [31], [106]-[108].

In addition to externally added catalysts, AAEMs can also be used as intrinsic catalysts for BM gasification and pyrolysis that enhance char reactivity, modify product distribution and the composition of liquid and gaseous products, and reduce the activation energy [9], [14], [18], [50], [52], [61], [62], [74], [75], [105], [107], [109]-[112]. They promote both heterogeneous char gasification reactions and homogeneous reactions, including the water-gas shift reaction and hydrocarbon reforming reactions [12], [75]. Their catalytic activity depends on the chemical form: solid AAEMs mainly catalyze heterogeneous reactions, whereas volatilized species contribute to homogeneous gas-phase reactions [100]. The relative catalytic activity generally follows the order: K > Na > Ca > Mg [74], [113], [114] or the following order for salts: K_2CO_3 > Na_2CO_3 > other alkali salts [31]. Accordingly, K is generally considered the most active catalyst for char gasification and methane reforming [52], [62], [115]. The higher catalytic activity of K than that of Ca is attributed to its monovalent nature and greater mobility, whereas divalent Ca forms stronger bonds with the carbon matrix and is retained more strongly within char [70], [75], [110], [113], [116].

Several mechanisms have been proposed to explain the catalytic activity of AAEMs in heterogeneous catalysis, including the oxygen transfer, active site, and catalytic desorption mechanisms. All of these mechanisms together describe how AAEMs promote char–gas reactions and facilitate the formation and release of gaseous products [100]. AAEMs have been reported to promote the formation of active carbon sites and enhance CO_2 adsorption and dissociation through chemical interactions [62], [96], [97]. Their catalytic role is further supported by acid-leaching studies, which showed that the removal of these metals greatly reduced char reactivity [117], [118]-[120]. However, acid

leaching may also modify the char structure, making it difficult to distinguish the effects of AAEM removal from treatment-induced structural changes [121].

AAEMs occur in BM as water-soluble, ion-exchangeable, and residual fractions [112], either as inorganic salts or bound within the organic matrix [31]. During thermal conversion, they migrate within the char and alter the carbon matrix, reducing activation energy and enhancing gasification rates [52], [110]. Therefore, their catalytic effectiveness depends not only on their concentration but also on their chemical form and interactions with other mineral phases. Therefore, gasification reactivity is related to inorganic elemental composition, particularly the K/Si ratio, whose higher values indicate catalytic promotion by K and inhibition by Si [12], [62], [122], [123]. Catalytic behavior may also be modified through interactions between AAEMs and other mineral species. For example, synergistic effects between K and Fe have been reported to enhance gasification reactivity through complementary catalytic effects [62].

Alkali species can increase the surface area and porosity of BM-derived char, thereby improving gasification reactivity [124], [125]. Biochar itself may also exhibit catalytic activity, particularly when enriched with AAEMs [39], [75], [107], [116], [126]. However, the catalytic roles of individual AAEMs can differ; for example, K does not always enhance the overall gasification rate, whereas Ca has been reported to act as an active catalyst during biomass gasification [80] . The catalytic activity depends strongly on ash chemistry [70] and the gasification atmosphere, because the chars produced under inert and reactive conditions differ in both their structures and catalytic properties [81]. However, excessive alkali may lead to surface deposits that block pores and reduce reactivity [31]. In addition, alkali metals are difficult to handle and may cause agglomeration in fluidized-bed reactors [29], [31], [59], [105].

1.3.4 Co-gasification

Co-gasification is a thermochemical conversion approach in which two or more feedstocks are simultaneously processed. Similar to co-combustion, which is widely applied as a cost-effective strategy for reducing CO_2 emissions in fossil fuel power plants [127], co-gasification uses interactions between different fuels to improve conversion performance and product quality. Although gasification technology is commercially well established, most co-gasification studies have been conducted at the laboratory or bench scale only.

A wide range of feedstock combinations for co-gasification has been investigated, including different combinations of coal, BM, plastics, and waste materials, to improve conversion efficiency and syngas quality [16], [18], [52], [53], [84], [126], [128]-[130]. In blended systems, differences in devolatilization behavior, ash chemistry, and mineral dispersion may cause additive, synergistic, or inhibitory effects. Positive synergy may be reflected by tar reduction, enhanced gas production, improved syngas quality, and increased carbon conversion [126]. Catalytic species from one feedstock may alter the reaction kinetics of another, making the interplay between feedstock composition, mineral chemistry, and reactor conditions essential for interpreting co-gasification performance [16].

Reactor configuration also plays a crucial role in co-gasification studies, as it influences heat and mass transfer, gas–solid contact, and reaction kinetics. Various experimental investigations have been conducted using different reactor systems, including fluidized-bed reactors [68], fixed-bed reactors [21], [68], [84], [109], [131]-[133], batch or semi-batch reactors [109], and TGA [35], [84], [105], [109], [133]. Fluidized-bed reactors

provide efficient mixing and heat transfer, whereas fixed-bed reactors offer well-controlled gas–solid contact and are particularly suitable for investigating reaction mechanisms and char conversion. Semi-batch systems employing preheated gasifying agents and drop-in feeding approaches have also been used to achieve rapid heating rates [109], [134]. Producer gas composition is typically analyzed using GC or FTIR methods [109], [131], [132]. TGA–MS is frequently used to study devolatilization and gas evolution because of its reproducibility and precise control of experimental conditions [20], [135], [136]. However, the small sample size and well-controlled thermal conditions in TGA–MS may not fully represent the reaction environment encountered in larger-scale reactors [69], [86], [137].

Whether solid-fuel blends, especially coal and BM systems, exhibit synergistic behavior remains a matter of debate. While some studies have reported no significant interaction, others have identified measurable synergistic effects [20], [121]. Mineral interactions are frequently proposed as one of the governing mechanisms of synergistic behavior. AAEMs present in BM can catalyze char–gas reactions and increase the reactivity of coal-derived char [16], [126]. For example, a study on cotton stalk and high-ash coal co-pyrolysis/gasification reported temperature-dependent synergistic enhancement of gas yields and highlighted the role of AAEMs and volatile–char interactions [131]. Increasing the BM proportion generally enhances the overall reactivity in blended systems [19], [52], [138].

Following the observation of synergy in BM and coal systems, similar concepts have been explored for other fossil fuels too, including OS [20]. However, limited experimental studies are available on OS co-gasification, especially in a CO_2 atmosphere. Consequently, the influence of mineral interactions on gas-phase reactions and producer gas composition has received comparatively little attention. To provide a broader understanding of feedstock interactions, previous co-pyrolysis studies involving BM and OS are also considered. Although these studies primarily focused on liquid products and pyrolysis behavior, they provide a valuable insight into the occurrence of additive and synergistic effects. The main observations from these studies are summarized in Table 2 and are later compared with the results obtained in the present work.

Table 2. Summary of previous studies on OS and BM co-processing

Feedstocks	Conditions	Main observation	Proposed mechanism	Ref.
OS + woody BM	N_2, CO_2, low T (≤630 °C)	No interaction between feedstocks, similar behavior in N_2 and CO_2	Additive behavior	Ceron et al. 2024 [139]
OS + woody BM	CO_2, low T (520 °C)	Enhanced decomposition and increased CO production; overall conversion remained close to linear	Predominantly additive behavior with slight interaction effects	Ceron et al. 2023 [140]

Feedstocks	Conditions	Main observation	Proposed mechanism	Ref.
OS + microalgae	N_2, high T (≤900 °C)	BM promoted OS liquid and gas production, whereas OS inhibited BM conversion; the inhibitory effect dominated the overall co-pyrolysis behavior	Catalytic promotion of OS by BM char; inhibition of BM by OS ash	Hu et al. 2016 [141]
OS + mushroom substrate	N_2, low T (≤590 °C)	Earlier decomposition, increased gas and oil yield; reduced solid residue	Catalytic effect of alkali-rich BM	Jiang et al. 2016 [111]
OS + wheat straw	N_2, low T (≤520 °C)	Increased gas yield; improved shale oil quality; reduced activation energy (180–400 °C)	Calcite-catalyzed oxygen transfer and biogas-kerogen interactions	Chen et al. 2017 [142]
OS + microalgae	N_2, high T (≤800 °C)	Improved pyrolysis oil quality; increased aromatic hydrocarbons; reduced oxygenates	Catalytic cracking/reforming	Yu et al. 2018 [143]
OS + pine	Inert (autoclave), low T (≤400 °C)	Temperature-dependent synergy in gas and oil yields; reduced solid residue under mild conditions	Cross-compound formation and heat-transfer effects	Johannes et al. 2013 [144]
OS + peanut shell	N_2, high T (≤900 °C)	Earlier decomposition, increased conversion and oil yield	Proposed temperature-dependent mineral-mediated catalysis (OS minerals at low T; BM AAEMs at high T)	Cui et al. 2023 [145]
OS + wheat straw	N_2, low T (≤521 °C)	Enhanced oil quality (H/C ratio), product redistribution	Temperature-dependent catalytic and free-radical interactions (OS minerals and BM-derived free radicals at low T; BM AAEMs at higher T)	Chen et al. 2022 [21]

Feedstocks	Conditions	Main observation	Proposed mechanism	Ref.
OS + corn stalk	N_2, low T (≤600 °C)	Earlier OS decomposition; reduced activation energy; suppressed release of H_2O and CO_2	Alkali-metal mediated oxygen-transfer mechanism	Zhai et al. 2022 [146]
OS + wood	N_2, low T, fast pyrolysis (≤600 °C)	Enhanced volatile release, reduced semicoke yield, increased CO_2 formation, improved oil quality	Free radical interaction and mineral-catalyzed oxygen transfer	Chen et al. 2020 [147]

Table 2 indicates that the reported interaction effects range from a predominantly additive behavior to clear synergistic responses. While several investigations reported enhanced gas or oil production, reduced activation energy, or improved product quality [21], [111], [141], [142]-[147], others observed predominantly additive behavior despite evidence of increased fuel decomposition [139], [140]. Collectively, these findings indicate that the occurrence and magnitude of interaction effects strongly depend on feedstock composition, reaction temperature, and operating conditions. Despite this, previous studies have focused almost exclusively on low-temperature co-pyrolysis under inert or weakly reactive atmospheres, where interaction effects were evaluated primarily through changes in shale oil yield and quality, volatile release, or apparent activation energy.

Several mechanisms have been proposed to explain interactions during BM and OS co-processing. The most frequently reported mechanisms involve mineral-mediated catalysis, in which OS minerals or BM-derived AAEMs promote the decomposition of the other feedstock [21], [111], [141], [142], [145]. Other proposed mechanisms include catalytic cracking and reforming [143], oxygen-transfer reactions [142], [146], free-radical interactions [21], [147], cross-compound formation [144], and heat-transfer effects [144]. The mineral fraction of OS has also been suggested to exhibit calcite-like catalytic behavior, promoting C–O bond cleavage and increasing CO_2 and CO formation [142]. Collectively, these studies suggest that BM and OS interactions arise from multiple overlapping mechanisms whose relative importance depends on feedstock composition, temperature, and reaction environment. However, the proposed mechanisms have generally been inferred from product distributions and kinetic behavior rather than direct verification.

Synergistic (or antagonistic) behavior is typically evaluated by comparing experimental results of blends with theoretical values calculated using linear additive (weighted average) models based on individual components [14], [89], [109], [111], [121], [131], [138], [142], [148], [149]. Positive deviations from linearity are generally interpreted as synergistic effects, whereas negative deviations indicate antagonistic behavior [130], [131], [150].

Although co-gasification offers opportunities for exploiting complementary feedstock properties, blending fuels with distinct thermal and mineral characteristics also

introduces complexity. BM devolatilizes at relatively low temperatures and contains high volatile matter and AAEMs content [31], whereas OS exhibits delayed decomposition because of its carbonate-rich mineral matrix [11]. Differences in decomposition windows, mineral speciation, and ash chemistry may lead to nonlinear behavior not predictable from individual fuel performance. Moreover, variations in particle density and ash fusion behavior may influence bed stability and gas–solid contact in reactor systems [9], [31]. These factors complicate the interpretation of synergistic or inhibitory effects and require careful experimental evaluation.

Although the understanding of BM and fossil fuel co-processing has considerably improved, systematic investigations of BM and OS co-gasification under a CO_2 atmosphere remain scarce. In particular, the effects of physicochemical properties of feedstock and mineral-mediated interactions on producer gas composition and conversion behavior have not yet been comprehensively evaluated.

2 Experimental

This dissertation is based on three different studies. Fuels and experimental methods are described in detail in the respective publications **(Papers I–III)**. This chapter provides a consolidated overview of the materials, experimental setups, and methods employed.

It also describes the Estonian BM and OS feedstocks used **(Papers I–II)**, followed by the description of the preliminary batch reactor and TGA–MS experiments **(Paper I)** and CO_2 co-gasification study conducted using TGA–MS and a fixed-bed reactor **(Paper III)**.

2.1 Materials

Feedstock characterization of 19 wood species grown in Estonia, including separate analyses of wood and bark, is presented in **Paper II**. Proximate, ultimate, and elemental analyses were performed using standardized methods. This study included only the characterization results for feedstocks used in the gasification experiments (**Paper III**).

BM and OS samples were dried and ground into powder prior to co-gasification. Samples were prepared in accordance with the ISO 14780 standard for both proximate and ultimate analyses. The prepared samples were stored in airtight plastic bags until use.

Birch (*Betula pendula*) and pine (*Pinus sylvestris*) were selected as BM feedstocks for the gasification experiments because of their abundance in Estonia. For co-gasification, the BM samples were blended with OS at weight percentages of 10%, 20%, and 30%. The resulting mixed samples were labeled according to their composition; for example, the sample denoted as OS–PineB_10 contained 90 wt% pine bark and 10 wt% OS.

2.2 Methods

Co-gasification experiments were performed using two different approaches: a fixed-bed reactor and TGA–MS. This allowed a comparison of the gasification process at different scales while maintaining similar temperatures, gas atmospheres, and heating conditions.

2.2.1 Fuel Compositional Analysis

The BM properties were measured following the European standards on solid biofuels. Moisture, ash, and volatile matter were measured as per ISO 18134-3, ISO 18122, and ISO 18123, respectively. Fixed carbon (FC) was calculated by difference as $\mathrm{FC}\,(\%) = 100 - \mathrm{ash} - \mathrm{volatiles} - \mathrm{moisture}$. The gross calorific value was determined using an IKA C5000 bomb calorimeter according to ISO 18125. C, H, N, and S were measured using a Vario Macro elemental analyzer (Elementar Analysensysteme GmbH, Langenselbold, Germany) following ISO 16948, while O was calculated by difference as $\mathrm{O}(\%) = 100 - \mathrm{C} - \mathrm{H} - \mathrm{N} - \mathrm{S} - \mathrm{Cl} - \mathrm{ash}$. A Primus II WD-XRF spectrometer (Rigaku Corporation, Tokyo, Japan) and iCAP Qc ICP–MS (Thermo Fisher Scientific, Bremen, Germany) were used to measure ash-forming elements according to ISO/TS 16996 and ISO 16968.

OS was characterized using standardized methods for mineral fuels. Moisture, ash, volatile matter, gross calorific value, elemental composition (CHNS), total inorganic carbon (TIC), and inorganic components were determined following ISO 579, EVS 669, ISO 562, ISO 1928, ISO 29541, an accredited in-house method (TJ-9) based on acid decomposition of carbonates and CO_2 quantification, and ISO 29581-2, respectively.

2.2.2 General Experimental Considerations

Heating rate and residence time strongly influence product distribution and gas composition during pyrolysis and gasification [31]. Low-to-moderate heating rates are commonly used in bench-scale studies because they result in higher char formation and increased surface area during pyrolysis and, consequently, higher gas production [14], [81]. Therefore, a heating rate of 50 °C/min was applied in both TGA–MS and fixed-bed reactor experiments to maintain consistency between experimental methods and interpretation of gasification behavior. Although higher heating rates may quicken devolatilization and reduce processing time [151], the selected heating rate was considered more suitable for investigating the potential interaction effects between feedstocks.

Residence time was determined based on mass-loss curves, with gasification considered complete when no further mass change was observed. Therefore, a residence time of 17 min was selected and applied in both TGA–MS and fixed-bed reactor experiments to ensure completion of the gasification process and comparability between the two systems.

A gasification temperature of 850 °C was selected based on literature recommendations [47], [51], [66], [125], [133], [141], [152], as this temperature range promotes char–CO_2 gasification reactions while ensuring sufficient decomposition of thermally stable feedstock components.

2.2.3 Fixed-bed Reactor and Gas Chromatography

Prior to the co-gasification experiments, a preliminary pyrolysis study (**Paper I**) was conducted using a preheated drop-in batch reactor described by Konist et al. [153] (Figure 1), enabling very high heating rates and rapid devolatilization, similar to the procedure described by Tong et al. [14].

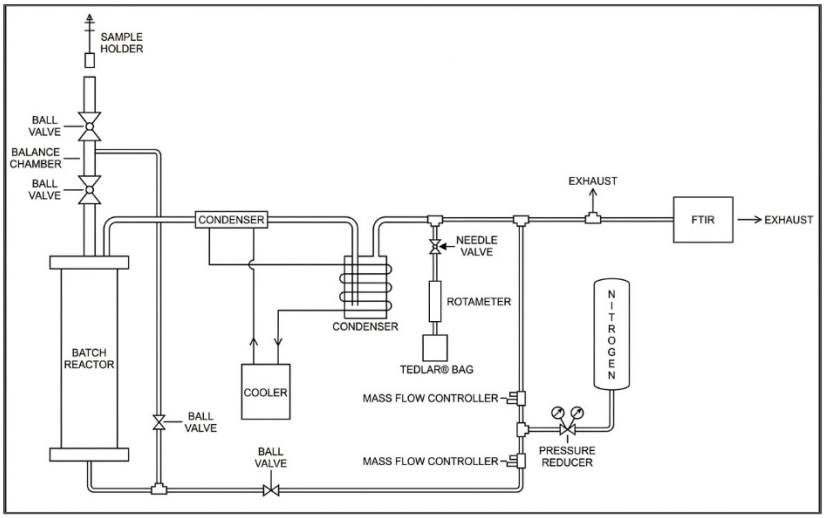


Figure 1. Schematic of the drop-in batch reactor (Paper I)

Although this reactor can also be used to investigate gasification under appropriate operating conditions, it was employed here primarily to study fast-heating pyrolysis behavior. Therefore, the experimental strategy was refined in **Paper III** by employing a

fixed-bed reactor that allows controlled adjustment of operating conditions, which is more appropriate for gasification-focused investigations (Figure 2).

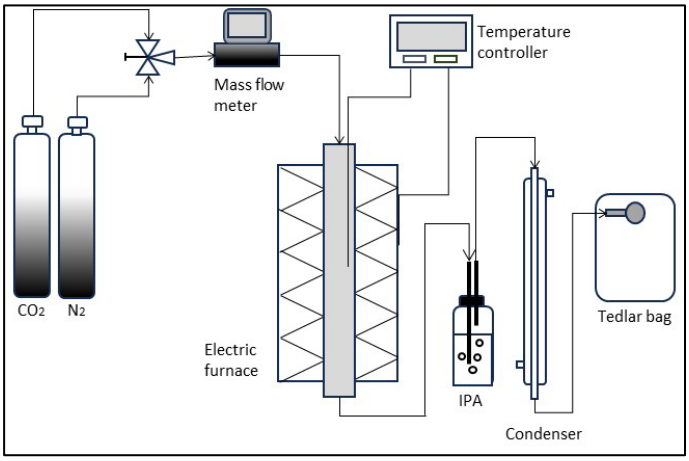


Figure 2. Schematic of the fixed-bed reactor (Paper III)

In the fixed-bed reactor, the gasification of BM and OS was carried out in a single system, allowing simultaneous pyrolysis and gasification. This integrated approach was selected to better represent industrial gasifier operation, where pyrolysis and gasification overlap within the same reactor and enable the capture of gases released during both stages, including CH_4, H_2, and CO [31].

The reactor was equipped with a wire-mesh sample holder to ensure effective heat transfer, gas penetration, and gas–solid interactions. For each experiment, 1 g of sample was processed using a two-stage procedure. The feedstock was initially heated under a N_2 atmosphere to allow pyrolysis. The heating rate was set to 50 °C/min (Section 2.2.2). Once the reactor temperature reached 850 °C, the gasifying atmosphere was switched to CO_2 to initiate gasification. A gas flow rate of 100 mL_{STP}/min was selected based on literature recommendations to ensure adequate gas–solid contact and efficient removal of volatiles, while avoiding poorly mixed conditions at low flow rates and reduced contact times at excessively high flow rates [131].

Solid residues were collected after each experiment for mass measurement and surface area determination. Tests were conducted in at least two independent runs per condition. The replicates showed good agreement. The observed variability, expressed as standard deviation, ranged from 0.01 to 1.6 wt%. Gas sampling was performed continuously for 34 min. Producer gas was collected in Tedlar® bags, and its composition was analyzed using a Shimadzu GC-2014 gas chromatograph with a thermal conductivity detector (TCD) and a valve system capable of quantifying H_2, CO, O_2, N_2, CO_2, and CH_4 in a single run. Permanent gas concentrations were determined using packed columns (Porapak N/MolSieve 5Å). The oven temperature was programmed from 35 to 120 °C at a heating rate of 20 °C/min, using helium (purity 99.996%) as the carrier gas at a flow rate of 35 mL/min. The GC was calibrated with certified gas standards. Reported gas concentrations are the as-measured volumetric concentrations in the collected gas (vol% in the bag) and therefore reflect the sampling/dilution conditions (presence of N_2 during pyrolysis and CO_2 during gasification). The limits of detection (LOD) were estimated using the standard deviation of the lowest calibration standard replicates and the calibration

slope. The resulting practical LODs were: CO ≈ 0.013 vol% (~130 ppm), H_2 ≈ 0.114 vol% (~1140 ppm), and CH_4 ≈ 0.018 vol% (~180 ppm).

2.2.4 TGA–MS

TGA is widely used to investigate thermal behavior and reaction kinetics during pyrolysis and gasification at small scales by continuously measuring mass loss as a function of temperature and time under controlled atmospheres. While TGA is well suited for screening studies and mechanistic comparisons, its small sample size and more uniform thermal conditions may not fully represent the reaction environment encountered in larger-scale reactors. Therefore, this work primarily used TGA for comparative analysis and fixed-bed experiments to evaluate gasification performance under more representative conditions.

The TGA–MS experiments were conducted using a NETZSCH STA 449 F3 Jupiter® TG-DSC system coupled with a NETZSCH QMS Aëolos® mass spectrometer. Approximately 5 mg of sample was placed in Al_2O_3 crucibles with a height-to-diameter ratio <1 to facilitate efficient release of evolved gases [154]. The samples were first subjected to pyrolysis under a N_2 (purity 99.999%) atmosphere, followed by gasification when the temperature reached 850 °C, by switching the gas flow to a mixture of 90% CO_2 (purity 99.995%) and 10% N_2. The heating rate was 50 °C/min, consistent with the fixed-bed reactor experiments. The experiment was terminated when no further mass loss was observed, corresponding to a residence time of 17 min. Buoyancy effects were corrected by performing blank runs with empty crucibles and subtracting the resulting baseline from sample measurements. Each measurement was performed at least in duplicate, with standard deviations ranging from 0.05 to 1.7 wt%.

A coupled mass spectrometer was used to monitor the H_2-release profile during gasification. The ion intensity at m/z = 2 was selected to evaluate the effect of mixed feedstocks, as signals from other producer gas ions overlapped with the background ions originating from N_2 and CO_2.

2.2.5 Surface Area

The specific surface areas (SSAs) of the solid residues were determined using N_2 adsorption–desorption isotherms based on the Brunauer–Emmett–Teller (BET) method [155]. Although both N_2 and CO_2 are commonly used for SSA measurements, with isotherms at 77 and 273 K, respectively, N_2 adsorption is more commonly preferred for porous material characterization because of its high stability, availability, and suitability over a broad pressure range [156].

SSA measurements were performed using a Quantachrome Autosorb analyzer. Prior to analysis, the samples were degassed under vacuum at 300 °C for 20 h to remove moisture and adsorbed gases.

2.2.6 Synergistic Behavior Investigation

Synergistic effects during co-gasification were evaluated by comparing the experimental behavior of BM and OS mixtures with theoretical predictions derived from the individual components. The assessment focused on two main parameters: mass-loss behavior obtained from TGA experiments and gas concentrations measured in the fixed-bed reactor.

The theoretical values of each mixture were calculated using a weighted average approach based on the mass fraction of BM and OS in the blend (Equation 12), where

Y_{BM} and Y_{OS} are gas concentrations of BM and OS, respectively, and x is the share of BM or OS in the mixture. This linear additive model assumes no interaction between the components and therefore serves as a reference for nonsynergistic behavior.

$$Y_{CAL} = x_{BM}Y_{BM} + x_{OS}Y_{OS} \quad (12)$$

Deviations between the experimental results and the calculated theoretical values were used to identify potential interactions. Positive or negative differences in mass-loss profiles or gas concentrations were interpreted as indications of synergistic or antagonistic behavior, respectively. To ensure that these deviations reflected genuine interactions rather than analytical variability, an uncertainty analysis was performed. Only deviations exceeding the combined uncertainty of the experimental and calculated values were considered significant. The uncertainty was estimated as follows:

1. Propagation of uncertainty:
   $$\sigma_{calc} = \sqrt{(x_{BM}\sigma_{BM})^2 + (x_{OS}\sigma_{OS})^2}, \quad (13)$$
2. Combined uncertainty for comparison:
   $$\sigma_{diff} = \sqrt{\sigma_{exp}^2 + \sigma_{calc}^2}, \quad (14)$$
3. Decision rule:
   $$\left|Y_{exp} - Y_{calc}\right| > \sigma_{diff}, \quad (15)$$

where σ_{BM} and σ_{OS} are standard deviations of the measured gas concentrations of pure BM and OS, respectively; σ_{exp} is the standard deviation of the measured gas concentration for the blend; σ_{calc} is the propagated uncertainty of the calculated (theoretical) value; and σ_{diff} is the combined uncertainty used when comparing experimental vs calculated values. The difference is considered resolvable if it exceeds the combined uncertainty and therefore cannot be explained solely by experimental variability.

3 Results and Discussion

The results are derived from the characterization of woody BM (**Paper II**), co-pyrolysis in a batch reactor and TGA–MS (**Paper I**), and co-gasification performed in a fixed-bed reactor and TGA–MS (**Paper III**).

3.1 Feedstock Characterization

Paper II demonstrates that woody BM is a heterogeneous resource, with the composition strongly influenced by species, plant fraction, and mineral uptake. It provides a comprehensive compositional dataset for 19 woody species grown in Estonia, including separate characterization of wood and bark fractions involving 27 parameters. Detailed results are presented in **Paper II**, while Table 3 and Table 4 summarize the proximate and ultimate analyses and inorganic element composition of the feedstocks used in gasification, respectively, presented in **Paper III**.

Chemical analyses revealed considerable compositional variability among BM, consistent with previous studies reporting differences related to BM type, species, plant fraction, and growing conditions [7], [36]. Principal component analysis (PCA) showed a compact clustering of wood samples with high VM (volatile matter), H, and O and low ash content, whereas bark samples were more dispersed. These results indicate that wood samples generally exhibit stable and predictable characteristics, whereas bark composition is more variable, which may influence ash-related thermal conversion (Figure 3). The loading plot (Figure 4) confirmed that this separation was primarily governed by mineral matter, with the first principal component (F1) representing a gradient from organic BM characteristics (VM, H, O, C, and GCV) to ash-related constituents and inorganic elements (Al, Na, Ca, Si, and ash). Notably, the birch bark clustered closer to the wood samples owing to its higher GCV, VM, and carbon content.

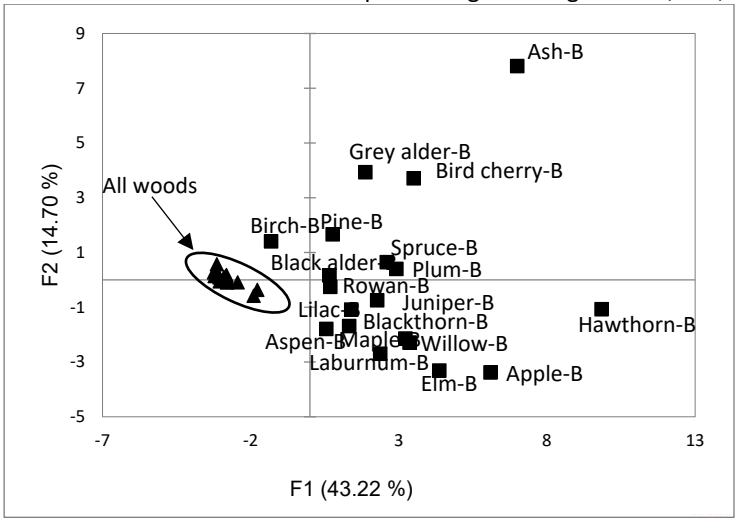


Figure 3. Dispersion of wood and bark samples based on the principal component analysis (PCA) from 27 variables (autoscaled) (Paper II); B, bark; W, wood; F1, principal component 1; F2, principal component 2

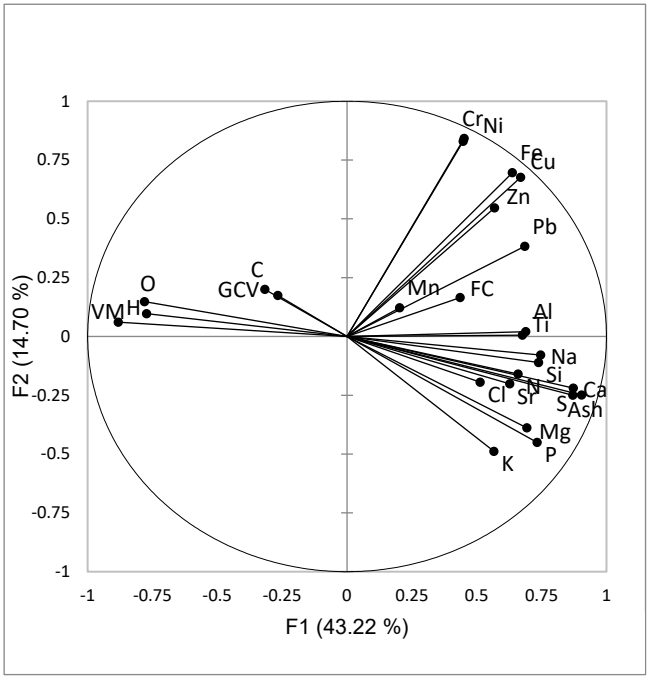


Figure 4. PCA loading plot showing the relationships between BM properties and elemental composition variables (Paper II); VM, volatile matter; H, hydrogen; O, oxygen; GCV, gross calorific value; C, carbon; FC, fixed carbon

Considerable variation was observed among the BMs regarding both total ash content and elemental composition, consistent with previous studies [123]. Bark samples generally exhibited higher FC, ash, Ca, and K contents than wood samples, whereas wood fractions contained higher VM. A notable exception was the markedly elevated Ca concentration in PineB, which was several times higher than that in the other BM samples. These differences are likely related to the higher mineral content of barks than that in wood [74], [157], [158].

FC content represents the solid carbon remaining after the release of volatiles and is therefore an important precursor for char formation during gasification. Higher FC content generally promotes the contribution of the char–CO_2 reaction. Rollinson et al. [159] similarly reported that higher FC/VM ratios correspond to lower activation energy and improved char reactivity. PineB and PineW exhibited FC/VM ratios of 0.30 and 0.17, respectively. This difference is consistent with the enhanced gasification performance observed for PineB during subsequent CO_2 gasification experiments (Section 3.3). In contrast, Gonzales et al. [160] reported that higher VM promoted CO formation during pyrolysis, indicating that the influence of VM and FC on gas production differs between pyrolysis and gasification conditions.

Trace element analysis (**Paper II**) revealed species- and fraction-specific differences that provide supplementary information for assessing feedstock utilization and potential ash-related challenges during thermochemical conversion. Among the investigated BM samples, silver birch and gray alder exhibited higher trace element concentrations than the other hardwood species, while Norway spruce bark contained approximately twice the heavy metal concentration of pine bark.

BM and OS represent fundamentally different fuels in terms of their physical and chemical characteristics (Table 3 and Table 4). BM is primarily composed of C and O, with an ash content of <5%, while OS contains >50% mineral matter. Due to its high mineral content and relatively low organic carbon fraction, OS exhibited a substantially lower calorific value than BM. The inorganic composition of OS is dominated by Ca and Si, followed by Mg, Al, Fe, and K, in various phases such as calcite, dolomite, quartz, pyrite, feldspar, and illite [161].

Table 3. Ultimate and proximate analyses for the BM and OS samples (Paper III)

Sample	C (%)	TIC (%)	H (%)	N (%)	S (%)	O (%)	W_{ar} (%)	A (%)	VM (%)	FC (%)	GCV (MJ/kg)
PineB	52.79	N/A	6.08	1.19	0.05	36.89	4.8	3.1	71.1	21.0	21.4
PineW	50.12	N/A	6.59	0.19	0.01	42.77	8.5	0.3	85.2	14.5	20.04
BirchB	56.34	N/A	7.00	0.44	0.02	34.83	3.7	1.4	80.1	18.5	24.18
BirchW	49.31	N/A	6.62	0.08	0.01	43.70	7.7	0.3	86.9	12.8	19.94
OS	27.49	5.99	2.75	0.06	1.47	16.80	0.5	51.4	47.7	0.9	9.6

PineB, pine bark; PineW, pine wood; BirchB, birch bark; BirchW, birch wood; OS, oil shale.
All values are reported on a dry basis (db), unless stated otherwise (ar, as received). TIC was determined only for OS, as BM contains negligible inorganic carbon.

Table 4. Inorganic elements of the fuels (ppm db) (Paper III)

Sample	Ca	Mg	Al	K	Si	Fe	P	Cr	Ni
PineB	12 947	459	87	2 095	102	186	310	138.2	91.4
PineW	718	241	16	530	28	41	103	0.3	0.1
BirchB	4 489	703	102	606	163	184	195	59.9	31.0
BirchW	1 036	421	14	473	21	39	51	0.3	0.3
OS	176 206	18 373	17 960	11 454	67 096	16 998	374	23	20

3.2 Thermal Decomposition Behavior and TGA–MS Analysis

The thermal decomposition behavior of BM samples and OS was initially investigated by TGA. The resulting mass-loss curves (Figure 5) revealed clear differences in the thermal decomposition behavior arising from differences in the organic composition and mineral structure of the feedstocks.

BM samples exhibited two main decomposition stages. In the first stage, the greatest mass loss occurred between 200 and 400 °C, owing to hemicellulose and cellulose decomposition, while the broader second stage between 400 and 900 °C corresponded to gradual lignin decomposition, consistent with previous studies [35], [109]. Similar decomposition temperature ranges were reported by Ochieng et al. [162], particularly for pine and birch (243–370 °C).

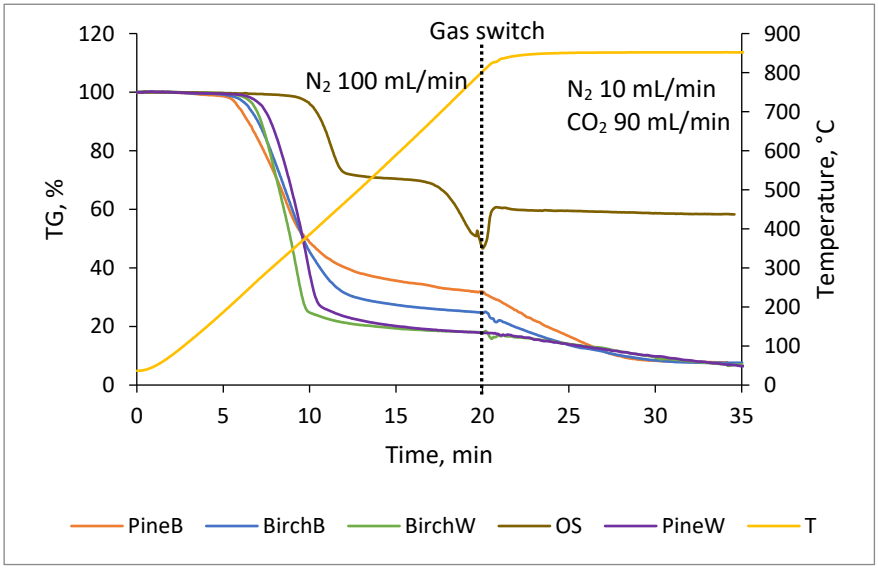


Figure 5. Mass loss curves of natural feedstocks (Paper III)

Mass-loss curves also revealed clear differences in the thermal behavior of wood and bark. Although bark decomposition initiated at lower temperatures (~210 °C) than wood (~280 °C), its subsequent mass loss was more gradual, resulting in substantially greater char retention at the gas-switch point. This behavior is consistent with proximate analysis results (Table 3), as bark samples exhibited lower VM and higher FC content. Bark generally contains more lignin and extractives than wood [74], [157], [158]. Its greater thermal stability likely promotes char formation, providing a larger carbon reservoir for subsequent gasification [69], [81]. Although the higher ash content of bark contributes to the increased residual mass before gas switch, this phenomenon cannot fully explain the observed difference, indicating that bark also forms a larger thermally stable char fraction.

In contrast, OS demonstrated greater thermal stability at lower temperatures, with the decomposition of its main organic components beginning at approximately 400 °C, nearly 200 °C later than that of BM. The decomposition proceeded through two distinct stages: kerogen decomposition (370–560 °C) followed by the decomposition of carbonate minerals (600–770 °C). This result is consistent with that of previous studies on OS [95], [163], [164]. During kerogen decomposition, cleavage of relatively weak C–O, C–S, and aliphatic C–C bonds releases volatile products [165]. Due to its low volatile content and high mineral matter, the OS retained significantly higher residual mass.

TGA–MS analysis in N_2 atmosphere confirmed that carbonate minerals, mainly calcite ($CaCO_3$) and dolomite ($CaMg(CO_3)_2$), decomposed at approximately 700 °C, releasing CO_2 (Figure 6). This decomposition behavior strongly depends on the gas atmosphere and CO_2 partial pressure [94]. Previous investigations using the same OS showed that CO_2 suppressed carbonate decomposition and shifted decarbonation to higher temperatures than achieved using N_2 [95]. Under CO_2, decomposition proceeded in two stages corresponding to the decomposition of dolomite and calcite (Figure 7) [95]. Similar behavior has been reported by Fang-Fang et al. [83], who observed delayed carbonate decomposition above 800 °C in CO_2 compared to that in N_2 atmosphere.

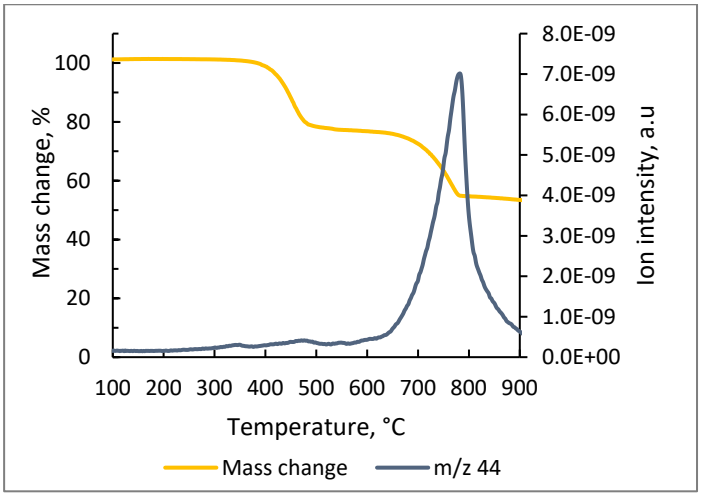


Figure 6. TGA–MS analysis of the same OS under N_2 atmosphere, showing mass change and CO_2 evolution (m/z = 44). The data are obtained from a repeat experiment performed under the same conditions as in Paper I

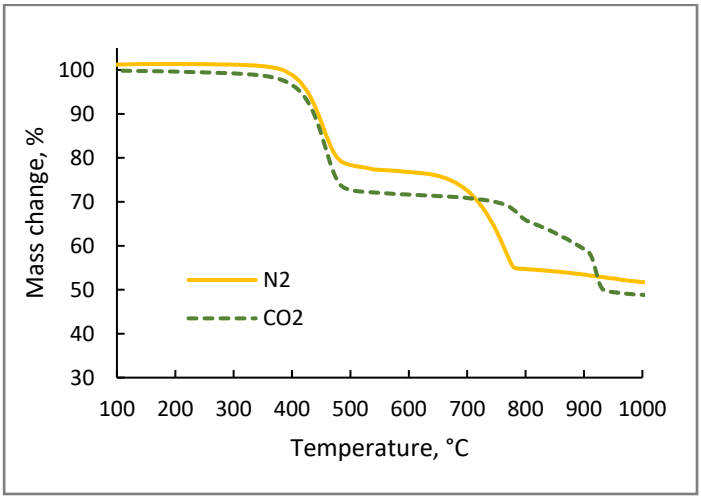


Figure 7. OS decomposition in N_2 and CO_2 atmospheres [95]

Based on previous findings [95], the two-stage procedure was selected to promote carbonate decomposition before gasification at 850 °C. Under N_2 atmosphere, carbonate minerals decompose during heating, resulting predominantly in oxide phases (CaO, MgO). The experimental design proposed herein was intended to examine the behavior of precalcined mineral phases during subsequent CO_2 gasification.

The mass increase observed for OS during the subsequent gasification stage was attributed to the carbonation of in situ formed CaO to $CaCO_3$, indicating that CaO reacted with CO_2 under the studied conditions, consistent with previous studies [47], [93], [142], [166]. Although the carbonation of precalcined CaO is thermodynamically limited at elevated temperatures [93], the observed reactivity may depend on the chemical form of Ca species present during CO_2 gasification.

A comparison of BM and OS blends (Figure 8) showed that increasing OS content progressively increased the residual mass, reflecting the high mineral content of OS. However, the main decomposition region remained largely unchanged, indicating that thermal decomposition was still dominated by the BM component.

The synergistic behavior was evaluated by comparing the experimental and calculated mass-loss curves. TGA results (Figure 8) showed close agreement between curves, indicating predominantly additive behavior under the applied conditions. Previous studies also reported similar findings for BM and coal mixtures, where synergistic effects were absent, weak, or observed mainly during the gasification stage rather than during pyrolysis [14], [20].

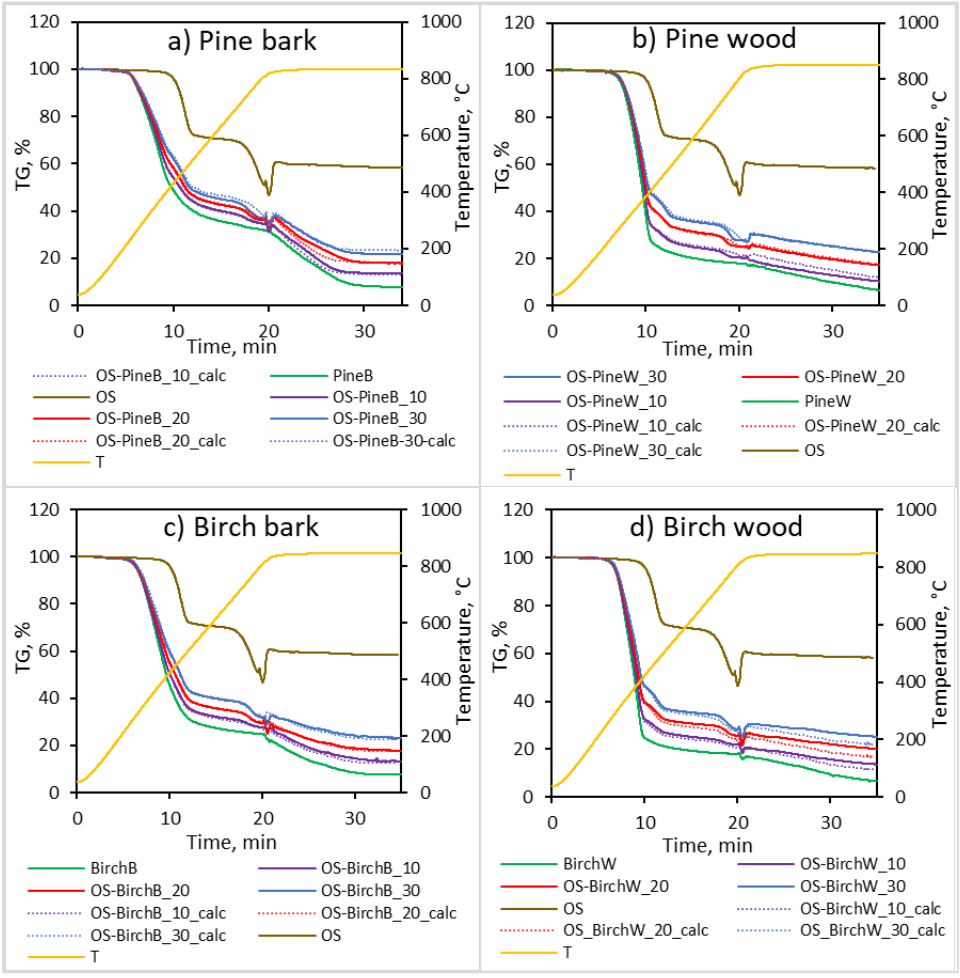


Figure 8. Comparison of experimental and calculated curves of TGA (Paper III)

TGA–MS was employed to monitor gas evolution during gasification (Figure 9). Signals commonly associated with H_2 (*m/z* = 2), CO_2 (*m/z* = 44), CO/N_2 (*m/z* = 28), and CH_4/O containing fragments (*m/z* = 16) were observed during the experiments. However, due to overlapping fragmentation patterns for *m/z* = 16 and 28, the evolution of CH_4 and CO

could not be interpreted. Therefore, this analysis focused primarily on H_2 (m/z = 2) evolution.

H_2 was released in two distinct stages. The first stage coincided with BM devolatilization (~250 °C), while the second followed the switch to a CO_2 atmosphere. Among the investigated fuels, BirchW exhibited the highest H_2 ion intensity at 10% OS addition, followed by lower intensities at higher OS contents. Because MS ion intensities provide only qualitative information, the observed differences should be interpreted as relative trends rather than quantitative changes in H_2 production.

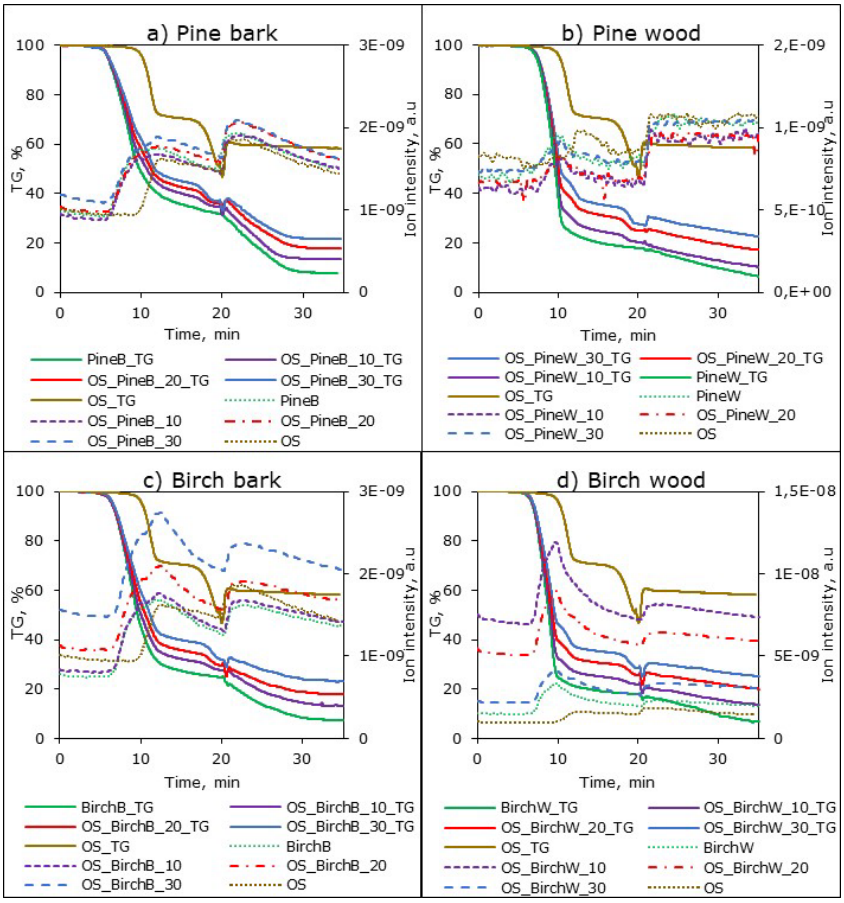


Figure 9. Mass loss curves with the simultaneous evaporation of m/z 2 indicating evaporation of H_2 (Paper III)

3.3 Producer Gas Composition

Table 5 summarizes the producer gas composition of the individual feedstocks. Under the applied conditions, CO was the dominant gaseous product, whereas H_2 and CH_4 concentrations remained comparatively low, consistent with a gasification regime dominated by char–CO_2 reactions [14], [81]. The CO concentration ranged from 5.35 to 16.10 vol%, while the H_2 concentration ranged from 1.26 to 2.47 vol%, with PineB producing more than three times higher CO concentration than PineW. Higher CO concentrations observed for bark feedstocks were consistent with the TGA results, which

indicated a greater retention of thermally stable carbon, likely associated with the higher lignin content of bark. CH_4 concentrations remained low for all BM samples (0.43–0.75 vol%). OS produced substantially lower gas concentrations, reflecting its high mineral content and lower fraction of organic carbon for gas formation.

Table 5. Producer gas composition of BM and OS feedstocks (mean ± standard deviation)

Feedstock	Gas concentration, vol%		
	CO	H_2	CH_4
PineB	16.10±0.10	2.47±0.04	0.62±0.01
PineW	5.35±0.50	1.26±0.10	0.43±0.03
BirchB	9.81±0.07	1.88±0.08	0.49±0.07
BirchW	9.70±1.39	2.05±0.28	0.75±0.16
OS	4.99±0.18	0.43±0.02	0.14±0.01

3.3.1 Relationships between Feedstock Properties and Producer Gas Concentration

To support the interpretation of the experimental results, an exploratory Pearson correlation analysis was performed using the investigated BM feedstocks. The complete correlation matrix is provided in Appendix 2. Due to the limited number of observations, the results should be interpreted as indicative trends rather than statistically robust relationships.

The analysis suggested that CO concentration was positively associated with FC, Ca, and K, and negatively with VM. Similar trends have been reported in previous studies, where feedstocks with a higher FC content exhibited enhanced carbon conversion and gasification performance [14], [167]. Positive associations between CO and both FC and AAEMs concentrations suggest that the gasification behavior was influenced by a combination of char availability and catalytic effects. However, because FC and mineral concentrations were strongly correlated across the investigated feedstocks, their individual contributions could not be distinguished.

H_2 exhibited generally weaker correlations with feedstock properties than CO, whereas CH_4 showed little or no correlation with feedstock composition, suggesting that its formation likely occurred through a different reaction pathway.

SSA indicated negative associations with ash content and major ash-forming elements such as Ca and K, and a positive association with VM. Similar observations were reported by Wu et al. [97], who showed that although naturally occurring AAEMs can influence gasification reaction pathways, development of the pore surface area is governed more strongly by conversion processes rather than by AAEM concentration. Furthermore, the feedstock exhibiting the highest SSA (BirchW) did not yield the largest producer gas concentration, which suggests that SSA alone is insufficient to explain the gasification behavior.

These observations are consistent with previous studies reporting that inorganic constituents, particularly K, can have a stronger effect on gasification reactivity than SSA alone [120] and that high SSA is not necessarily associated with a higher char reactivity [80], [99], [168], [169]. Similarly, He et al. [169] also reported that BM char reactivity is more strongly related to the catalytic index than to the SSA alone. Nevertheless, literature findings regarding the role of SSA remain inconclusive [125], [170], indicating

that the relationship between SSA and reactivity is dependent on feedstock characteristics and operating conditions.

3.4 Co-gasification and Synergy Quantification

To evaluate whether interactions occurred between BM and OS during co-gasification, the experimental gas concentrations were compared with the values predicted by a linear additive model. Figure 10 presents the CO, H_2, and CH_4 concentrations obtained during the co-gasification of BM and OS blends. Nonadditive behavior was evaluated using a linear additive model (Equation 12), where experimental values exceeding the calculated ones indicated synergy, agreement indicated additive behavior, and lower experimental values suggested antagonistic effects.

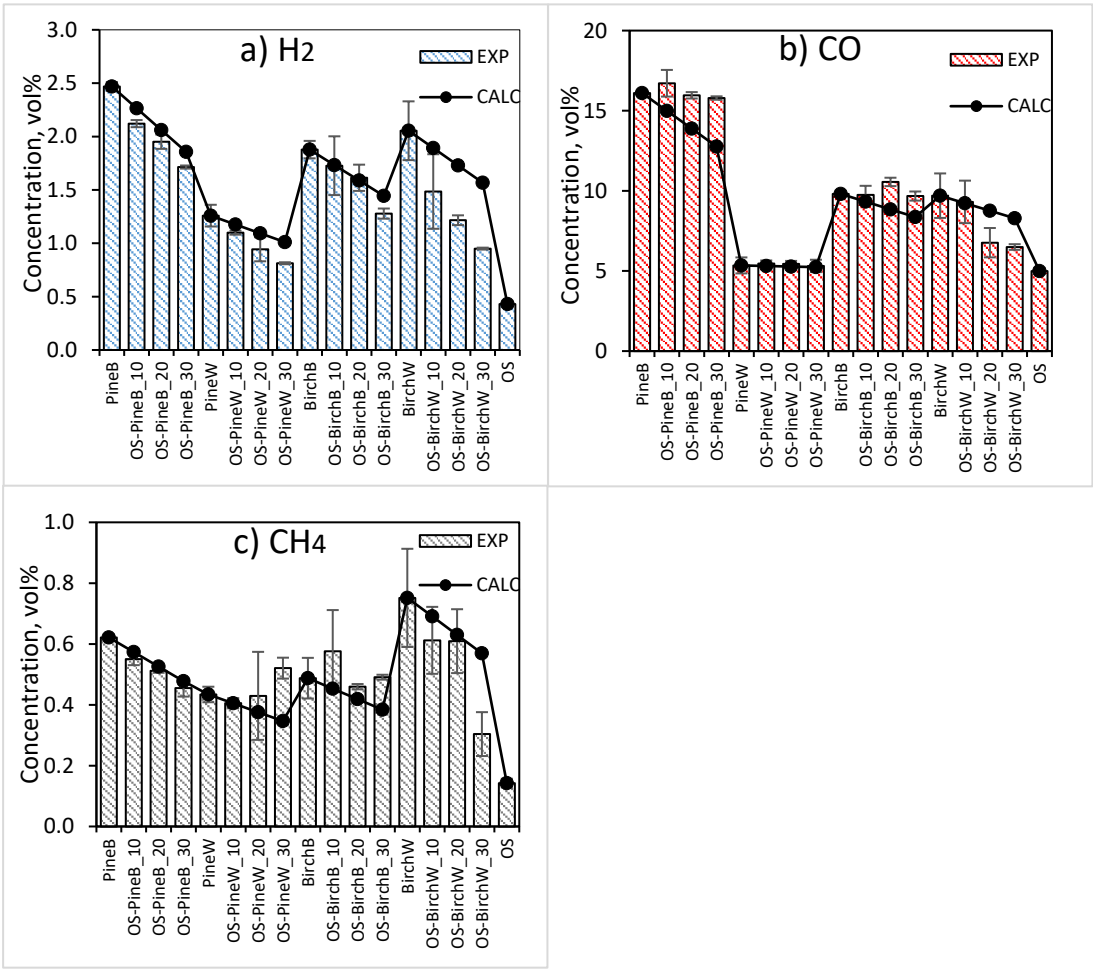


Figure 10. Gas concentrations and corresponding calculated values during gasification (Paper III)

According to the additive model, increasing the OS content should decrease the CO concentration because of the low CO concentration of OS alone. However, the observed deviations were strongly dependent on the feedstock. Bark-based blends generally exhibited positive deviations from additive behavior, whereas wood-based blends

showed largely additive or inhibitory behavior. PineB blends displayed the strongest synergy, as the experimental CO concentration remained nearly constant (16.0–15.8 vol%) despite adding more OS, indicating sustained formation of CO beyond theoretical predictions. Similar behavior was observed for BirchB blends, particularly at higher OS blending ratios.

In contrast, H_2 concentration showed a predominantly additive or inhibitory behavior, decreasing systematically with increasing OS addition. However, low H_2 concentrations do not necessarily indicate the absence of synergy, since CO_2 gasification primarily promotes CO rather than H_2 formation. Although enhanced H_2 evolution following OS addition to BM was observed in TGA–MS experiments, this effect was not clearly detected in fixed-bed experiments. This difference may reflect the different experimental environments and the distinct information provided by the two techniques. TGA employs small sample masses and minimizes diffusion limitations, whereas the higher sample mass used in the fixed-bed reactor may result in temperature gradients (the inner regions remain cooler than the surface) that may influence the evolution and detection of gaseous products [86].

CH_4 formation remained limited under the applied conditions because methane is mainly generated during pyrolysis and is further suppressed at elevated temperatures through reforming reactions [66]. Since CO_2 was introduced only after the reactor reached 850 °C, VOC-related secondary reactions were likely limited [78]. Synergistic behavior would therefore be reflected by a lower experimental CH_4 concentration than that predicted by the additive model because of enhanced methane reforming (reverse reactions 6 and 7). However, no clear systematic deviation from the calculated trend was observed. Only the BirchW sample with 30% OS showed a possible suppression of CH_4, although this would require further confirmation.

3.4.1 Uncertainty Evaluation

To evaluate whether the observed deviations exceeded experimental variability, uncertainty propagation was applied as described in Section 2.2.6. Deviations larger than the combined uncertainty (σ_{diff}) were considered resolvable and therefore distinguishable from experimental variability (Table 6). Although the same analysis was performed for both H_2 and CH_4, detailed results are presented only for CO, because H_2 showed predominantly additive or inhibitory behavior, while CH_4 showed no consistent nonadditive trend across the investigated blends.

Table 6. Experimental and calculated CO concentrations for BM and OS blends with propagated uncertainties

Sample	Y_{exp} (vol%)	σ_{exp}	Y_{calc} (vol%)	σ_{calc}	σ_{diff}	Y_{exp}-Y_{calc} (vol%)
OS-PineB_10	16.71	0.83	14.99	0.09	0.84	**1.72**
OS-PineB_20	15.96	0.20	13.88	0.08	0.22	**2.08**
OS-PineB_30	15.79	0.11	12.77	0.09	0.14	**3.02**
OS-PineW_10	5.47	0.19	5.31	0.45	0.49	0.16
OS-PineW_20	5.44	0.19	5.27	0.40	0.44	0.16
OS-PineW_30	5.31	0.39	5.24	0.35	0.52	0.07
OS-BirchB_10	9.75	0.56	9.32	0.07	0.57	0.43
OS-BirchB_20	10.56	0.26	8.84	0.07	0.27	**1.72**

Sample	Y_{exp} (vol%)	σ_{exp}	Y_{calc} (vol%)	σ_{calc}	σ_{diff}	Y_{exp}-Y_{calc} (vol%)
OS-BirchB_30	9.67	0.29	8.36	0.13	0.31	**1.31**
OS-BirchW_10	9.31	1.33	9.23	1.25	1.82	0.08
OS-BirchW_20	6.76	0.92	8.76	1.11	1.44	**-1.99**
OS-BirchW_30	6.49	0.18	8.29	0.97	0.99	**-1.79**

Y_{exp}, experimentally measured CO concentration; Y_{calc}, value calculated using the linear additive model; σ_{exp}, standard deviation of measured CO for the blend; σ_{calc}, the propagated uncertainty of the calculated value; σ_{diff}, the combined uncertainty used for comparison
Bold values indicate deviations exceeding the combined uncertainty ($|Y_{exp}-Y_{calc}|>\sigma_{diff}$), representing synergistic or antagonistic effects depending on the sign of the deviation

Table 6 reveals positive deviations exceeding combined uncertainty for all PineB blends, indicating synergistic behavior. PineW blends remained largely additive. BirchB blends showed positive deviation at higher OS blending ratios (20–30 wt%), whereas the 10 wt% blend remained within the combined uncertainty. In contrast, BirchW blends containing 20% and 30% OS exhibited negative deviations (-1.99 and -1.79 vol%, respectively), indicating antagonistic behavior and suppression of CO formation.

3.5 Solid Residue Characteristics

Solid residue yields provide insights into char conversion behavior during gasification. Table 7 summarizes the residue yields and the corresponding BET surface areas obtained from the fixed-bed reactor. BM residue yields ranged from 9.7 to 17.2 wt%, indicating incomplete char conversion, consistent with previous studies reporting higher char residues during CO_2 than O_2 gasification because of the absence of exothermic oxidation reactions [66].

Table 7. Residue yield and BET surface area of gasification residues

Sample	Residue yield, wt%	SSA, m^2/g
PineB	17.2	435
PineW	16.2	672
BirchB	14.2	505
BirchW	9.7	682
OS	56.6	9.7

Wood-derived chars exhibited higher SSAs than bark-derived chars. BirchW showed the highest SSA value (682 m^2/g), which indicates that the SSA was influenced more by the BM fraction (wood vs. bark) than by species (pine vs. birch). Relatively small increases in ash content (0.3–3.1 wt%) substantially decreased char SSA (681–434 m^2/g), suggesting that ash limited the pore development during gasification. The SSA values of woody chars were within the range reported in the literature (220–779 m^2/g) [125], [169], [171], [172].

In contrast to BM chars, OS residue exhibited very low SSA (9.7 m^2/g), indicating limited pore development during gasification. This behavior is consistent with that reported in a previous study showing that the SSA of OS semicoke strongly depends on thermal treatment conditions and ranged from 15.5 to 58.8 m^2/g at 500–800 °C in N_2

[173]. Although increasing the temperature initially promotes pore development, further heating leads to carbonate decomposition and a subsequent decrease in SSA. The high mineral content of OS likely contributes to pore blockage or sintering during thermal conversion, limiting the development of porous structures. Similar behavior has been reported previously, with OS residues exhibiting an SSA of 4.2 m^2/g after CO_2 gasification compared with 27.5 m^2/g for semicoke produced under N_2 at 900 °C, despite comparable residue yields [95]. In contrast, CO_2 and H_2O gasification of BM has been reported to increase the SSA and pore volume compared to that achieved with N_2 pyrolysis because of enhanced char conversion and pore development [64]. These findings suggest substantial differences in pore development and structural evolution between BM chars and OS semicoke during gasification.

Figure 11 illustrates the relationship between the residue yield and SSA of the solid residues obtained from co-gasification. The addition of OS systematically reduced the SSA across all blends, which is expected given the substantially lower SSA of the OS residue compared with that of BM chars. For comparison, a simple mass-weighted SSA was calculated from the individual feedstocks. Experimental SSA values were consistently lower than these calculated values, with differences ranging from 73 to 300 m^2/g, suggesting that the decrease in surface area cannot be explained solely by dilution of the OS residue. Instead, mineral-rich OS may additionally influence pore development and pore accessibility during gasification. The observed reduction in SSA may be partly attributed to the formation of mineral layers on the char surface, which can block or restrict access to pore structures. Such a mechanism has been proposed by Perander et al. [29], who observed the formation of $CaCO_3$ and K_2CO_3 deposits on char surfaces during CO_2 gasification.

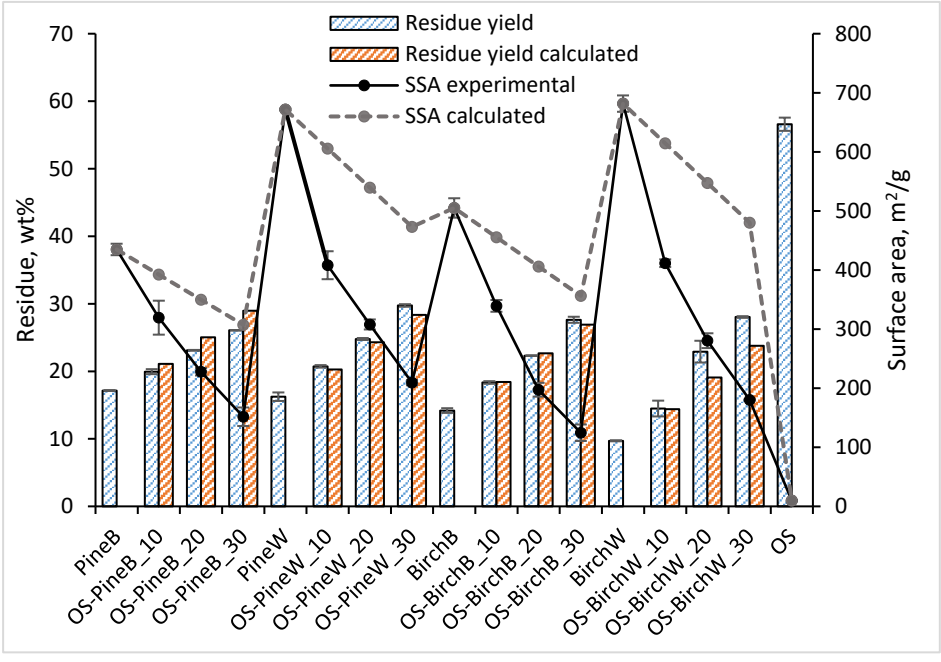


Figure 11. Solid residue yield and BET surface area of OS and BM blends obtained in the fixed-bed reactor (experimental data from Paper III; calculated SSA values and residue yields added for comparison)

A comparison of experimental and calculated residue yields showed lower residue yields for PineB and OS blends than those predicted by the linear additive model, indicating enhanced solid conversion and possible synergistic behavior (Figure 11). This observation is consistent with the enhanced CO formation observed for PineB blends during co-gasification. However, this correspondence between CO enhancement and lower residue yield was not observed for all blends. Although BirchB blends also showed enhanced CO formation, this was not accompanied by a corresponding decrease in residue yield. For the remaining blends, residue yield deviations either remained within experimental uncertainty or indicated reduced conversion relative to the additive model.

3.6 Factors Influencing Synergistic Behaviour

The results demonstrate that OS did not influence all BM samples uniformly, indicating that the interaction between the two feedstocks strongly depended on the initial characteristics of the BM. Bark blends exhibited the strongest enhancement in CO formation. Also, PineB differed from the other BM samples primarily owing to its higher FC content and inorganic elements (Table 3 and Table 4).

The higher FC content of PineB may have contributed to its higher CO concentration by providing a larger carbon reservoir for subsequent char–CO_2 conversion, consistent with the greater char retention of bark observed during thermal decomposition (Figure 5). However, FC alone cannot explain the observed feedstock-dependent behavior, as CO concentration did not scale directly with FC content across the investigated BM samples.

The enhanced gasification behavior of PineB blends may be linked to their relatively high concentrations of inherent Ca (1.3 wt%) and K (0.2 wt%). Both elements are well-established catalysts for the char–CO_2 reaction [48], [70], [75], [96], [97], [105], [110], [113], [116], providing a plausible mechanistic basis for the enhanced CO formation observed. However, the present data do not allow the individual contributions of K, Ca, or other AAEMs to be distinguished, as their concentrations varied together across the investigated feedstocks.

The catalytic effectiveness of AAEMs may depend not only on their concentration but also on their chemical form and association with the carbon matrix and other mineral species. Organically associated AAEMs can exhibit higher catalytic activity than externally added minerals owing to their better dispersion and closer contact with the carbon matrix. This may help explain why the bark samples, which contained higher concentrations of inherent AAEMs, showed greater CO formation. In contrast, for biomass samples with lower inherent AAEM concentrations, the addition of mineral-rich OS did not produce the same degree of enhancement, despite the high Ca content of OS. This suggests that Ca concentration alone may not determine the catalytic response and that the original association and dispersion of AAEMs within the biomass matrix may also be important. This interpretation is consistent with previous studies. Lin et al. [105] reported a stronger catalytic effect of organically bound Ca^{2+} than added CaO, and Perander et al. [29] similarly observed higher reactivity for organically bound Ca species than that of externally added crystalline Ca-oxalate. Likewise, Tong et al. [14] reported that enhanced CO formation during coal and BM co-gasification was strongly associated with the catalytic role of BM-derived K. Thus, the relatively high inherent AAEM content of PineB may be particularly important, because AAEMs naturally associated with the biomass are generally better dispersed and in closer contact with the carbon matrix than mineral species introduced with OS, potentially making them more catalytically effective.

The addition of OS clearly modified the gasification behavior of the bark-based blends. Given the high mineral content of OS, its mineral fraction represents a plausible contributor to this effect. Although the role of mineral matter in OS gasification remains less extensively studied than in BM gasification, previous studies indicate that mineral composition is more important than total ash content alone. Tang et al. [50] reported that high total ash content may suppress reactivity, whereas specific oxides such as K_2O and CaO can promote pyrolysis and CO_2 gasification of OS.

The presence of CaO is particularly relevant under the conditions applied in the present study. During the preceding pyrolysis step, carbonate minerals in OS decompose, resulting in the formation of oxide phases, including CaO, which is therefore available when the atmosphere is subsequently switched to CO_2 for gasification. CaO has been reported to promote the chemisorption of CO_2 and participate in oxygen-transfer mechanisms during char gasification [105], [174], [175], providing a plausible catalytic pathway for OS-derived CaO to enhance char-CO_2 conversion. However, the magnitude of this effect depended strongly on the biomass type, with the clearest enhancement observed for the bark-based blends. This suggests that OS-derived Ca species alone cannot fully explain the observed behavior and that their effect may depend on interactions with the biomass-derived char and its inherent mineral matter.

Previous BM and OS co-processing studies (Table 2) have proposed several mineral-mediated mechanisms, including oxygen transfer, catalytic cracking and reforming, and interactions between BM-derived AAEMs and OS minerals. These studies indicate that interactions may occur in both directions, with BM-derived minerals affecting OS conversion and OS-derived minerals affecting biomass conversion. The present results are consistent with such a combined mineral effect, although the direction and relative contribution of these interactions cannot be distinguished from the present experiments. The observed synergy is therefore interpreted as a collective mineral-mediated effect rather than a unidirectional catalytic process.

A common catalytic pathway that could link these mineral effects is AAEM-assisted oxygen transfer during char–CO_2 conversion [100], [101], [102], [176]. AAEMs have been reported to facilitate CO_2 adsorption and increase the availability of reactive carbon sites on the char surface [62], [96], [97]. In these mechanisms, AAEM species can act as oxygen-transfer mediators between CO_2 and reactive carbon sites through successive oxidation and reduction steps, facilitating oxygen transfer from CO_2 to reactive carbon sites. The resulting C–O surface complexes subsequently decompose and release CO, while the catalytic species are regenerated. Similar mechanism has been proposed by Zhai et al. [146] for BM and OS co-pyrolysis, where BM-derived alkali metals were suggested to facilitate oxygen exchange between oxygen-containing surface groups and reacting species.

The specific mineral-mediated pathways cannot be resolved from the present experiments. Targeted experiments would therefore be required to distinguish the contribution of individual mineral species and verify the proposed mechanism. Ash leaching of BM followed by controlled doping of individual AAEM species could help determine whether the observed enhancement originates from biomass-derived minerals and identify the relative contributions of K and Ca [29], [80]. Similarly, separating or modifying the OS mineral fraction would help distinguish the catalytic contribution of OS-derived minerals from that of BM-derived AAEMs [122]. Surface-sensitive techniques, such as XPS (X-Ray Photoelectron Spectroscopy), Raman or FTIR spectroscopic methods could further provide information on changes in the chemical

states, carbon structure, and the formation of oxygen-containing surface intermediates during char–CO_2 conversion [104], [112], [171], [172].

The different behavior observed in the TGA and fixed-bed experiments suggests that the manifestation of nonadditive effects is also influenced by the experimental environment. One important difference is the sample mass: approximately 5 mg was used in the TGA, compared with 1 g in the fixed-bed reactor, corresponding to a 200-fold difference. The small and thin sample layer in the TGA allows uniform and well-controlled heating with short heat transfer distances, but provides relatively limited opportunity for contact between BM and OS particles. In contrast, the substantially larger sample mass and bed volume in the fixed-bed reactor provide greater opportunity for particle–particle contact, although temperature gradients, thermal lag, and longer transport distances may also occur. The higher-than-predicted residue yields observed for some blends (Figure 11) may indicate that these conditions also limited the extent of solid conversion, leaving part of the char less completely gasified. Thus, the fixed-bed environment may simultaneously promote feedstock interactions through greater particle contact while limiting overall conversion through heat transfer effects. These competing effects may partly explain why the manifestation of nonadditive behavior differed between the two experimental systems.

Particle properties may further contribute to these differences. OS exhibits substantially higher bulk density (1.22–1.72 t/m^3 [44]) compared to woody BM (typically 0.4–0.7 t/m^3 [177]), which can influence bed packing and contact between BM and mineral-rich OS particles. These observations suggest that reactor configurations providing more intensive particle mixing and feedstock contact, such as fluidized beds, could be particularly useful for further investigating the interaction effects observed in this study.

Overall, the present work extends previous studies, which have inferred BM and OS interactions largely from changes in pyrolysis products, such as shale oil yield, volatile release, and activation energy (Table 2), by demonstrating that these interactions also influence producer gas composition during high-temperature CO_2 gasification. The manifestation of these interaction depends on both feedstock characteristics and the experimental environment, supporting a combined rather than a single-factor explanation. Further targeted experiments are required to distinguish the individual contributions and verify the proposed catalytic mechanisms.

4 Conclusions

The transition toward climate-neutral energy systems requires the development of highly efficient and sustainable methods for utilizing both renewable and fossil fuel resources. In Estonia, where biomass and oil shale remain key domestic energy sources, improving their thermochemical conversion pathways is of particular importance. Co-gasification in a CO_2 atmosphere is a potential route for both enhanced resource utilization and carbon management while promoting CO-rich producer gas formation through char–CO_2 reactions. However, the occurrence and extent of interaction effects between biomass and mineral-rich oil shale under such conditions remain insufficiently understood.

This work provides a systematic experimental investigation of feedstock-dependent interactions during the co-gasification of lignocellulosic biomass and Estonian oil shale in a CO_2 atmosphere. A multimethod approach combining fixed-bed gasification, thermogravimetric analysis, and surface area analysis of gasification residues was used to evaluate the producer gas composition, residue yield, and synergistic behavior.

Comprehensive chemical characterization of 19 woody species grown in Estonia, including dominant forest species and less common or ornamental species, revealed clear compositional differences between wood and bark fractions. Wood samples formed a relatively homogeneous group characterized by high volatile matter and low ash content, whereas bark samples exhibited greater compositional variability and higher fixed carbon and ash contents. In contrast, oil shale was characterized by a high mineral matter content dominated by Ca and a comparatively low organic-carbon fraction.

TGA revealed predominantly additive thermal decomposition behavior of biomass and oil shale blends, whereas fixed-bed experiments showed clear synergistic interactions, demonstrating that their manifestation depends on the experimental scale. Co-gasification behavior was strongly feedstock-dependent, and the most pronounced synergistic effects were observed for bark blends. These results highlight the importance of feedstock selection for enhancing CO production during CO_2 gasification. The interaction effects were expressed primarily through enhanced CO formation, while H_2 and CH_4 showed limited evidence of systematic nonadditive behavior. PineB blends exhibited the strongest combined evidence of enhanced gasification, with increased CO formation accompanied by lower residue yield than predicted by the additive model. In particular, addition of 10% oil shale afforded a CO concentration of up to 16.7 vol%, exceeding the additive-model predictions. In contrast, wood samples exhibited largely additive or inhibitory behavior. Uncertainty analysis further confirmed that the observed CO enhancements in bark blends exceeded experimental variability and represented measurable synergistic behavior.

The feedstock-dependent response was associated with differences in both carbon availability and mineral composition. Bark samples generally contained more fixed carbon and higher concentrations of inherent AAEMs than the corresponding wood fractions. The relatively high Ca and K contents of bark provide a plausible basis for enhanced char–CO_2 conversion, while literature evidence suggests that inherently associated AAEMs may be particularly effective because of their close contact and dispersion within the carbon matrix. OS provided an additional mineral contribution, particularly through Ca-containing phases. The formation of CaO during the pyrolysis stage is especially relevant, as CaO can promote CO_2 chemisorption and participate in

oxygen-transfer mechanisms during char gasification. Overall, the observed behavior is consistent with a combined mineral-mediated effect involving biomass-derived AAEMs and OS-derived mineral species, although their individual contributions could not be distinguished experimentally.

The comparison between TGA and fixed-bed experiments further indicates that the experimental environment influences how strongly nonadditive effects are expressed. Despite the more uniform thermal conditions in the TGA, non-additive effects were more clearly observed in the fixed-bed reactor. The larger sample mass and different bed environment may increase opportunities for feedstock interactions, while also introducing greater thermal gradients that can affect the extent of solid conversion.

This study establishes a compositional baseline for Estonian woody biomass and advances the understanding of feedstock-dependent interactions during biomass and oil shale co-gasification in CO_2. It demonstrates that oil shale addition can enhance biomass gasification, but the effect is not uniform and depends on both biomass characteristics and the experimental environment. These findings provide a useful basis for selecting suitable biomass feedstocks to promote the production of CO-rich producer gas. The findings provide a basis for targeted mechanistic and kinetic studies, optimization of feedstock combinations and process conditions, and, ultimately, evaluation of the potential for scale-up to larger co-gasification systems. More broadly, the results support further investigation of biomass and oil shale co-gasification as a potential alternative pathway for resource utilization.

The proposed mechanistic interpretations were inferred from experimental observations and feedstock characteristics rather than directly verified. Further mechanistic studies, including multirate experiments and selective demineralization, are therefore needed to distinguish intrinsic catalytic effects from structural and reactor-related influences.

Future work should also explore alternative gasification atmospheres, particularly combined CO_2–steam systems, to assess their influence on gas composition, carbon conversion, and potential synergetic effects. The introduction of steam may alter gasification pathways by promoting gas-phase and heterogeneous reactions, potentially enhancing gas production and increasing the H_2 concentration in the producer gas.

A more complete characterization of the product distribution would also be valuable. Separating pyrolysis and gasification product streams and extending the analysis to tar formation could provide further insight into stage-specific reaction pathways and the influence of oil shale on biomass conversion. Finally, integrating experimental results with kinetic and equilibrium modeling could improve the understanding and prediction of nonadditive behavior.

List of Figures

Figure 1. Schematic of the drop-in batch reactor (Paper I)..... 28
Figure 2. Schematic of the fixed-bed reactor (Paper III) 29
Figure 3. Dispersion of wood and bark samples based on the principal component analysis (PCA) from 27 variables (autoscaled) (Paper II); B, bark; W, wood; F1, principal component 1; F2, principal component 2..... 32
Figure 4. PCA loading plot showing the relationships between BM properties and elemental composition variables (Paper II); VM, volatile matter; H, hydrogen; O, oxygen; GCV, gross calorific value; C, carbon; FC, fixed carbon 33
Figure 5. Mass loss curves of natural feedstocks (Paper III) 35
Figure 6. TGA–MS analysis of the same OS under N_2 atmosphere, showing mass change and CO_2 evolution (m/z = 44). The data are obtained from a repeat experiment performed under the same conditions as in Paper I..... 36
Figure 7. OS decomposition in N_2 and CO_2 atmospheres [95] 36
Figure 8. Comparison of experimental and calculated curves of TGA (Paper III)..... 37
Figure 9. Mass loss curves with the simultaneous evaporation of m/z 2 indicating evaporation of H_2 (Paper III) 38
Figure 10. Gas concentrations and corresponding calculated values during gasification (Paper III)..... 40
Figure 11. Solid residue yield and BET surface area of OS and BM blends obtained in the fixed-bed reactor (experimental data from Paper III; calculated SSA values and residue yields added for comparison) 43

List of Tables

Table 1. Main reactions in the BM and OS gasification process [31], [84], [85] 19
Table 2. Summary of previous studies on OS and BM co-processing 23
Table 3. Ultimate and proximate analyses for the BM and OS samples (Paper III) 34
Table 4. Inorganic elements of the fuels (ppm db) (Paper III) 34
Table 5. Producer gas composition of BM and OS feedstocks (mean ± standard deviation) 39
Table 6. Experimental and calculated CO concentrations for BM and OS blends with propagated uncertainties..... 41
Table 7. Residue yield and BET surface area of gasification residues..... 42

References

[1] International Energy Agency, “Estonia 2023. Energy Policy Review,” 2023. [Online]. Available: www.iea.org

[2] V. Oja, R. Rooleht, and Z. S. Baird, “Physical and thermodynamic properties of kukersite pyrolysis shale oil: Literature review,” *Oil Shale*, vol. 33, no. 2, pp. 184–197, 2016, doi: 10.3176/OIL.2016.2.06.

[3] O. Järvik and V. Oja, “Molecular Weight Distributions and Average Molecular Weights of Pyrolysis Oils from Oil Shales: Literature Data and Measurements by Size Exclusion Chromatography (SEC) and Atmospheric Solids Analysis Probe Mass Spectroscopy (ASAP MS) for Oils from Four D…,” *Energy and Fuels*, vol. 31, no. 1, pp. 328–339, Jan. 2016, doi: 10.1021/ACS.ENERGYFUELS.6B02452.

[4] J. Kann, A. Elenurm, I. Rohtla, N. Golubev, A. Kaidalov, and B. Kindorkin, “About Thermal Low-Temperature Processing of Oil Shale by Solid Heat Carrier Method,” *Oil Shale*, vol. 21, no. 3, 2004.

[5] J. Kann, A. Raukas, and A. Siirde, “About the gasification of kukersite oil shale,” *Oil Shale*, vol. 30, no. 2 SUPPL., pp. 283–293, 2013, doi: 10.3176/oil.2013.2S.08.

[6] M. Binder, M. Kraussler, M. Kuba, and M. Luisse, “IEA Bioenergy: Task 33. Hydrogen from biomass gasification,” 2018.

[7] S. V. Vassilev, D. Baxter, L. K. Andersen, and C. G. Vassileva, “An overview of the chemical composition of biomass,” *Fuel*, vol. 89, no. 5, pp. 913–933, May 2010, doi: 10.1016/j.fuel.2009.10.022.

[8] M. V. Gil, M. P. González-Vázquez, R. García, F. Rubiera, and C. Pevida, “Assessing the influence of biomass properties on the gasification process using multivariate data analysis,” *Energy Convers. Manag.*, vol. 184, pp. 649–660, 2019, doi: 10.1016/j.enconman.2019.01.093.

[9] M. P. Kannan and G. N. Richards, “Gasification of biomass chars in carbon dioxide: dependence of gasification rate on the indigenous metal content,” *Fuel*, vol. 69, no. 6, pp. 747–753, Jun. 1990, doi: 10.1016/0016-2361(90)90041-N.

[10] A. Nzihou, B. Stanmore, and P. Sharrock, “A review of catalysts for the gasification of biomass char, with some reference to coal,” *Energy*, vol. 58, pp. 305–317, Sep. 2013, doi: 10.1016/j.energy.2013.05.057.

[11] M. Koel, “Estonian oil shale,” Oil Shale. Accessed: Dec. 02, 2025. [Online]. Available: https://www.kirj.ee/public/oilshale/Est-OS.htm

[12] A. Abdalazeez, T. Li, W. Wang, and S. Abuelgasim, “A brief review of CO2 utilization for alkali carbonate gasification and biomass/coal co-gasification: Reactivity, products and process,” *Journal of CO2 Utilization*, vol. 43, p. 101370, Jan. 2021, doi: 10.1016/j.jcou.2020.101370.

[13] Z. He *et al.*, “The enhanced rich H2 from co-gasification of torrefied biomass and low rank coal: The comparison of dry/wet torrefaction, synergetic effect and prediction,” *Fuel*, vol. 287, p. 119473, Mar. 2021, doi: 10.1016/j.fuel.2020.119473.

[14] S. Tong *et al.*, “Gas-pressurized torrefaction of biomass wastes: Co-gasification of gas-pressurized torrefied biomass with coal,” *Bioresour. Technol.*, vol. 321, p. 124505, Feb. 2021, doi: 10.1016/j.biortech.2020.124505.

[15] Y. Zhang, Y. Zheng, M. Yang, and Y. Song, “Effect of fuel origin on synergy during co-gasification of biomass and coal in CO2,” *Bioresour. Technol.*, vol. 200, no. 1, pp. 789–794, Jan. 2016, doi: 10.1016/j.biortech.2015.10.076.

[16] D. Mallick, P. Mahanta, and V. Suryakant, “Co-gasification of coal and biomass blends : Chemistry and engineering,” *Fuel*, vol. 204, pp. 106–128, 2017, doi: 10.1016/j.fuel.2017.05.006.

[17] IEA Bioenergy, “Implementation of bioenergy in Estonia - Country Report,” 2021. [Online]. Available: https://www.keskkonnaagentuur.ee/sites/default/files/elfinder/article_files/puidubilanss_2017_0.pdf

[18] A. Ramos, E. Monteiro, V. Silva, and A. Rouboa, “Co-gasification and recent developments on waste-to-energy conversion: A review,” *Renewable and Sustainable Energy Reviews*, vol. 81, pp. 380–398, Jan. 2018, doi: 10.1016/J.RSER.2017.07.025.

[19] J. Wei *et al.*, “A review on reactivity characteristics and synergy behavior of biomass and coal Co-gasification,” *Int. J. Hydrogen Energy*, vol. 46, no. 33, pp. 17116–17132, 2021, doi: 10.1016/j.ijhydene.2021.02.162.

[20] Z. Yang *et al.*, “Recent advances in co-thermochemical conversions of biomass with fossil fuels focusing on the synergistic effects,” *Renewable and Sustainable Energy Reviews*, vol. 103, pp. 384–398, Apr. 2019, doi: 10.1016/J.RSER.2018.12.047.

[21] B. Chen *et al.*, “Study of the Co-pyrolysis characteristics of oil shale with wheat straw based on the hierarchical collection,” *Energy*, vol. 239, p. 122144, Jan. 2022, doi: 10.1016/J.ENERGY.2021.122144.

[22] Mais Baqain, “Oil Shale Oxyfuel CFB Combustion,” 2024, doi: 10.23658/taltech.26/2024.

[23] A. Lyons Cerón, “Co-Pyrolysis of Biomass and Oil Shale,” 2024, doi: 10.23658/taltech.27/2024.

[24] A. Konist, T. Pihu, D. Neshumayev, and I. Külaots, “Low grade fuel - oil shale and biomass co-combustion in CFB boiler,” *Oil Shale*, vol. 30, no. 2 SUPPL., pp. 294–304, 2013, doi: 10.3176/oil.2013.2S.09.

[25] G. Collodi, G. Azzaro, N. Ferrari, and S. Santos, “Demonstrating Large Scale Industrial CCS through CCU – A Case Study for Methanol Production,” *Energy Procedia*, vol. 114, pp. 122–138, Jul. 2017, doi: 10.1016/J.EGYPRO.2017.03.1155.

[26] P. J. Inocencio-García, J. C. Solarte-Toro, and C. A. Cardona Alzate, “Experimental comparison of CO2-assisted and conventional downdraft biomass gasification of corn cob and pine wood,” *Environmental Science and Pollution Research*, vol. 33, pp. 1971–1991, Feb. 2025, doi: 10.1007/s11356-025-36909-z.

[27] L. Zhang, J. Huang, Y. Fang, and Y. Wang, “Gasification Reactivity and Kinetics of Typical Chinese Anthracite Chars with Steam and CO2,” *Energy and Fuels*, vol. 20, no. 3, pp. 1201–1210, May 2006, doi: 10.1021/EF050343O.

[28] D. P. Ye, J. B. Agnew, and D. K. Zhang, “Gasification of a South Australian low-rank coal with carbon dioxide and steam: kinetics and reactivity studies,” *Fuel*, vol. 77, no. 11, pp. 1209–1219, Sep. 1998, doi: 10.1016/S0016-2361(98)00014-3.

[29] M. Perander *et al.*, “Catalytic effect of Ca and K on CO2 gasification of spruce wood char,” *Fuel*, vol. 150, pp. 464–472, Jun. 2015, doi: 10.1016/j.fuel.2015.02.062.

[30] I. Stupak *et al.*, “Sustainable utilisation of forest biomass for energy—Possibilities and problems: Policy, legislation, certification, and recommendations and guidelines in the Nordic, Baltic, and other European countries,” *Biomass Bioenergy*, vol. 31, no. 10, pp. 666–684, Oct. 2007, doi: 10.1016/J.BIOMBIOE.2007.06.012.

[31] Prabir. Basu, *Biomass gasification and pyrolysis : practical design and theory*. Academic Press, 2010.

[32] N. Van Minh *et al.*, "Biomass gasification for hydrogen-rich syngas production: Feedstock engineering, reactor design and sustainability assessment," *Biomass Bioenergy*, vol. 213, p. 109386, Oct. 2026, doi: 10.1016/J.BIOMBIOE.2026.109386.

[33] J. S. Tumuluru, S. Sokhansanj, C. T. Wright, R. D. Boardman, and N. A. Yancey, "A review on biomass classification and composition, co-firing issues and pretreatment methods," *American Society of Agricultural and Biological Engineers Annual International Meeting 2011, ASABE 2011*, vol. 3, pp. 2053–2083, 2011, doi: 10.13031/2013.37191.

[34] Keskkonnaportaal, "EESTI METSAD - Statistiline metsainvesteerimine 2024," 2024.

[35] H. Yang, R. Yan, H. Chen, D. H. Lee, and C. Zheng, "Characteristics of hemicellulose, cellulose and lignin pyrolysis," *Fuel*, vol. 86, no. 12–13, pp. 1781–1788, Aug. 2007, doi: 10.1016/J.FUEL.2006.12.013.

[36] S. V. Vassilev, C. G. Vassileva, and V. S. Vassilev, "Advantages and disadvantages of composition and properties of biomass in comparison with coal: An overview," *Fuel*, vol. 158, pp. 330–350, Oct. 2015, doi: 10.1016/J.FUEL.2015.05.050.

[37] AECOM & Fichtner Consulting Engineers, "Advanced Gasification Technologies – Review and Benchmarking: Review of current status of advanced gasification technologies - Task report 2," 2021.

[38] J. Werkelin, D. Lindberg, D. Boström, B. J. Skrifvars, and M. Hupa, "Ash-forming elements in four Scandinavian wood species part 3: Combustion of five spruce samples," *Biomass Bioenergy*, vol. 35, no. 1, pp. 725–733, Jan. 2011, doi: 10.1016/j.biombioe.2010.10.010.

[39] H. De Lasa, E. Salaices, J. Mazumder, and R. Lucky, "Catalytic Steam Gasification of Biomass: Catalysts, Thermodynamics and Kinetics," *Chem. Rev.*, vol. 111, no. 9, pp. 5404–5433, Sep. 2011, doi: 10.1021/CR200024W.

[40] L. Cao *et al.*, "Biorenewable hydrogen production through biomass gasification: A review and future prospects," *Environ. Res.*, vol. 186, p. 109547, Jul. 2020, doi: 10.1016/J.ENVRES.2020.109547.

[41] X. M. Jiang, X. X. Han, and Z. G. Cui, "Progress and recent utilization trends in combustion of Chinese oil shale," *Prog. Energy Combust. Sci.*, vol. 33, no. 6, pp. 552–579, Dec. 2007, doi: 10.1016/J.PECS.2006.06.002.

[42] Z. Kang, Y. Zhao, and D. Yang, "Review of oil shale in-situ conversion technology," *Appl. Energy*, vol. 269, p. 115121, Jul. 2020, doi: 10.1016/J.APENERGY.2020.115121.

[43] M. Bachmann, R. Ilp, and T. Metusala, *Kukersite and mudstone: the story of our energy*. Motor, 2014. Accessed: Dec. 19, 2025. [Online]. Available: https://www.ester.ee/record=b3068808*est

[44] E. Väli, I. Valgma, and E. Reinsalu, "Usage of Estonian Oil Shale," *Oil Shale*, vol. 25, no. 2s, p. 101, 2008, doi: 10.3176/oil.2008.2s.02.

[45] R. Kuusik, M. Uibu, K. Kirsimäe, R. Mõtlep, and T. Meriste, "Open-air deposition of Estonian oil shale ash: Formation, state of art, problems and prospects for the abatement of environmental impact," *Oil Shale*, vol. 29, no. 4, pp. 376–403, 2012, doi: 10.3176/oil.2012.4.08.

[46] J. Speight, “Shale oil and gas production processes,” *Shale Oil and Gas Production Processes*, pp. 1–1031, Jan. 2019, doi: 10.1016/C2015-0-02189-X.

[47] J. O. Jaber, S. D. Probert, P. T. Williams, and M. Tahat, “Gasification potential and kinetics of Jordanian oil shales using CO2 as the reactant gas,” *Energy Sources*, vol. 22, no. 6, pp. 573–585, 2000, doi: 10.1080/00908310050013785.

[48] C. S. M. de Lecea, M. Almela-Alarcón, and A. Linares-Solano, “Calcium-catalysed carbon gasification in CO2 and steam,” *Fuel*, vol. 69, no. 1, pp. 21–27, Jan. 1990, doi: 10.1016/0016-2361(90)90253-M.

[49] R. Qudaih, I. Talab, S. Syed, I. Janajreh, and M. Hamdan, “Material characterization and gasification of Jordanian oil shale,” *International Journal of Energy, Environment and Economics*, vol. 19, no. 4, pp. 339–354, 2013.

[50] L. Tang *et al.*, “CO2 gasification and pyrolysis reactivity evaluation of oil shale,” *Energy Procedia*, vol. 158, pp. 1694–1699, 2019, doi: 10.1016/J.EGYPRO.2019.01.394.

[51] C. Higman and M. van der Burgt, *Gasification. 2nd. ed. Chapter 2. The Thermodynamics of Gasification*. Gulf Professional Publishing, 2003. doi: 10.1016/B978-075067707-3/50002-4.

[52] M. Wang *et al.*, “Brief review on petroleum coke and biomass/coal co-gasification: Syngas production, reactivity characteristics, and synergy behavior,” *Fuel*, vol. 304, p. 121517, Nov. 2021, doi: 10.1016/J.FUEL.2021.121517.

[53] S. Mariyam, M. Shahbaz, T. Al-Ansari, H. R. Mackey, and G. McKay, “A critical review on co-gasification and co-pyrolysis for gas production,” *Renewable and Sustainable Energy Reviews*, vol. 161, p. 112349, Jun. 2022, doi: 10.1016/J.RSER.2022.112349.

[54] Donald L. Klass, *Biomass for Renewable Energy, Fuels, and Chemicals*. Elsevier, 1998.

[55] I. Narváez, A. Orío, M. P. Aznar, and J. Corella, “Biomass gasification with air in an atmospheric bubbling fluidized bed. Effect of six operational variables on the quality of the produced raw gas,” *Ind. Eng. Chem. Res.*, vol. 35, no. 7, pp. 2110–2120, 1996, doi: 10.1021/ie9507540.

[56] B. Yan *et al.*, “Insights into the role of gasification media in gasification process: Principles, advantages, bottlenecks and prospects,” *Appl. Energy*, vol. 409, no. 3, p. 127543, Apr. 2026, doi: 10.1016/j.apenergy.2026.127543.

[57] M. L. Valderrama Rios, A. M. González, E. E. S. Lora, and O. A. Almazán del Olmo, “Reduction of tar generated during biomass gasification: A review,” *Biomass Bioenergy*, vol. 108, pp. 345–370, Jan. 2018, doi: 10.1016/j.biombioe.2017.12.002.

[58] J. Shen, X. S. Wang, M. Garcia-Perez, D. Mourant, M. J. Rhodes, and C. Z. Li, “Effects of particle size on the fast pyrolysis of oil mallee woody biomass,” *Fuel*, vol. 88, no. 10, pp. 1810–1817, Oct. 2009, doi: 10.1016/J.FUEL.2009.05.001.

[59] V. Seebauer, J. Petek, and G. Staudinger, “Effects of particle size, heating rate and pressure on measurement of pyrolysis kinetics by thermogravitics analysis,” *Fuel*, vol. 76, no. 13, pp. 1277–1282, Oct. 1997, doi: 10.1016/S0016-2361(97)00106-3.

[60] A. L. Cerón, A. Konist, H. Lees, and O. Järvik, “Effect of woody biomass gasification process conditions on the composition of the producer gas,” *Sustainability (Switzerland)*, vol. 13, no. 21, 2021, doi: 10.3390/su132111763.

[61] Y. Gao *et al.*, "Syngas Production from Biomass Gasification: Influences of Feedstock Properties, Reactor Type, and Reaction Parameters," *ACS Omega*, vol. 8, no. 35, pp. 31620–31631, Sep. 2023, doi: 10.1021/acsomega.3c03050.

[62] X. Li *et al.*, "Catalytic effects of key compositions in biomass ashes on coal gasification reactivity and structural evolution characteristic during gasification process," *J. Clean. Prod.*, vol. 499, no. 4, p. 145197, Mar. 2025, doi: 10.1016/j.jclepro.2025.145197.

[63] H. Song *et al.*, "Recent development of biomass gasification for H2 rich gas production," *Applications in Energy and Combustion Science*, vol. 10, p. 100059, 2022, doi: 10.1016/j.jaecs.2022.100059.

[64] S. Wang, D. Kong, R. Shan, J. Gu, H. Yuan, and Y. Chen, "Comparative study on the effect of H2O/air/CO2 on the gasification results of wheat straw," *Biomass Bioenergy*, vol. 197, p. 107807, Jun. 2025, doi: 10.1016/J.BIOMBIOE.2025.107807.

[65] N. Mahinpey and A. Gomez, "Review of gasification fundamentals and new findings: Reactors, feedstock, and kinetic studies," *Chem. Eng. Sci.*, vol. 148, pp. 14–31, Jul. 2016, doi: 10.1016/j.ces.2016.03.037.

[66] N. Sadhwani, S. Adhikari, and M. R. Eden, "Biomass Gasification Using Carbon Dioxide: Effect of Temperature, CO2/C Ratio, and the Study of Reactions Influencing the Process," *Ind. Eng. Chem. Res.*, vol. 55, no. 10, pp. 2883–2891, Mar. 2016, doi: 10.1021/acs.iecr.5b04000.

[67] J. Gil, J. Corella, M. P. Aznar, and M. A. Caballero, "Biomass gasification in atmospheric and bubbling fluidized bed: Effect of the type of gasifying agent on the product distribution," *Biomass Bioenergy*, vol. 17, no. 5, pp. 389–403, Nov. 1999, doi: 10.1016/S0961-9534(99)00055-0.

[68] A. G. Collot, Y. Zhuo, D. R. Dugwell, and R. Kandiyoti, "Co-pyrolysis and co-gasification of coal and biomass in bench-scale fixed-bed and fluidized bed reactors," *Fuel*, vol. 78, no. 6, pp. 667–679, 1999, doi: 10.1016/S0016-2361(98)00202-6.

[69] M. J. Antal and M. Grønli, "The Art, Science, and Technology of Charcoal Production†," *Ind. Eng. Chem. Res.*, vol. 42, no. 8, pp. 1619–1640, Apr. 2003, doi: 10.1021/IE0207919.

[70] H. Risnes *et al.*, "Calcium addition in straw gasification," *Fuel*, vol. 82, no. 6, pp. 641–651, Apr. 2003, doi: 10.1016/S0016-2361(02)00337-X.

[71] P. Lahijani, Z. A. Zainal, M. Mohammadi, and A. R. Mohamed, "Conversion of the greenhouse gas CO2 to the fuel gas CO via the Boudouard reaction: A review," *Renewable and Sustainable Energy Reviews*, vol. 41, pp. 615–632, 2015, doi: 10.1016/J.RSER.2014.08.034.

[72] X. Liu *et al.*, "Combined experimental and theoretical analysis of stage-dependent gasification kinetics and carbon structure evolution of char in CO2 atmosphere," *Carbon N. Y.*, vol. 254, p. 121500, Apr. 2026, doi: 10.1016/J.CARBON.2026.121500.

[73] A. Molina, A. Montoya, and F. Mondragón, "CO2 strong chemisorption as an estimate of coal char gasification reactivity," *Fuel*, vol. 78, no. 8, pp. 971–977, Jun. 1999, doi: 10.1016/S0016-2361(98)00220-8.

[74] S. Zhang, Y. Xu, X. Bie, Q. Li, Y. Zhang, and H. Zhou, "Mechanisms in CO2 gasification and co-gasification of combustible solid waste: A critical review," *Gas*

Science and Engineering, vol. 128, p. 205368, Aug. 2024, doi: 10.1016/J.JGSCE.2024.205368.

[75] J. Wang *et al.*, "Mechanistic insights into size-dependent biochar gasification and AAEM-Catalyzed reactivity via in-situ Raman spectroscopy," *Fuel*, vol. 425, p. 139496, Dec. 2026, doi: 10.1016/J.FUEL.2026.139496.

[76] J. Cai *et al.*, "Relationships between char CO2 gasification reactivity and char physicochemical properties from biomasses with different leaching pretreatments," *Biomass Bioenergy*, vol. 210, no. 1, p. 109131, Jul. 2026, doi: 10.1016/j.biombioe.2026.109131.

[77] P. Liu *et al.*, "CO2 assisted steam gasification for hydrogen-rich syngas from rice straw: Evolution of carbon structure and its effect," *Green Energy and Resources*, vol. 4, no. 2, p. 100175, Jun. 2026, doi: 10.1016/J.GERR.2026.100175.

[78] S. H. Cho, J. Lee, K. H. Kim, Y. J. Jeon, and E. E. Kwon, "Carbon dioxide assisted co-pyrolysis of coal and ligno-cellulosic biomass," *Energy Convers. Manag.*, vol. 118, pp. 243–252, 2016, doi: 10.1016/j.enconman.2016.03.093.

[79] S. Mozaffari, O. Järvik, and Z. S. Baird, "Effect of N2 and CO2 on shale oil from pyrolysis of Estonian oil shale," *International Journal of Coal Preparation and Utilization*, vol. 42, no. 10, pp. 2908–2922, 2022, doi: 10.1080/19392699.2021.1914025.

[80] J. Kramb, A. Gómez-Barea, N. DeMartini, H. Romar, T. R. K. C. Doddapaneni, and J. Konttinen, "The effects of calcium and potassium on CO2 gasification of birch wood in a fluidized bed," *Fuel*, vol. 196, pp. 398–407, 2017, doi: 10.1016/j.fuel.2017.01.101.

[81] H. C. Butterman and M. J. Castaldi, "CO2 as a carbon neutral fuel source via enhanced biomass gasification," *Environ. Sci. Technol.*, vol. 43, no. 23, pp. 9030–9037, Dec. 2009, doi: 10.1021/es901509n.

[82] S. Mozaffari, O. Järvik, and Z. S. Baird, "Composition of gas from pyrolysis of Estonian oil shale with various sweep gases," *Oil Shale*, vol. 38, no. 3, pp. 215–227, 2021, doi: 10.3176/OIL.2021.3.03.

[83] X. Fang-Fang, W. Ze, L. Wei-Gang, and S. Wen-Li, "Study on thermal conversion of huadian oil shale under N2 and CO2 atmospheres," *Oil Shale*, vol. 27, no. 4, pp. 309–320, 2010, doi: 10.3176/oil.2010.4.04.

[84] Z. Wang, K. G. Burra, T. Lei, and A. K. Gupta, "Co-gasification characteristics of waste tire and pine bark mixtures in CO2 atmosphere," *Fuel*, vol. 257, p. 116025, Dec. 2019, doi: 10.1016/J.FUEL.2019.116025.

[85] T. Detchusananard, K. Im-orb, P. Ponpesh, and A. Arpornwichanop, "Biomass gasification integrated with CO2 capture processes for high-purity hydrogen production: Process performance and energy analysis," *Energy Convers. Manag.*, vol. 171, no. March, pp. 1560–1572, 2018, doi: 10.1016/j.enconman.2018.06.072.

[86] P. Ollero, A. Serrera, R. Arjona, and S. Alcantarilla, "Diffusional effects in TGA gasification experiments for kinetic determination," *Fuel*, vol. 81, no. 15, pp. 1989–2000, Oct. 2002, doi: 10.1016/S0016-2361(02)00126-6.

[87] J. M. Calo and M. T. Perkins, "A heterogeneous surface model for the 'steady-state' kinetics of the boudouard reaction," *Carbon N. Y.*, vol. 25, no. 3, pp. 395–407, Jan. 1987, doi: 10.1016/0008-6223(87)90011-X.

[88] Y. H. Chan, S. N. F. Syed Abdul Rahman, H. M. Lahuri, and A. Khalid, "Recent progress on CO-rich syngas production via CO2 gasification of various wastes: A

critical review on efficiency, challenges and outlook," *Environmental Pollution*, vol. 278, Jun. 2021, doi: 10.1016/J.ENVPOL.2021.116843.

[89] V. Nemanova, A. Abedini, T. Liliedahl, and K. Engvall, "Co-gasification of petroleum coke and biomass," *Fuel*, vol. 117, no. PART A, pp. 870–875, Jan. 2014, doi: 10.1016/J.FUEL.2013.09.050.

[90] D. Sutton, B. Kelleher, and J. R. H. Ross, "Review of literature on catalysts for biomass gasification," *Fuel Processing Technology*, vol. 73, no. 3, pp. 155–173, Nov. 2001, doi: 10.1016/S0378-3820(01)00208-9.

[91] D. Dayton, "A Review of the Literature on Catalytic Biomass Tar Destruction: Milestone Completion Report," 2002, Accessed: Oct. 28, 2025. [Online]. Available: http://www.osti.gov/bridge

[92] S. Fang *et al.*, "High-yield hydrogen production via dolomite/ilmenite synergistic catalytic gasification in a fluidized bed reactor," *Fuel*, vol. 425, p. 139486, Dec. 2026, doi: 10.1016/J.FUEL.2026.139486.

[93] N. Gao, M. Śliz, C. Quan, A. Bieniek, and A. Magdziarz, "Biomass CO2 gasification with CaO looping for syngas production in a fixed-bed reactor," *Renew. Energy*, vol. 167, pp. 652–661, Apr. 2021, doi: 10.1016/j.renene.2020.11.134.

[94] J. M. Valverde, A. Perejon, S. Medina, and L. A. Perez-Maqueda, "Thermal decomposition of dolomite under CO2: insights from TGA and in situ XRD analysis," *Physical Chemistry Chemical Physics*, vol. 17, no. 44, pp. 30162–30176, Nov. 2015, doi: 10.1039/c5cp05596b.

[95] Tallinna Tehnikaülikool and Tartu Ülikool, "Innovaatiliste ja keskkonnasõbralike põlevkivi või selle saaduste töötlemise tehnoloogiate arendamine (RITA1/01-60)," 2021.

[96] P. Lahijani, M. Mohammadi, and A. R. Mohamed, "Investigation of synergy and inhibition effects during co-gasification of tire char and biomass in CO2 environment," *Biomass Convers. Biorefin.*, vol. 12, no. 6, pp. 2229–2241, Oct. 2020, doi: 10.1007/S13399-020-01028-X.

[97] H. Wu, K. Yip, F. Tian, Z. Xie, and C. Z. Li, "Evolution of Char Structure during the Steam Gasification of Biochars Produced from the Pyrolysis of Various Mallee Biomass Components," *Ind. Eng. Chem. Res.*, vol. 48, no. 23, pp. 10431–10438, 2009, doi: 10.1021/IE901025D.

[98] L. R. Radović, P. L. Walker, and R. G. Jenkins, "Importance of carbon active sites in the gasification of coal chars," *Fuel*, vol. 62, no. 7, pp. 849–856, Jul. 1983, doi: 10.1016/0016-2361(83)90041-8.

[99] C. Schneider, S. Rincón Prat, and T. Kolb, "Determination of active sites during gasification of biomass char with CO2 using temperature-programmed desorption. Part 1: Methodology & desorption spectra," *Fuel*, vol. 267, p. 116726, May 2020, doi: 10.1016/J.FUEL.2019.116726.

[100] J. Yu, Q. Guo, Y. Gong, L. Ding, J. Wang, and G. Yu, "A review of the effects of alkali and alkaline earth metal species on biomass gasification," *Fuel Processing Technology*, vol. 214, no. 2, p. 106723, Apr. 2021, doi: 10.1016/j.fuproc.2021.106723.

[101] S. G. Chen and R. T. Yang, "Unified Mechanism of Alkali and Alkaline Earth Catalyzed Gasification Reactions of Carbon by CO2 and H2O," *Energy & Fuels*, vol. 11, no. 2, pp. 421–427, Mar. 1997, doi: 10.1021/EF960099O.

[102] D. W. Mckee, “GASIFICATION OF GRAPHITE IN CARBON DIOXIDE AND WATER VAPOR-THE CATALYTIC EFFECTS OF ALKALI METAL SALTS,” *Carbon N. Y.*, vol. 20, no. 1, pp. 59–66, 1982.

[103] M. Shahbaz, S. Yusup, A. Inayat, D. O. Patrick, and M. Ammar, “The influence of catalysts in biomass steam gasification and catalytic potential of coal bottom ash in biomass steam gasification: A review,” *Renewable and Sustainable Energy Reviews*, vol. 73, pp. 468–476, 2017, doi: 10.1016/j.rser.2017.01.153.

[104] M. Hervy *et al.*, “Evolution of dolomite composition and reactivity during biomass gasification,” *Appl. Catal. A Gen.*, vol. 572, pp. 97–106, Feb. 2019, doi: 10.1016/J.APCATA.2018.12.014.

[105] X. Lin, C. Li, X. He, J. Dai, D. Xu, and Y. Wang, “Study on the mechanism of calcium catalyzed CO2 gasification of lignite,” *Fuel Processing Technology*, vol. 213, p. 106689, Mar. 2021, doi: 10.1016/J.FUPROC.2020.106689.

[106] H. Liu *et al.*, “Catalytic performance of novel Ni catalysts supported on SiC monolithic foam in carbon dioxide reforming of methane to synthesis gas,” *Catal. Commun.*, vol. 9, no. 1, pp. 51–54, Jan. 2008, doi: 10.1016/J.CATCOM.2007.05.002.

[107] M. Faizan and H. Song, “Critical review on catalytic biomass gasification: State-of-Art progress, technical challenges, and perspectives in future development,” *J. Clean. Prod.*, vol. 408, p. 137224, Jul. 2023, doi: 10.1016/J.JCLEPRO.2023.137224.

[108] D. Li, Y. Nakagawa, and K. Tomishige, “Development of Ni-based catalysts for steam reforming of tar derived from biomass pyrolysis,” *Chinese Journal of Catalysis*, vol. 33, no. 4, pp. 583–594, 2012, doi: 10.1016/s1872-2067(11)60359-8.

[109] J. Li, K. R. G. Burra, Z. Wang, X. Liu, and A. K. Gupta, “Co-gasification of high-density polyethylene and pretreated pine wood,” *Appl. Energy*, vol. 285, p. 116472, Mar. 2021, doi: 10.1016/j.apenergy.2021.116472.

[110] D. Feng, Y. Zhao, Y. Zhang, H. Xu, L. Zhang, and S. Sun, “Catalytic mechanism of ion-exchanging alkali and alkaline earth metallic species on biochar reactivity during CO2/H2O gasification,” *Fuel*, vol. 212, pp. 523–532, Jan. 2018, doi: 10.1016/J.FUEL.2017.10.045.

[111] H. Jiang *et al.*, “Preliminary Study on Copyrolysis of Spent Mushroom Substrate as Biomass and Huadian Oil Shale,” *Energy and Fuels*, vol. 30, no. 8, pp. 6342–6349, Aug. 2016, doi: 10.1021/ACS.ENERGYFUELS.6B01085.

[112] J. Yu, W. Xia, C. Areeprasert, L. Ding, K. Umeki, and G. Yu, “Catalytic effects of inherent AAEM on char gasification: A mechanism study using in-situ Raman,” *Energy*, vol. 238, p. 122074, Jan. 2022, doi: 10.1016/J.ENERGY.2021.122074.

[113] K. Wang, J. Zhang, B. H. Shanks, and R. C. Brown, “The deleterious effect of inorganic salts on hydrocarbon yields from catalytic pyrolysis of lignocellulosic biomass and its mitigation,” *Appl. Energy*, vol. 148, pp. 115–120, Jun. 2015, doi: 10.1016/J.APENERGY.2015.03.034.

[114] Y. Huang *et al.*, “Effects of metal catalysts on CO2 gasification reactivity of biomass char,” *Biotechnol. Adv.*, vol. 27, no. 5, pp. 568–572, Sep. 2009, doi: 10.1016/J.BIOTECHADV.2009.04.013.

[115] P. Nanou, G. Van Rossum, W. P. M. Van Swaaij, and S. R. A. Kersten, “Evaluation of catalytic effects in gasification of biomass at intermediate temperature and pressure,” *Energy and Fuels*, vol. 25, no. 3, pp. 1242–1253, Mar. 2011, doi: 10.1021/EF101557B.

[116] D. Feng *et al.*, “Effects of K and Ca on reforming of model tar compounds with pyrolysis biochars under H2O or CO2,” *Chemical Engineering Journal*, vol. 306, pp. 422–432, Dec. 2016, doi: 10.1016/J.CEJ.2016.07.065.

[117] K. Mitsuoka, S. Hayashi, H. Amano, K. Kayahara, E. Sasaoaka, and M. A. Uddin, “Gasification of woody biomass char with CO2: The catalytic effects of K and Ca species on char gasification reactivity,” *Fuel Processing Technology*, vol. 92, no. 1, pp. 26–31, Jan. 2011, doi: 10.1016/j.fuproc.2010.08.015.

[118] T. Suzuki, H. Nakajima, N. Ikenaga, H. Oda, and T. Miyake, “Effect of mineral matters in biomass on the gasification rate of their chars,” *Biomass Convers. Biorefin.*, vol. 1, no. 1, pp. 17–28, Feb. 2011, doi: 10.1007/s13399-011-0006-2.

[119] A. Aho *et al.*, “Pyrolysis of pine and gasification of pine chars – Influence of organically bound metals,” *Bioresour. Technol.*, vol. 128, no. 2, pp. 22–29, Jan. 2013, doi: 10.1016/j.biortech.2012.10.093.

[120] A. Phounglamcheik *et al.*, “CO2 Gasification Reactivity of Char from High-Ash Biomass,” *ACS Omega*, vol. 6, no. 49, pp. 34115–34128, Dec. 2021, doi: 10.1021/acsomega.1c05728.

[121] L. Zhou, H. Zheng, K. Xiong, Y. Zhao, and S. Liu, “Comparative study on the co-gasification of coal and biomass: effects of pre-mixing versus separate pyrolysis on synergistic behaviors and kinetics,” *J. Anal. Appl. Pyrolysis*, vol. 196, p. 107748, Jun. 2026, doi: 10.1016/J.JAAP.2026.107748.

[122] Z. Chang, M. Chu, C. Zhang, S. Bai, H. Lin, and L. Ma, “Influence of inherent mineral matrix on the product yield and characterization from Huadian oil shale pyrolysis,” *J. Anal. Appl. Pyrolysis*, vol. 130, pp. 249–255, 2018, doi: 10.1016/j.jaap.2017.12.022.

[123] C. Dupont, T. Nocquet, J. A. Da Costa, and C. Verne-Tournon, “Kinetic modelling of steam gasification of various woody biomass chars: Influence of inorganic elements,” *Bioresour. Technol.*, vol. 102, no. 20, pp. 9743–9748, Oct. 2011, doi: 10.1016/J.BIORTECH.2011.07.016.

[124] P. Lahijani, G.D. Najafpour, and M. Mohammadi, “Influence of Inherent Alkali Content and Surface Area of Biomass Char on its CO 2 Gasification Reactivity,” *Iranica Journal of Energy and Environment*, vol. 8, pp. 1–5, 2017, doi: 10.5829/idosi.ijee.2017.08.01.01.

[125] G. Duman, M. A. Uddin, and J. Yanik, “The effect of char properties on gasification reactivity,” *Fuel Processing Technology*, vol. 118, pp. 75–81, Feb. 2014, doi: 10.1016/J.FUPROC.2013.08.006.

[126] A. C. A. Zahra, A. M. Y. W. Alahakoon, L. Zhu, T. Prakoso, A. Abudula, and G. Guan, “Biochar-assisted gasification of raw biomass: a review on the reactivity and synergistic effect on tar reforming,” *Resources Chemicals and Materials*, vol. 4, no. 3, p. 100115, Sep. 2025, doi: 10.1016/J.RECM.2025.100115.

[127] M. V. Gil, D. Casal, C. Pevida, J. J. Pis, and F. Rubiera, “Thermal behaviour and kinetics of coal/biomass blends during co-combustion,” *Bioresour. Technol.*, vol. 101, no. 14, pp. 5601–5608, 2010, doi: 10.1016/j.biortech.2010.02.008.

[128] L. Emami Taba, M. F. Irfan, W. A. M. Wan Daud, and M. H. Chakrabarti, “The effect of temperature on various parameters in coal, biomass and CO-gasification: A review,” *Renewable and Sustainable Energy Reviews*, vol. 16, no. 8, pp. 5584–5596, Oct. 2012, doi: 10.1016/j.rser.2012.06.015.

[129] M. Shahbaz, T. Al-Ansari, M. Inayat, S. A. Sulaiman, P. Parthasarathy, and G. McKay, “A critical review on the influence of process parameters in catalytic co-

gasification: Current performance and challenges for a future prospectus," *Renewable and Sustainable Energy Reviews*, vol. 134, p. 110382, Dec. 2020, doi: 10.1016/j.rser.2020.110382.

[130] I. I. Ahmed, N. Nipattummakul, and A. K. Gupta, "Characteristics of syngas from co-gasification of polyethylene and woodchips," *Appl. Energy*, vol. 88, no. 1, pp. 165–174, Jan. 2011, doi: 10.1016/J.APENERGY.2010.07.007.

[131] P. Yang *et al.*, "Synergistic effect of the cotton stalk and high-ash coal on gas production during co-pyrolysis/gasification," *Bioresour. Technol.*, vol. 336, p. 125336, 2021, doi: 10.1016/j.biortech.2021.125336.

[132] X. Liu, K. G. Burra, Z. Wang, J. Li, D. Che, and A. K. Gupta, "On deconvolution for understanding synergistic effects in co-pyrolysis of pinewood and polypropylene," *Appl. Energy*, vol. 279, p. 115811, Dec. 2020, doi: 10.1016/J.APENERGY.2020.115811.

[133] Q. Liu *et al.*, "High H2/CO ratio syngas production from chemical looping co-gasification of biomass and polyethylene with CaO/Fe2O3 oxygen carrier," *Energy Convers. Manag.*, vol. 199, p. 111951, Nov. 2019, doi: 10.1016/J.ENCONMAN.2019.111951.

[134] I. I. Ahmed and A. K. Gupta, "Kinetics of woodchips char gasification with steam and carbon dioxide," *Appl. Energy*, vol. 88, no. 5, pp. 1613–1619, May 2011, doi: 10.1016/j.apenergy.2010.11.007.

[135] K. Jayaraman, M. V. Kok, and I. Gokalp, "Pyrolysis, combustion and gasification studies of different sized coal particles using TGA-MS," *Appl. Therm. Eng.*, vol. 125, pp. 1446–1455, Oct. 2017, doi: 10.1016/J.APPLTHERMALENG.2017.07.128.

[136] M. Puig-Gamero, J. Lara-Díaz, J. L. Valverde, L. Sanchez-Silva, and P. Sánchez, "Dolomite effect on steam co-gasification of olive pomace, coal and petcoke: TGA-MS analysis, reactivity and synergistic effect," *Fuel*, vol. 234, pp. 142–150, Dec. 2018, doi: 10.1016/J.FUEL.2018.07.014.

[137] Y. C. Lin, J. Cho, G. A. Tompsett, P. R. Westmoreland, and G. W. Huber, "Kinetics and mechanism of cellulose pyrolysis," *Journal of Physical Chemistry C*, vol. 113, no. 46, pp. 20097–20107, 2009, doi: 10.1021/jp906702p.

[138] M. Puig-Gamero, Á. Alcazar-Ruiz, P. Sánchez, and L. Sanchez-Silva, "Binary Blends Versus Ternary Blends in Steam Cogasification by Means of TGA–MS: Reactivity and H2/CO Ratio," *Ind. Eng. Chem. Res.*, vol. 59, no. 28, pp. 12801–12811, Jul. 2020, doi: 10.1021/ACS.IECR.0C01399.

[139] A. Lyons Ceron, R. Ochieng, S. Sarker, O. Järvik, and A. Konist, "Co-Pyrolysis of Woody Biomass and Oil Shale—A Kinetics and Modelling Study," *Energies (Basel).*, vol. 17, no. 5, Feb. 2024, doi: 10.3390/EN17051055.

[140] A. Lyons Cerón and A. Konist, "Co-Pyrolysis of Woody Biomass and Oil Shale in a Batch Reactor in CO2, CO2-H2O, and Ar Atmospheres," *Energies (Basel).*, vol. 16, no. 7, Apr. 2023, doi: 10.3390/en16073145.

[141] Z. Hu, X. Ma, and L. Li, "The synergistic effect of co-pyrolysis of oil shale and microalgae to produce syngas," *Journal of the Energy Institute*, vol. 89, no. 3, pp. 447–455, Aug. 2016, doi: 10.1016/J.JOEI.2015.02.009.

[142] B. Chen, X. Han, M. Mu, and X. Jiang, "Studies of the Co-pyrolysis of Oil Shale and Wheat Straw," *Energy and Fuels*, vol. 31, no. 7, pp. 6941–6950, Jul. 2017, doi: 10.1021/ACS.ENERGYFUELS.7B00871.

[143] Z. Yu *et al.*, “Catalytic characteristics of the fast pyrolysis of microalgae over oil shale: Analytical Py-GC/MS study,” *Renew. Energy*, vol. 125, pp. 465–471, Sep. 2018, doi: 10.1016/J.RENENE.2018.02.136.

[144] I. Johannes, L. Tiikma, and H. Luik, “Synergy in co-pyrolysis of oil shale and pine sawdust in autoclaves,” *J. Anal. Appl. Pyrolysis*, vol. 104, no. 3, pp. 341–352, Nov. 2013, doi: 10.1016/j.jaap.2013.06.015.

[145] S. Cui, T. Yang, Y. Zhai, Y. Zhu, Z. Yu, and X. Kai, “Investigation on the characteristics and interaction of co-pyrolysis of oil shale and peanut shell,” *Fuel*, vol. 340, p. 127502, May 2023, doi: 10.1016/J.FUEL.2023.127502.

[146] Y. Zhai, Y. Zhu, S. Cui, Y. Tao, X. Kai, and T. Yang, “Study on the co-pyrolysis of oil shale and corn stalk: Pyrolysis characteristics, kinetic and gaseous product analysis,” *J. Anal. Appl. Pyrolysis*, vol. 163, p. 105456, May 2022, doi: 10.1016/J.JAAP.2022.105456.

[147] B. Chen *et al.*, “Studies of fast co-pyrolysis of oil shale and wood in a bubbling fluidized bed,” *Energy Convers. Manag.*, vol. 205, p. 112356, Feb. 2020, doi: 10.1016/j.enconman.2019.112356.

[148] J. Li *et al.*, “Synergistic effects during co-pyrolysis and co-gasification of polypropylene and polystyrene,” *Appl. Energy*, vol. 336, p. 120750, Apr. 2023, doi: 10.1016/J.APENERGY.2023.120750.

[149] Z. Zhang, S. Pang, and T. Levi, “Influence of AAEM species in coal and biomass on steam co-gasification of chars of blended coal and biomass,” *Renew. Energy*, vol. 101, pp. 356–363, Feb. 2017, doi: 10.1016/J.RENENE.2016.08.070.

[150] J. Fermoso, M. V. Gil, C. Pevida, J. J. Pis, and F. Rubiera, “Kinetic models comparison for non-isothermal steam gasification of coal–biomass blend chars,” *Chemical Engineering Journal*, vol. 161, no. 1–2, pp. 276–284, Jul. 2010, doi: 10.1016/J.CEJ.2010.04.055.

[151] C. Higman and M. van der Burgt, *Gasification. 2nd. ed. Chapter 3. The Kinetics of Gasification and Reactor Theory*. Gulf Professional Publishing, 2003. doi: 10.1016/B978-075067707-3/50003-6.

[152] C. Franco, F. Pinto, I. Gulyurtlu, and I. Cabrita, “The study of reactions influencing the biomass steam gasification process,” *Fuel*, vol. 82, no. 7, pp. 835–842, May 2003, doi: 10.1016/S0016-2361(02)00313-7.

[153] A. Konist, A. Valtsev, L. Loo, T. Pihu, M. Liira, and K. Kirsimäe, “Influence of oxy-fuel combustion of Ca-rich oil shale fuel on carbonate stability and ash composition,” *Fuel*, vol. 139, pp. 671–677, Jan. 2015, doi: 10.1016/j.fuel.2014.09.050.

[154] S. Vyazovkin *et al.*, “ICTAC Kinetics Committee recommendations for collecting experimental thermal analysis data for kinetic computations,” *Thermochim. Acta*, vol. 590, pp. 1–23, Aug. 2014, doi: 10.1016/J.TCA.2014.05.036.

[155] S. Brunauer, P. H. Emmett, and E. Teller, “Adsorption of Gases in Multimolecular Layers,” *J. Am. Chem. Soc.*, vol. 60, no. 2, pp. 309–319, Feb. 1938, doi: 10.1021/JA01269A023.

[156] K. Sing, “The use of nitrogen adsorption for the characterisation of porous materials,” *Colloids Surf. A Physicochem. Eng. Asp.*, vol. 187–188, pp. 3–9, Aug. 2001, doi: 10.1016/S0927-7757(01)00612-4.

[157] D. Lv, M. Xu, X. Liu, Z. Zhan, Z. Li, and H. Yao, “Effect of cellulose, lignin, alkali and alkaline earth metallic species on biomass pyrolysis and gasification,” *Fuel*

Processing Technology, vol. 91, no. 8, pp. 903–909, Aug. 2010, doi: 10.1016/J.FUPROC.2009.09.014.

[158] D. M. Neiva *et al.*, "Lignin from Tree Barks: Chemical Structure and Valorization," *ChemSusChem*, vol. 13, no. 17, pp. 4537–4547, Sep. 2020, doi: 10.1002/cssc.202000431.

[159] A. N. Rollinson and M. K. Karmakar, "On the reactivity of various biomass species with CO2 using a standardised methodology for fixed-bed gasification," *Chem. Eng. Sci.*, vol. 128, pp. 82–91, May 2015, doi: 10.1016/J.CES.2015.02.007.

[160] M. P. González-Vázquez, R. García, M. V. Gil, C. Pevida, and F. Rubiera, "Comparison of the gasification performance of multiple biomass types in a bubbling fluidized bed," *Energy Convers. Manag.*, vol. 176, pp. 309–323, Nov. 2018, doi: 10.1016/j.enconman.2018.09.020.

[161] E. Bondar and M. Koel, "Application of supercritical fluid extraction to organic geochemical studies of oil shales," *Fuel*, vol. 77, no. 3, pp. 211–213, Feb. 1998, doi: 10.1016/S0016-2361(97)00188-9.

[162] R. Ochieng, A. L. Cerón, A. Konist, and S. Sarker, "A combined analysis of the drying and decomposition kinetics of wood pyrolysis using non-isothermal thermogravimetric methods," *Energy Conversion and Management: X*, vol. 20, no. 12, p. 100424, Oct. 2023, doi: 10.1016/j.ecmx.2023.100424.

[163] J. O. Jaber and S. D. Probert, "Pyrolysis and gasification kinetics of Jordanian oil-shales," *Appl. Energy*, vol. 63, no. 4, pp. 269–286, Aug. 1999, doi: 10.1016/S0306-2619(99)00033-1.

[164] D. Yang, F. Xu, A. Konist, and O. Järvik, "Insights into property-associated decomposition characteristics of oil shale from various deposits," *Fuel*, vol. 428, p. 140413, Jan. 2027, doi: 10.1016/J.FUEL.2026.140413.

[165] F. Zhao, Z. Yang, L. Zhang, C. Zhang, T. Wang, and H. Zhang, "The effect of temperature on pyrolysis products during oil shale thermal decomposition," *Sci. Rep.*, vol. 15, no. 1, Jul. 2025, doi: 10.1038/s41598-025-11050-6.

[166] S. Link *et al.*, "Catalytic effect of oil shale ash on CO2 gasification of leached wheat straw and reed chars," *Energy*, vol. 152, pp. 906–913, 2018, doi: 10.1016/j.energy.2018.04.013.

[167] J. Guo *et al.*, "Influence of process parameters on the exergy analysis of biomass fluidized bed gasification," *Renewable and Sustainable Energy Reviews*, vol. 226, p. 116320, Jan. 2026, doi: 10.1016/J.RSER.2025.116320.

[168] R. Wu, J. Beutler, C. Price, and L. L. Baxter, "Biomass char particle surface area and porosity dynamics during gasification," *Fuel*, vol. 264, p. 116833, Mar. 2020, doi: 10.1016/J.FUEL.2019.116833.

[169] J. He *et al.*, "Experimental study on the key factors affecting the gasification performance between different biomass: Compare citrus peel with pine sawdust," *Int. J. Hydrogen Energy*, vol. 47, no. 71, pp. 30428–30439, 2022, doi: 10.1016/j.ijhydene.2022.07.004.

[170] R. Roncancio and J. P. Gore, "CO2 char gasification: A systematic review from 2014 to 2020," *Energy Conversion and Management: X*, vol. 10, p. 100060, 2021, doi: 10.1016/j.ecmx.2020.100060.

[171] S. Liu *et al.*, "Catalytic pyrolysis of pine wood over char-supported Fe: Bio-oil upgrading and catalyst regeneration by CO2/H2O," *Fuel*, vol. 307, p. 121778, 2022, doi: 10.1016/j.fuel.2021.121778.

[172] M. Zhang, G. Fan, N. Liu, M. Yang, X. Li, and Y. Wu, “Tar removal in pine pyrolysis catalyzed by bio-char supported nickel catalyst,” *J. Anal. Appl. Pyrolysis*, vol. 169, p. 105843, 2023, doi: 10.1016/j.jaap.2022.105843.

[173] H. Pikkor, H. Lees, A. Konist, O. Järvik, and B. Maaten, “Steam Activation of Oil Shale to Enhance the Porosity of Produced Semicoke,” *Energy Sources, Part A: Recovery, Utilization and Environmental Effects*, vol. 44, no. 4, pp. 9064–9073, 2022, doi: 10.1080/15567036.2022.2128471.

[174] J. T. Sears, H. S. Muralidhara, and C. Y. Wen, “Reactivity Correlation for the Coal Char-C02 Reaction,” *Collect. Czech. Chem. Commun*, vol. 19, no. 110, p. 452, 1980.

[175] D. Cazorla-Amorós, A. Linares-Solano, C. Salinas-Martinez De Lecea, and J. P. Joly, “A Temperature-Programmed Reaction Study of Calcium-Catalyzed Carbon Gasification,” *Energy & Fuels*, vol. 6, pp. 287–293, 1992.

[176] D. Cazorla-Amoros, A. Linares-Solano, F. H. M. Dekker, and F. Kapteijn, “ISOTOPIC STEADY-STATE AND STEP-RESPONSE STUDY ON CARBON GASIFICATION CATALYZED BY CALCIUM,” *Carbon N. Y.*, vol. 33, no. 8, p. 114771154, 1995, doi: 10.1016/0008-6223(95)00068-O.

[177] P. D. Miles and W. Brad. Smith, “Specific gravity and other properties of wood and bark for 156 tree species found in North America,” *Res. Note NRS-38. Newtown Square, PA: U.S. Department of Agriculture, Forest Service, Northern Research Station. 35 p.*, vol. 38, pp. 1–35, 2009, doi: 10.2737/NRS-RN-38.

[178] M. M. Mukaka, “A guide to appropriate use of Correlation coefficient in medical research,” *Malawi Med. J.*, vol. 24, no. 3, p. 69, 2012.

Acknowledgements

I would like to express my deepest gratitude to my supervisors, Prof. Alar Konist and Prof. Oliver Järvik, for their guidance and encouragement throughout my doctoral studies. I appreciate their oversight and the opportunity to carry out this research.

I am sincerely thankful to my colleagues at Department of Energy Technology for making the research environment both professional and enjoyable.

I am deeply thankful to my family and friends for their constant support. Most importantly, I would like to thank my husband, Mihkel, who stood by me throughout this journey. I am also grateful to my son and daughter, Karl and Stella, whose arrival brought both renewed motivation and a joyful challenge to completing this work.

Abstract

Co-gasification of Biomass and Oil Shale in a CO_2 Atmosphere

The transition of Estonia toward climate neutrality requires reducing the carbon intensity of its energy system while maintaining energy security. Oil shale and biomass are key domestic energy resources. Therefore, their efficient utilization and valorization remain strategically important. While oil shale has been extensively studied for obtaining liquid fuels, its gasification, as well as that of biomass in Estonia, remains underexplored. Hence, development of gasification represents a promising alternative for more sustainable utilization of these resources. Co-gasification of biomass and oil shale under a CO_2 atmosphere offers a potential route for simultaneous energy production and carbon utilization.

CO_2 was selected as the gasifying medium because it participates directly in char conversion and promotes the formation of CO-rich producer gas through the char–CO_2 reaction. In addition to its relevance for CO_2 utilization, CO_2 gasification provides a reaction environment dominated by char–CO_2 interactions, making it suitable for investigating feedstock-dependent and mineral-mediated effects.

Synergistic effects have been widely reported for biomass co-gasification with coal and other feedstocks, suggesting that interaction effects can greatly influence the conversion behavior. Given the high mineral content of oil shale, similar mineral-mediated interactions may occur in biomass and oil shale systems. However, the occurrence of such interactions under CO_2 gasification conditions remains poorly understood.

This thesis provides a systematic investigation of feedstock-dependent interactions during the co-gasification of lignocellulosic biomass and Estonian kukersite oil shale. The work includes comprehensive chemical characterization of 19 woody species. The wood and bark fractions were analyzed separately. Laboratory-scale gasification experiments were conducted using pine and birch wood and bark samples. A multimethod approach involving fixed-bed gasification, gas chromatography, thermogravimetric analysis coupled with mass spectrometry (TGA–MS), and structural characterization of the solid residue was applied to investigate the gasification behavior, producer gas composition, and nonadditive behavior. TGA indicated predominantly additive behavior, whereas fixed-bed experiments revealed clear nonadditive effects, highlighting the importance of reactor-scale conditions in the manifestation of synergy.

The compositional analysis revealed significant heterogeneity between wood and bark fractions, with bark exhibiting higher fixed carbon and ash content, while wood showed higher volatile matter, providing a basis for interpreting feedstock-dependent gasification behavior. The gasification results demonstrated strong feedstock-dependency, with bark-based blends exhibiting clear nonadditive enhancement of CO concentration, most notably for pine bark with 10 wt% oil shale addition, reaching up to 16.7 vol%, with deviations between experimental and calculated values exceeding the combined uncertainty, whereas wood-based samples showed largely additive or inhibitory behavior. Under fixed-bed conditions, H_2 showed mainly additive or inhibitory behavior, while CH_4 concentrations remained low and showed no consistent interaction pattern.

Surface area analysis showed that wood-derived chars had significantly higher surface areas (up to ~680 m^2/g) than bark-derived chars (435–505 m^2/g), and yet the former generated lower CO concentrations during gasification. Despite a systematic decrease in

surface area with increasing oil shale ratio, bark-based blends maintained higher reactivity, indicating that feedstock composition and mineral content exerted a stronger influence over surface area in controlling the gasification performance.

The feedstock-dependent response was associated with differences in both carbon availability and mineral composition. Higher fixed carbon content provides a larger carbon reservoir for subsequent char–CO_2 conversion, while inherent biomass AAEMs and OS-derived mineral species provide plausible catalytic contributions. The results are therefore consistent with a combined mineral-mediated effect involving both feedstocks, although their individual contributions and the specific catalytic pathway could not be distinguished experimentally. The comparison between TGA and fixed-bed experiments further indicates that the experimental environment influences how strongly these interactions are expressed.

This work establishes a compositional baseline for Estonian woody biomass resources and advances the understanding of biomass and oil shale interactions during CO_2 co-gasification. The findings highlight the importance of feedstock selection and provide a basis for targeted mechanistic and kinetic studies, optimization of feedstock combinations and process conditions, and ultimately evaluation of the potential for scale-up. More broadly, the results support further investigation of biomass–oil shale co-gasification as a potential alternative pathway for resource utilization.

Lühikokkuvõte

Biomassi ja põlevkivi koosgaasistamine CO_2 keskkonnas

Kliimaneutraalsusele üleminek eeldab tõhusamate ja jätkusuutlikumate meetodite arendamist nii taastuvate kui ka fossiilsete ressursside kasutamiseks. Eestis on biomass ja põlevkivi peamised energiaallikad, mistõttu on nende väärindamine kaasaegsete termokeemiliste muundamisprotsesside abil jätkuvalt strateegiliselt oluline. Kuigi põlevkivi kasutamist vedelkütuste tootmiseks on põhjalikult uuritud, on nii põlevkivi gaasistamist kui ka biomassi gaasistamist Eestis seni vähe käsitletud. Biomassi ja põlevkivi koosgaasistamist CO_2 keskkonnas ning nendevahelist koosmõju on väga vähe eksperimentaalselt uuritud, kuigi selline lähenemine pakub võimalust ressursside jätkusuutlikumaks kasutamiseks ja CO_2 väärindamiseks.

Gaasistusagensina kasutati CO_2, kuna see võimaldab samaaegselt CO_2 väärindamist ja CO-rikka generaatorgaasi tootmist. Kirjanduse põhjal on CO_2-gaasistamine tundlik kütuse mineraalse koostise suhtes, mistõttu sobib see hästi erinevate kütuste koosmõju uurimiseks.

Varasemates uuringutes on biomassi koosgaasistamisel teiste kütustega täheldatud sünergiat, mida on muu hulgas seostatud kütuste mineraalse koostisega. Põlevkivi suure mineraalse koostise tõttu võivad sarnased koostoimed esineda ka biomassi ja põlevkivi koosgaasistamisel, kuid varasemalt pole neid uuritud. Käesolev töö on esimene eksperimentaalne uuring Eesti biomassi ja kukersiitpõlevkivi koosgaasistamise kohta CO_2 keskkonnas. Töö eesmärk oli uurida lignotselluloosse biomassi ja põlevkivi koosgaasistamise käitumist, generaatorgaasi koostist ja mitteaditiivseid efekte. Selleks kombineeriti mitut eksperimentaalset meetodit, sealhulgas gaasistamist fikseeritud kihiga reaktoris, gaasikoostise määramist gaaskromatograafiaga, termogravimeetrilist analüüsi koos massispektromeetriaga (TGA–MS) ning tahke jäägi eripinna määramist.

Töö hõlmas 19 Eestis kasvava puuliigi keemilist iseloomustamist, analüüsides eraldi tüvepuitu ja koort. Analüüsid näitasid puidu ja koore koostise selgeid erinevusi, kus kooreproove iseloomustasid suurem seotud süsiniku sisaldus ja tuhasus, puiduproove aga suurem lendosade sisaldus. Kasutatud põlevkivi iseloomustati samuti analoogselt biomassiga. Kütuste põhjalik karakteriseerimine võimaldas hinnata nende omaduste seoseid generaatorgaasi koostise ja tahke jäägiga ning tõlgendada gaasistamisel täheldatud erinevusi.

Koosgaasistamiseks kasutati männi ja kase tüvepuitu ja koort. TGA tulemused viitasid valdavalt aditiivsele käitumisele, samas kui fikseeritud kihiga reaktoris tehtud katsed näitasid, et biomassi ja põlevkivi vahel esineb koosmõju (sünergia), mille ulatus sõltub kasutatavast biomassi liigist ja taime osast. Kahe katsesüsteemi erinevad tulemused näitavad, et mitteaditiivsete efektide avaldumine sõltub ka eksperimentaalsest keskkonnast. Positiivne koosmõju avaldus kõige selgemalt koorepõhistes segudes, kus täheldati arvutuslikust suuremaid CO kontsentratsioone. Erinevused ületasid eksperimentaalse määramatuse, kinnitades mitteaditiivset käitumist. Suurim CO kontsentratsioon (16.7 vol%) määrati männikoore segus, mis sisaldas 10% põlevkivi. Seevastu tüvepuidupõhised segud näitasid valdavalt aditiivset või inhibeerivat käitumist. H_2 kontsentratsioon üldiselt vähenes põlevkivi sisalduse suurenemisega, samas kui CH_4 kontsentratsioon jäi madalaks ja ei näidanud selget muutustrendi.

Tahke jäägi eripinna analüüs näitas, et tüvepuidust saadud söe eripind oli oluliselt suurem (kuni ~680 m^2/g) võrreldes kooreproovidest saadud söega (~435–505 m^2/g), kuid sellele vaatamata oli tüvepuidu gaasistamisel CO kontsentratsioon madalam. Põlevkivi

osakaalu suurenedes vähenes eripind süstemaatiliselt, kuid koorepõhised segud säilitasid kõrgema reaktsioonivõime, mis näitab, et gaasistamise efektiivsust mõjutasid eripinnast enam lähteaine koostis ja mineraalainete sisaldus.

Tulemused näitavad, et lähteaine koostis mõjutab oluliselt biomassi ja põlevkivi vahelist koosmõju. Kooreproovide suurem seotud süsiniku sisaldus tagab pürolüüsi järel suurema süsinikuvaru järgnevaks söe–CO_2 reaktsiooniks, samas kui biomassile omased leelis- ja leelismuldmetallid võivad katalüüsida süsiniku gaasistamist. Põlevkivi lisab süsteemi täiendava mineraalse komponendi, eelkõige Ca ühendid. Tulemused on seega kooskõlas kombineeritud efektiga, millesse võivad panustada nii biomassi enda AAEM-id kui ka põlevkivist pärinevad mineraalid. Nende individuaalset panust ja täpset katalüütilist mehhanismi ei olnud käesolevate katsete põhjal siiski võimalik eristada. TGA ja fikseeritud kihiga reaktori tulemuste erinevus viitab lisaks sellele, et koosmõju avaldumist võivad mõjutada proovi mass, osakeste vaheline kontakt ning soojus- ja massiülekande tingimused.

Käesolevas töös esitatud põlevkivi ja biomassi vaheline koosmõju tõlgendus põhineb peamiselt kütuste koostise analüüsil ja eksperimentaalsete gaasistamise katsete tulemustel. Seega jäi antud töö ulatusest välja tulemuste kineetiline valideerimine, sealhulgas kütuste koosgaasistamine erinevatel kuumutuskiirustel ja selektiivne demineraliseerimine. Täiendavad uuringud annaksid olulist informatsiooni, et eristada katatüütilisi efekte ja täpsemalt hinnata mineraalide rolli gaasistamise reaktsioonides.

Tulemused näitavad, et põlevkivi lisamine biomassi gaasistamisele võib teatud tingimustel soodustada CO moodustumist, kuid mõju sõltub nii biomassi omadustest kui ka eksperimentaalsetest tingimustest. Töö loob põhjaliku lähteandmestiku Eesti puitbiomassi koostise kohta ning täiendab arusaama lähteaine omaduste ja mineraalainete rollist biomassi ja põlevkivi koosgaasistamisel. Saadud tulemused loovad aluse sihipärasteks mehhanistlikeks ja kineetilisteks uuringuteks, lähteainesegude ja protsessitingimuste optimeerimiseks ning pikemas perspektiivis protsessi skaleerimise võimaluste hindamiseks. Ühtlasi toetavad tulemused biomassi ja põlevkivi koosgaasistamise edasist uurimist ühe võimaliku alternatiivse väärindamissuunana.

Appendix 1 (Publications)

Publication I

Järvik, O., Sulg, M., Cascante Cirici, P., Eldermann, M., Konist, A., Gusca, J., & Siirde, A. (2020). **Co-Pyrolysis and Co-Gasification of Biomass and Oil Shale.** *Environmental and Climate Technologies*, *24*(1), 624–637. https://doi.org/10.2478/rtuect-2020-0038

Environmental and Climate Technologies
2020, vol. 24, no. 1, pp. 624–637
https://doi.org/10.2478/rtuect-2020-0038
https://content.sciendo.com

Co-Pyrolysis and Co-Gasification of Biomass and Oil Shale

Oliver JARVIK[1], Mari SULG[2], Pau CASCANTE CIRICI[3], Meelis ELDERMANN[4], Alar KONIST[5], Julija GUSCA[6], Andres SIIRDE[7]*

[1,2,3,5,7]*School of Engineering: Department of Energy Technology, Tallinn University of Technology, Ehitajate tee 5, Tallinn, 19086, Estonia*

[4]*Viru Keemia Grupp AS, Järveküla tee 14, Kohtla-Järve, 30328, Estonia*

[6]*Institute of Energy Systems and Environment, Riga Technical University, Azenes iela 12/1, Riga, LV-1048, Latvia*

***Abstract* – The European Union has set an ambitious goal to transform to a carbon neutral economy. The present paper focuses on thermal treatment of oil shale and biomass blends that could be considered as an important pathway for achieving the carbon neutral goal locally in Estonia. The concept of co-pyrolysis and co-gasification of biomass and oil shale offers various advantages such as higher liquid product yield and higher char conversion than if the oil shale and biomass particles were processed individually. In the paper, an overview of the planned actions for merging oil shale industry carbon neutral economy is given. The selected approaches are justified with information found in scientific literature and initial experimental results. Further, the possible future developments for gasification and pyrolysis in Estonia are also highlighted.**

***Keywords* – CFB (circulating fluidized bed); char; fixed bed reactor; heating rate.**

1. INTRODUCTION

Biomass is an abundant raw material and a source for energy, fuels and (organic) chemicals. Producing fuels and chemicals allows more economical use of local biomass and waste. This is especially attractive for countries, like Estonia, that have large amounts of forested land.

Thermal treatment of different organic (polymeric) materials in an oxygen deprived environment, termed pyrolysis or gasification (depending on temperature), has received a lot of attention as a promising method to produce oil, chemicals and syngas. Studies have indicated that thermal treatment produces fuel (liquid or gas) at a lower cost than other common technologies, such as biochemical [1], [2]. Thermal treatment can be applied to a wide range of feedstock, including wastes and oil shale [3], which allows the use of different feedstock depending on what is economically feasible and readily available [4]. Such flexibility also means the raw materials could be varied to produce different types and amounts of products to meet changing demands. In addition, a locally important feedstock, such as oil shale could be used, either on its own or for co-pyrolysis/co-gasification with biomass to optimize the properties of the resulting liquid and/or gaseous product(s).

* Corresponding author.
E-mail address: andres.siirde@taltech.ee

©2020 Oliver Jarvik, Mari Sulg, Pau Cascante Cirici, Meelis Eldermann, Alar Konist, Julija Gusca, Andres Siirde.
This is an open access article licensed under the Creative Commons Attribution License (http://creativecommons.org/licenses/by/4.0), in the manner agreed with Sciendo.

Pyrolysis and gasification are complex processes involving hundreds of chemical species, many different reactions, and mass and heat transfer processes. The composition and structure of the raw materials and the conditions used all play a role in determining the composition of the evolving products [5], [6]. Performing co-pyrolysis/co-gasification, by mixing biomass with something like plastic wastes, tires or oil shale, also affects the process and the resulting products. On one hand, this can improve the yield and properties of the products and enable the use of a wider variety of feedstock, but it also adds complexity [7]–[9]. Further, compared to thermal treatment of just one raw material (for example coal), synergetic effects in co-pyrolysis and co-gasification are sometimes reported [10], [11]. It is also suggested that inorganic constituents can act as catalysts [6], [12].

The data on co-gasification of biomass and oil shale seems to be very scarce [13]. There are few studies on co-pyrolysis of oil shale and biomass at temperatures ranging from 340 °C in an autoclave [14] to 520 °C in a cylindrical retort [15].

The current paper presents a broad range of conditions and techniques that are used in the ongoing study intended to develop knowledge in the field of co-pyrolysis and co-gasification of oil shale and biomass. The results obtained provide valuable input to the analysis of the perspectives of Estonia's carbon neutrality and also to the oil shale industry for developing innovative and environmentally friendly technologies for oil shale processing. Firstly, it will provide basic information about the possibilities for further valorisation of feedstock for example into platform chemicals and polymer monomers. Secondly, valuable data is obtained to cope with the targets of the European Union climate and energy package and Renewable Energy Directive.

2. Methods and Materials

2.1. Raw Material

The selected approaches are applied to Kukersite oil shale, biomass and their mixtures. Proximate and ultimate analysis of the biomass (bark of Scots pine; *Pinus sylvestris* as an example) and oil shale are shown in Table 1. To eliminate the effect of moisture content, samples are dried at 105 °C and stored in desiccators. Particle size of the sample is in between 0.25 mm and 0.5 mm.

Table 1. Examples of Proximate and Ultimate Analysis of Bark and Oil Shale

	Loss on ignition at 550 °C, wt. %	**Ash content at 815 °C (dry matter), wt. %**	**Carbonate CO_2, wt. %**	**Elemental composition, wt. %**				
				C	**H**	**N**	**S**	**O**
Oil shale	41.38	47.35	17.6	33.78	3.71	0.09	1.73	60.69
Bark (Scots pine)	96.95			52.79	6.08	1.19	0.04	43.10

2.2. Testing Procedure

The general test plan is as follows:

1) Sample preparation – particle size-reduction;
2) Preliminary characterization of fuels – it involves elemental composition, content of heavy metals, calorific value, ash content, moisture content, adsorption parameters, etc.;

3) Thermal treatment of materials in thermogravimetric analyser (TGA) under different conditions (pyrolysis or gasification). Different heating rates and carrier gases can be used (usually below 40 °C/min) to test a wide range of conditions. As the sample amount is limited, it is mostly used for screening, although valuable data on evolving gases is obtained;
4) Thermal treatment of materials in a fixed bed reactor is used to obtain larger amounts of material that can be further analysed and characterized. For the solid residue (char), the same analyses are carried out as for preliminary characterization of fuels. Evolved gases and condensed oil are further characterized.

2.3. Experimental Set-Up and Equipment

The experimental part of the research is performed in the Department of Energy Technology (DET) of the Tallinn University of Technology. The co-pyrolysis and co-gasification experiments are being performed in a laboratory-scale fixed bed reactor (Fig. 1), described in more detail in [16]. It is equipped with control (temperature control by means of thermocouples and gas flow by means of mass flow controllers) and data acquisition system (NI SCXI-1000 chassis with modules NI-1102 and NI-1124). Non-condensable gases may be analysed either with Fourier transformed infrared (FTIR) spectrometer (*DX-4000, Gasmet*) which can be configured to measure simultaneously H_2O, CO_2, CO, NO, NO_2, N_2O, SO_2, NH_3, CH_4, HCl, HF, C_xH_y. The FTIR is coupled with a Zirconia oxygen sensor for determination of the O_2 content. Concentration of volatile organic compounds (VOCs) is measured using a flame ionization detector (*Fidamat* 6*, Siemens*). Samples of the evolving gases may also be extracted to the gas sampling bag for the later analysis (of CO, H_2 and CH_4).

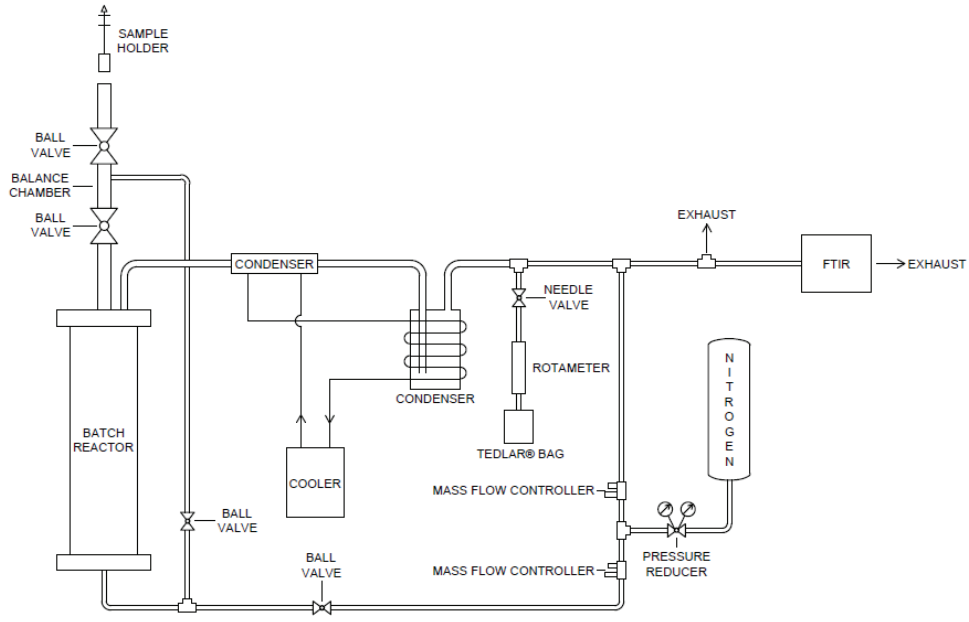


Fig. 1. Fixed bed reactor set-up.

The kinetics of the gasification and pyrolysis processes including also heat effects are measured with a *Netzsch STA* 449 *F*3 *Jupiter*® thermogravimetric analyser. It is equipped with a water vapor generator and high-speed furnace to simulate processes under different conditions and different heating rates. Evolved gases are analysed with *Netzsch QMS* 403 *D Aëolos*® mass spectrometer.

Determination of adsorption parameters (specific surface area and porosity, including calculation of multipoint BET, void volume and micropore specific surface area) is performed using a Quantachrome Autosorb iQ-C gas sorption analyser. It is useful for physisorption and chemisorption studies (former in H_2 and oxidizing environments) to fully characterize the feed materials and the remaining solid residues.

The mobility of heavy metals is analysed using ICP-MS (*Thermo iCAP Qc Quadrupole*) after acid digestion and treatment.

Gases and liquids will be analysed in gas chromatograph (*Agilent* 7890*A GC*) with MS and FID detectors and LC (*Waters e*2695) with PID and MS detector, respectively.

General sample characterisation (including chemical composition of solids) is performed in a dedicated accredited laboratory in DET according to international standards and validated methods.

3. Results and Discussion

Despite the efforts taken to reduce the use of solid fossil fuels, combustion of these fuels is still one of the main sources of electricity and heat, both in Estonia and globally. This is mainly because these fossil fuels are widely available, and the technologies used are reliable and available when needed. Oil shale provides approximately 80 % of Estonia's electricity needs, making Estonia one of the least energy independent countries of Europe [17]. The oil shale sector is known from wider publicity about its large environmental footprint. However, it is not often known that, during the last 25 years, significant improvements in reducing the environmental impact of the oil shale-related industries (both energy and shale oil production) has been achieved. This is mainly as a result of utilizing fluidized bed combustion technologies. At the same time, new technologies are emerging that could possibly provide even more efficient utilization of oil shale and provide cleaner and more economical energy. To find the balance between the needs (energy) and expectations (clean environment), it is necessary to develop more sustainable ways to utilize local conventional fuels (such as oil shale). Also, latest developments in the energy sector are mostly driven by the EU's legislative constraints and climate agreements suggest that further development of the oil shale industry is urgently needed. It is suggested that instead of oil shale combustion, its gasification or valorisation to shale oil could be more sustainable [18].

Estonian oil shale pyrolysis process is rather well studied and shale oil is extensively researched [19]–[21]. In the pyrolysis reactors, the conditions have been optimized to maximize the yield of shale oil. Shale oil is mostly used as fuel oil and its value depends on the crude oil market. To increase the value of shale oil, it should be further processed using upgrading (for example with the aid of gas) or separation of valuable compounds to be used in the chemical industry. Dibasic phenols have been the main valuable products separated from the Kiviter shale oil (low heating rate). Recently a project for oil shale valorisation was started with the aim to use partial oxidation of kerogen for production of dicarboxylic acids [22], showing the potential of oil shale as a source of valuable products. However, little is known about the liquids obtained during its co-pyrolysis with biomass. Based on the coal and

biomass pyrolysis liquid characterization, it could be expected that, depending on the type of feedstock, the obtained products could be "modified" [23].

The composition and yield of the products obtained during their thermal treatment is dependent on the type/composition of the feedstock that is used in the process, process temperature, heating rate, reaction time and the feed particle size [24]–[26]. In the following sections, a short overview describing the effects of these different parameters on pyrolysis and gasification processes is given together with the parameters selected in the current study and their possible impact on the process and products.

3.1. Feedstock

Biomass (based on the species analysed as well as storage conditions) could have significant variation in its physical as well as chemical properties. The composition of oil shale, mainly its organic content, however, also chemical composition of organic matter, is also varying. The parameters of feedstock affecting its thermal treatment and composition of obtained products are the size of the particles, ratio of oil shale to biomass, ash content, moisture content (which determines the concentration of steam in the gas phase). The feedstock blending ratio is reported to directly affect the formation of combustible gases (mostly H_2, CO and CH_4 but also higher hydrocarbons) in co-gasification [27]. Additionally, biomass blending with coal is reported to initiate gasification process at lower temperatures [28], produces more tar and less char [27].

In the course of the research, we have chosen to keep the size of the feed particles small to reduce the diffusion related phenomena and to reduce the time needed to heat the particles. Also, to avoid adding complexity, the samples are always dried. Rather, moisture (in the form of vapour/steam) can be introduced into the reactor in a controlled manner. Steam is a commonly used "additive" in gasification of biomass or coal as it allows to effectively change the composition (for example H_2 or CO content) of obtained gas [29].

An important feature that distinguishes oil shale is its high mineral matter content. This mineral matter is largely composed of carbonate minerals that start to decompose at temperatures of around 700 °C (Fig. 2). During decomposition a significant amount of CO_2 is formed. The extent of carbonate decomposition depends on the final temperature and residence time [30].

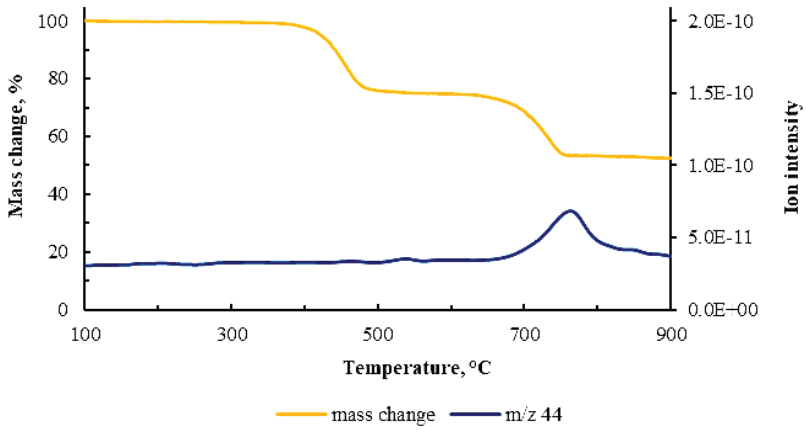


Fig. 2. Decomposition of oil shale and evolution of CO_2 in N_2 atmosphere.

As can be seen from Fig. 2, the sample displays mass loss steps typical for oil shale – the decomposition step for organic matter in the temperature range of 370 to 560 °C and the decomposition of carbonate minerals in the temperature range of 600 to 770 °C. These have respective mass losses of 24.7 % and 21.9 %. Additionally, about 0.5 % of moisture is present (mass loss up to 200 °C). The residual mass of the sample is 52.8 %. The blue line on Fig. 1 shows the evolution of m/z 44, CO_2. As it is evolving at temperatures above 700 °C, it confirms that the second mass loss step is the decomposition of carbonate minerals while little or no CO_2 is evolving during decomposition of organic matter.

3.2. Temperature and Heating Rates

Temperature is quite influential as far as the results of the pyrolysis products are concerned. For example, during the pyrolysis of biomass (and other feedstock) the composition of evolving gases changes as temperature is changed as does the amount of char. It has been studied that at higher temperatures more non-condensable gases [31]–[33], mainly CO + H_2, are formed. In contrast, if the process is done with lower temperatures, solid products like charcoal, bio-coal or torrefied fuels are produced [23].

Together with temperature the heating rate also has a large influence on the yield and composition of the product that can be obtained in the processes. For example, if the material is heated rapidly to a moderate final temperature, more liquids will be obtained [34] whilst increasing the temperature and maintaining the high heating rate results in higher gas yields [35], [36].

In the current study, the main emphasis is on the gaseous and liquid products. Therefore, the sample is introduced to the pre-heated reactor (so-called drop-in method). In this way we achieve the highest possible heating rate to increase the yield of gases/liquids (depending on the final temperature). It is expected that the study will provide sufficient data for upgrading the process.

Low heating rate thermal treatment studies indicate that there is two-step decomposition (pyrolysis) taking place at temperatures below 500 °C (Fig. 3). At higher heating rate (in fixed bed reactor) the decomposition of oil shale and biomass seems to be simultaneous (Fig. 4).

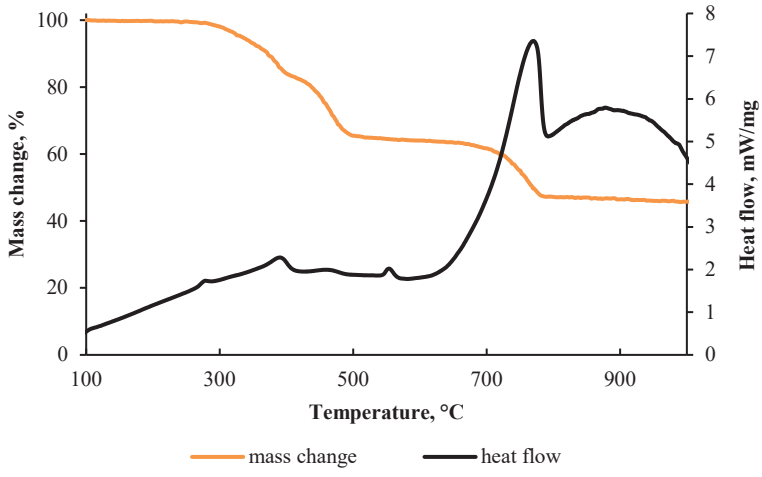


Fig. 3. Decomposition of oil shale and biomass mixture (80:20 w:w) in N_2 atmosphere.

In Fig. 3, the mass loss and heat flow during pyrolysis of oil shale and biomass mixture is shown. Compared to the oil shale decomposition presented in Fig. 2, the mass loss during co-pyrolysis starts at approximately 100 °C lower temperature (around 280 °C) which corresponds to the starting point of wood pyrolysis [37]. Heat effects associated with pyrolysis are rather small compared to that of decomposition of carbonate minerals.

Based on the decomposition data from TGA and gas analysis data (Fig. 4), the estimated heating rate (from 25 to 300 °C) of a sample in fixed bed reactor is around 140 °C/min.

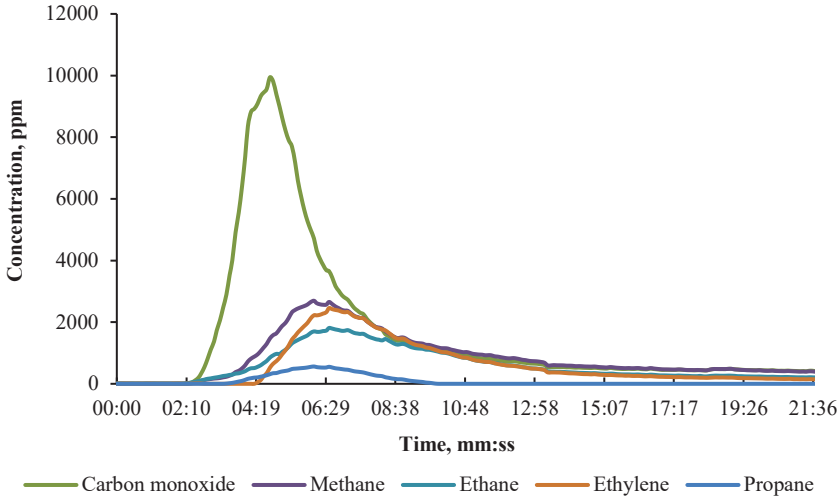


Fig. 4. Evolution of different gases during oil shale and biomass co-pyrolysis at 550 °C in the fixed bed reactor.

At high heating rates there is no possibility to measure real time mass loss, however, the process can be monitored through gas analysis. The gas analysis shows that at pyrolysis conditions relatively large amount of higher non-condensable (at around 0 °C) hydrocarbons is formed. Further studies are underway to determine the possible catalytic effect of oil shale on biomass co-pyrolysis (for oil production) and co-gasification (especially for production of syngas with high CO and H_2 content).

3.3. Reactors

There are different reactors available for co-pyrolysis or co-gasification. The selection of a reactor for the thermal treatment defines the occurrence of the reactions and exact processes involved in different reactor zones which are interrelated with temperature effects. There are different types of reactors used for pyrolysis and gasification. Fast pyrolysis reactors have been developed for the purposes of laboratories and pilot-scale demonstrations, including CFB, free fall etc. types [10]. Operational gasification (pilot) plants are gathered in the International Energy Agency (IEA) database [38]. For coal and biomass co-gasification, a total of five plants at least in the technology readiness level (TRL) 4–5 have been built. Plants utilizing down draft fixed bed gasifier and Integrated Gasification Combined Cycle (IGCC) have failed to reach commercial operation. Currently, according to IEA, only two pilot scale plants (pressurized entrained flow gasifier and fixed bed gasifier) in the Research Institutes of Sweden are operational. Regarding biomass and coal co-pyrolysis, two TRL 6–7 fast

pyrolysis plants in the world are operational, however, at least one pilot scale fast pyrolysis plant is also operational in the VTT technical research centre of Finland.

Despite the unfavourable statistic, the studies of pyrolysis and gasification are continuing. For this purpose, different reactors are utilized, including fixed bed, downdraft fixed bed, updraft fixed bed, (circulating) fluidized bed, tubular, entrained flow and circulating radial-flow moving bed reactors [10].

The reactor used in the current study is a batch fixed bed reactor which was chosen for its simplicity. As this type of reactor is used for developing new processes (or studying for example solid-supported catalysts), it serves as an excellent reactor type for oil shale and biomass blends gasification and pyrolysis.

3.4. Char

Char is sometimes considered as a leftover of pyrolysis or gasification processes, however, depending on its properties, bio-char can be used as fertilizer or soil improver [39], [40] or other value-added product (e.g. catalyst carrier). Compared to the use of conventional fertilizers, the addition of bio-char to the soil will reduce CO_2, CH_4 and N_2O emissions [41], [42]. Despite its beneficial properties, it is still advantageous to reduce the amount of char formation if the goal is to use fuels as a source of liquids or gaseous products [43], [44]. This will be achieved as temperature is increased as is shown in Table 2. As it can be seen for pyrolysis of biomass, the mass losses obtained in the fixed bed reactor are between 80–88 % which is commonly reported in literature [45]. Interpretation of oil shale thermal treatment results is more challenging because of the high content of carbonates in mineral part of oil shale.

The mass losses of co-pyrolysis calculated (based on Eq. (1)) from the obtained losses in pyrolysis of biomass and oil shale are 42.62 %, 45.54 % and 56.88 % at 550 ºC, 750 ºC and 900 ºC, respectively. These values are higher than those obtained experimentally in co-pyrolysis, indicating possible synergy between the materials.

$$ML_{\text{theor}} = \frac{m_{\text{BM}} \cdot ML_{\text{BM}} + m_{\text{OS}} \cdot ML_{\text{OS}}}{m_{\text{SUM}}}, \tag{1}$$

where

ML_{theor}	Calculated mass loss at specific temperature, %;
ML_{BM}	Experimental mass loss of biomass at specific temperature, %;
ML_{OS}	Experimental mass loss of oil shale at specific temperature, %;
m_{BM}	Mass of biomass, g;
m_{OS}	Mass of oil shale, g;
m_{SUM}	Mass of oil shale and biomass blend, g.

Still, as the easiest option, char can also be beneficially used to extract energy from residual carbon. Estonia has extensive experience in utilizing char (called semi-coke) as an energy source in solid heat carrier shale oil production processes (so-called Galoter process including Petroter and Enefit technologies) [46].

Oil shale pyrolysis residue, semi-coke (or char), is known by its environmental hazard [47]. Still, considering different beneficial options for char utilization, solid residues from co-pyrolysis and co-gasification experiments needs to be fully characterized.

TABLE 2. MASS LOSSES DURING THERMAL TREATMENT OF OIL SHALE, BIOMASS AND THEIR BLENDS

Sample	Temperature, °C	Mass loss, wt.%
Bark (Scots pine)	550	80.60
	750	85.45
	900	87.62
Oil shale	550	24.54
	750	26.54
	900	42.24
Oil shale + bark	550	39.56
	750	46.67
	900	60.46

3.5. (Co-)Gasification: Current Situation and Future Directions

Gasification is considered an economically efficient process when it comes to utilization of low-grade fuels [48], [49]. Gasification of oil shale was historically carried out in chamber ovens and resulted gas which had medium calorific value and relatively high sulphur content. High sulphur content of chamber oven gas made it unusable (according to the current standards) in most applications. When combining the accumulated knowledge with modern gasification processes, it might be possible to reconsider oil shale gasification, and more preferably co-gasification with biomass, as an economically and environmentally viable process. This could be achieved with CFB gasifiers that have a high fuel flexibility. Based on the experience and current trends in combustion related studies, as well as trends in pyrolysis and gasification studies, it is generally accepted that CFB technology is the preferred technology. This technology is well suited for high ash content fuels like oil shale and allows more simple and precise control of gasification environment and temperature control compared to other, more conventional gasification technologies. CFB technology also ensures uniform temperature distribution which is an important parameter considering the effect of temperature on gasification products. Currently, however, there is no information available on gasification of oil shale in CFB reactors. The current study is intended to provide data on the CFB gasification conditions and resulting gas composition (including tar formation) useful for scientists and decision makers. Consequently, the results of the study will be used to upgrade gasification to a CFB unit that is currently under development in DET.

An important goal in future studies is to evaluate the possibility of utilization of CFB gasification technologies for oil shale and biomass co-gasification that could easily be adopted on a large scale. It is important to comprehensively tackle the currently known problems, like de-fluidization of the fluidized bed caused by the agglomeration of biomass ash with low melting point and excessive tar formation and accumulation in downstream pipes [50] that have resulted in failure of pilot and large-scale installations.

Additional studies should also focus on environmental aspects of provided processes. This includes greenhouse gas and sulphur emission related problems. Because sulphur is a dangerous pollutant (for the environment and for catalyst if obtained gases are further used in synthesis), its removal from streams is of high importance. Therefore, the fate and behaviour of sulphur compounds should be studied to determine the operational conditions for maximizing the extent of sulphur bound to the mineral part of oil shale in co-pyrolysis

and co-gasification processes. Most importantly, it must be ensured that all environmental aspects of the proposed technologies are considered so that the stakeholders and the wider public accept the technologies.

3.6. (Co-)Pyrolysis: Current Situation and Future Directions

Estonian oil shale chemical industry is relying on an old, out-dated Kiviter process. This process is known by its large environmental footprint and issues with pyrolytic water [51], however it produces oil with higher content of methylresorcinols. On the other hand, it is known that biomass pyrolysis oils have a complex chemical composition and they contain many useful oxygen and nitrogen compounds that can be used for producing chemicals [2]. Therefore, biomass and oil shale co-pyrolysis oil could potentially contain different valuable compounds that would help to extend the chemical industry and make it environmentally acceptable.

After completing this study, an immediate direction for further research would be to develop applications in detail for the most valuable chemicals found in the co-pyrolysis oils. Certainly, some basic platform chemicals and polymer monomers can be produced [2], but beyond this there are a lot of high-tech applications that should be investigated. For example, the phenolic compounds can be used to create carbon aerogels, which can then be used in capacitors and batteries, insulation, adsorption and filtration and other applications [52]–[54]. Such phenols are also valuable precursors of adhesive resins for certain plastics. There is large potential to investigate other high value applications of chemicals from co-pyrolysis liquids.

4. CONCLUSIONS

Co-pyrolysis and/or co-gasification of oil shale and biomass seem to be a feasible intermittent step for achieving the final goal of transforming Estonia to a carbon neutral economy and is meaningful in regards to circular economy goals (effective use of wood waste for co-pyrolysis and co-gasification). However, as this conclusion is based on the literature reviews on thermal treatment of coal and biomass blends, further oil shale specific experimental data is needed. An important feature distinguishing oil shale from most of the coals is its high mineral matter content which means careful selection of process parameters is needed. Experiments do show that heating rate has a strong effect on the process and the main focus should be on thermal treatment of blends at high heating rates. Not only yield of products, but also environmental aspects need to be considered. To take full advantage of the feedstock, all process streams must be researched.

REFERENCES

[1] Anex R. P. *et al.* Techno-economic comparison of biomass-to-transportation fuels via pyrolysis, gasification, and biochemical pathways. *Fuel* 2010:89(S1):S29–S35. https://doi.org/10.1016/j.fuel.2010.07.015
[2] Isikgor H. F., Becer C. R. Lignocellulosic biomass: a sustainable platform for the production of bio-based chemicals and polymers. *Polym. Chem.* 2015:6(25):4497–4559. https://doi.org/10.1039/C5PY00263J
[3] Bridgwater A. V. Review of fast pyrolysis of biomass and product upgrading. *Biomass and Bioenergy* 2012:38:68–94. https://doi.org/10.1016/j.biombioe.2011.01.048
[4] Mohan D., Pittman C. U. Jr., Steele P. H. Pyrolysis of Wood/Biomass for Bio-oil: A Critical Review. *Energy Fuels* 2006:20(3):848–889. https://doi.org/10.1021/ef0502397
[5] Özsin G., Pütün A. E. Kinetics and evolved gas analysis for pyrolysis of food processing wastes using TGA/MS/FT-IR. *Waste Management* 2017:64:315–326. https://doi.org/10.1016/j.wasman.2017.03.020

[6] Ranzi E., Debiagi P. E. A., Frassoldati A. Mathematical Modeling of Fast Biomass Pyrolysis and Bio-Oil Formation. Note I: Kinetic Mechanism of Biomass Pyrolysis. *ACS Sustain. Chem. Eng.* 2017:5(4):2867–2881. https://doi.org/10.1021/acssuschemeng.6b03096

[7] Sharypov V. I. *et al.* Co-pyrolysis of wood biomass and synthetic polymers mixtures. Part III: Characterisation of heavy products. *J. Anal. Appl. Pyrolysis* 2003:67(2):325–340. https://doi.org/10.1016/S0165-2370(02)00071-2

[8] Sharypov V. I. *et al.* Co-pyrolysis of wood biomass and synthetic polymer mixtures. Part I: influence of experimental conditions on the evolution of solids, liquids and gases. *J. Anal. Appl. Pyrolysis*, 2002:64(1):15–28. https://doi.org/10.1016/S0165-2370(01)00167-X

[9] Zhou C.-H., Xia X., Lin C.-X., Tong D.-S., Beltramini J. Catalytic conversion of lignocellulosic biomass to fine chemicals and fuels. *Chem. Soc. Rev.* 2011:40(11):5588–5617. https://doi.org/10.1039/c1cs15124j

[10] Kamble A. D., Saxena V. K., Chavan P. D., Mendhe V. A. Co-gasification of coal and biomass an emerging clean energy technology: Status and prospects of development in Indian context. *Int. J. Min. Sci. Technol.* 2019:29(2):171–186. https://doi.org/10.1016/j.ijmst.2018.03.011

[11] Quan C., Gao N. Copyrolysis of Biomass and Coal: A Review of Effects of Copyrolysis Parameters, Product Properties, and Synergistic Mechanisms. *Biomed Research International* 2016:6197867. https://doi.org/10.1155/2016/6197867

[12] Park D. K., Kim S. D., Lee S. H., Lee J. G. Co-pyrolysis characteristics of sawdust and coal blend in TGA and a fixed bed reactor. *Bioresource Technology* 2010:101(15):6151–6156. https://doi.org/10.1016/j.biortech.2010.02.087

[13] Hu Z., Ma X., Li L. The synergistic effect of co-pyrolysis of oil shale and microalgae to produce syngas. *J. Energy Inst.* 2016:89(3):447–455. https://doi.org/10.1016/j.joei.2015.02.009

[14] Krasulina J., Luik H., Palu V., Tamvelius H. Thermochemical Co-liquefication of Estonian Oil Shale With Peat and Pine Bark. *Oil Shale* 2012:29(3):222–236. https://doi.org/10.3176/oil.2012.3.03

[15] Chen B., Han X., Mu M., Jiang X. Studies of the Co-pyrolysis of Oil Shale and Wheat Straw. *Energy & Fuels* 2017:31(7):6941–6950. https://doi.org/10.1021/acs.energyfuels.7b00871

[16] Konist A., Valtsev A., Loo L., Pihu T., Liira M., Kirsimäe K. Influence of oxy-fuel combustion of Ca-rich oil shale fuel on carbonate stability and ash composition. *Fuel* 2015:139:671–677. https://doi.org/10.1016/j.fuel.2014.09.050

[17] World Energy Council. World Energy Resources 2016. 2016. London, United Kingdom.

[18] Kann J., Raukas A., Siirde A. About the Gasification of Kukersite Oil Shale. *Oil Shale* 2013:30(2S):283–293, 2013. https://doi.org/10.3176/oil.2013.2S.08

[19] Kann J., Elenurm A., Rohtla I., Golubev N., Kaidalov A., Kindorkin B. About thermal low-temperature processing of oil shale by solid heat carrier method. *Oil Shale* 2004:21(3):195–203.

[20] Oja V., Rooleht R., Baird S. Z. Physical and thermodynamic properties of kukersite pyrolysis shale oil: literature review. *Oil Shale* 2016:33(2):184–197. https://doi.org/10.3176/oil.2016.2.06

[21] Järvik O., Oja V. Molecular Weight Distributions and Average Molecular Weights of Pyrolysis Oils From Oil Shales: Literature Data and Measurements by Size Exclusion Chromatography (SEC) and Atmospheric Solids Analysis Probe Mass Spectroscopy (ASAP MS) or Oils from Four Different Deposits. *Energy and Fuels* 2017:31(1):328–339. https://doi.org/10.1021/acs.energyfuels.6b02452

[22] Veski R., Veski S. Aliphatic dicarboxylic acids from oil shale organic matter – historic review. *Oil Shale* 2019:36(1):76–95. https://doi.org/10.3176/oil.2019.1.06

[23] Varma A. K., Shankar R., Mondal P. A Review on Pyrolysis of Biomass and the Impacts of Operating Conditions on Product Yield, Quality, and Upgradation. In Sarangi P., Nanda S., Mohanty P. (eds) *Recent Advancements in Biofuels and Bioenergy Utilization*. Springer, Singapore 2018, pp. 227–259. https://doi.org/10.1007/978-981-13-1307-3_10

[24] Abnisa F., Wan Daud W. M. A. A review on co-pyrolysis of biomass: An optional technique to obtain a high-grade pyrolysis oil. *Energy Convers. Manag.* 2014:87:71–85. https://doi.org/10.1016/j.enconman.2014.07.007

[25] Dhaundiyal A., Tewari P. Kinetic Parameters for the Thermal Decomposition of Forest Waste Using Distributed Activation Energy Model (DAEM). *Environmental and Climate Technologies* 2017:19(1):15–32. https://doi.org/10.1515/rtuect-2017-0002

[26] Dhaundiyal A., Singh S. B. Mathematical insight to non-isothermal pyrolysis of pine needles for different probability distribution functions. *Biofuels* 2018:9(5):647–658. https://doi.org/10.1080/17597269.2017.1329495

[27] Emami-Taba L., Irfan M. F., Wan Daud W. M. A., Chakrabarti M. H. Fuel blending effects on the co-gasification of coal and biomass – A review. *Biomass and Bioenergy* 2013:57:249–263. https://doi.org/10.1016/j.biombioe.2013.02.043

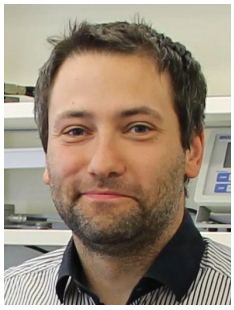
[28] Huber W. G., Iborra S., Corma A. Synthesis of Transportation Fuels from Biomass: Chemistry, Catalysts, and Engineering. *ChemInform*, 2006. https://doi.org/10.1002/chin.200652240

[29] Ptasinski K. J. *Efficiency of biomass energy: an exergy approach to biofuels, power, and biorefineries*. Wiley, 2016. https://doi.org/10.1002/9781119118169

[30] Plamus K., Soosaar S., Ots A., Neshumayev D. Firing Estonian Oil Shale of Higher Quality in CFB Boilers – Environmental and Economic Impact. *Oil Shale* 2011:28(1S):113. https://doi.org/10.3176/oil.2011.1S.04

[31] Williams P. T., Besler S. The influence of temperature and heating rate on the slow pyrolysis of biomass. *Renew. Energy* 1996:7(3):233–250. https://doi.org/10.1016/0960-1481(96)00006-7

[32] Williams P. T., Besler S., Taylor D. T. The pyrolysis of scrap automotive tyres: The influence of temperature and heating rate on product composition. *Fuel* 1990:69(12):1474–1482. https://doi.org/10.1016/0016-2361(90)90193-T
[33] Guizani C., Jeguirim M., Valin S., Limousy L., Salvador S. Biomass Chars: The Effects of Pyrolysis Conditions on Their Morphology, Structure, Chemical Properties and Reactivity. *Energies* 2017:10(6):796. https://doi.org/10.3390/en10060796
[34] Debdoubi A., El amarti A., Colacio E., Blesa M. J., Hajjaj L. H. The effect of heating rate on yields and compositions of oil products from esparto pyrolysis. *Int. J. Energy Res.* 2006:30(15):1243–1250. https://doi.org/10.1002/er.1215
[35] Waheed Q. M. K., Nahil M. A., Williams P. T. Pyrolysis of waste biomass: investigation of fast pyrolysis and slow pyrolysis process conditions on product yield and gas composition. *J. Energy Inst.* 2013:86(4):233–241. https://doi.org/10.1179/1743967113Z.00000000067
[36] Dhaundiyal A., Singh S. B., Hanon R., Muammel M. Rawat. Determination of Kinetic Parameters for the Thermal Decomposition of Parthenium hysterophorus. *Environmental and Climate Technologies* 2018:22(1):5–22. https://doi.org/10.1515/rtuect-2018-0001
[37] Bhatia S. C. *Advanced renewable energy systems*. Woodhead Publishing India, 2014.
[38] Task33 Database. [Online]. [Accessed: 14-Jun-2019]. Available: http://task33.ieabioenergy.com/content/Task 33 Projects.
[39] Shen Q., Hedley M., Camps Arbestain M., Kirschbaum M. U. Can biochar increase the bioavailability of phosphorus? *Journal of Soil Science and Plant Nutrition* 2016:16(2). https://doi.org/10.4067/S0718-95162016005000022
[40] Yadav A., Ansari K. B., Simha P., Gaikar V. G., Pandit A. B. Vacuum pyrolysed biochar for soil amendment. *Resour. Technol.* 2016:2:S177–S185. https://doi.org/10.1016/j.reffit.2016.11.004
[41] Augustenborg C. A., Hepp S., Kammann C., Hagan D., Schmidt O., Müller C. Biochar and Earthworm Effects on Soil Nitrous Oxide and Carbon Dioxide Emissions. *J. Environ. Qual.* 2012:41(4):1203. https://doi.org/10.2134/jeq2011.0119
[42] Nelissen V., Saha B. K., Ruysschaert G., Boeckx P. Effect of different biochar and fertilizer types on N_2O and NO emissions. *Soil Biol. Biochem.* 2014:70:244–255. https://doi.org/10.1016/j.soilbio.2013.12.026
[43] Kirsanovs V., Blumberga D., Dzikevics M., Kovals A. Design of Experimental Investigations on the Effect of Equivalence Ratio, Fuel Moisture Content and Fuel Consumption on Gasification Process. *Energy Procedia* 2016:95:189–194. https://doi.org/10.1016/j.egypro.2016.09.045
[44] Kirsanovs V., Blumberga D., Veidenbergs I., Rochas C., Vigants E., Vigants G. Experimental investigation of downdraft gasifier at various conditions. *Energy Procedia* 2017:128:332–338. https://doi.org/10.1016/j.egypro.2017.08.321
[45] Ronsse F., S. van Hecke, Dickinson D., Prins W. Production and characterization of slow pyrolysis biochar: influence of feedstock type and pyrolysis conditions. *GCB Bioenergy* 2013:5(2):104–115. https://doi.org/10.1111/gcbb.12018
[46] Golubev N. Solid heat carrier technology for oil shale retorting. *Oil Shale* 2003:20(3):324–332.
[47] Reinik J. *et al.* Characterization of water extracts of oil shale retorting residues form gaseous and solid heat carrier processes. *Fuel Process. Technol.* 2015:131:443–451. https://doi.org/10.1016/j.fuproc.2014.12.024
[48] Raukas A., Siirde A. New trends in Estonian oil shale industry. *Oil Shale* 2012:29(3):203–205. https://doi.org/10.3176/oil.2012.3.01
[49] Kirsanovs V. *et al.* Biomass Gasification for District Heating. *Energy Procedia* 2017:113:217–223. https://doi.org/10.1016/j.egypro.2017.04.057
[50] Vélez J. F., Chejne F., Valdés C. F., Emery E. J., Londoño C. A. Co-gasification of Colombian coal and biomass in fluidized bed: An experimental study. *Fuel* 2009:88(3):424–430. https://doi.org/10.1016/j.fuel.2008.10.018
[51] Järvik O., Viiroja A., Kamenev S., Kamenev I. Activated sludge process coupled with intermittent ozonation for sludge yield reduction and effluent water quality control. *J. Chem. Technol. Biotechnol.* 2011:86(7). https://doi.org/10.1002/jctb.2610
[52] Paguio R. R., Saito K. M., Hund J. F., Jimenez R. M. Synthesis of Resorcinol Formaldehyde Aerogel Using UV Photo-Initiators for Inertial Confinement Fusion Experiments. *MRS Proc.* 2011:1306. https://doi.org/10.1557/opl.2011.476
[53] Peikolainen A.-L., Perez-Cabalerro F., Koel M. Low-Density Organic Aerogels From Oil Shale By-Product 5-Methylresorcinol. *Oil Shale* 2008:25(3):348–358. https://doi.org/10.3176/oil.2008.3.06
[54] Peikolainen A.-L., Volobujeva O., Aav R., Uibu M., Koel M. Organic acid catalyzed synthesis of 5-methylresorcinol based organic aerogels in acetonitrile. *J. Porous Mater.* 2012:19(2):189–194. https://doi.org/10.1007/s10934-011-9459-8



Oliver Jarvik PhD is a senior researcher at the Department of Energy Technology at Tallinn University of Technology (TalTech). He defended his PhD in 2011 on the topic of wastewater treatment by means of integrated chemical and biochemical oxidation. Since then he has studied thermodynamic properties of oils, shale oil conversion processes and implemented projects related to environmental effects of oil shale combustion. Oliver Jarvik is also the director of the bachelor study programm entitled "Chemical, Environmental and Energy Technology" at TalTech.
E-mail: oliver.jarvik@taltech.ee
ORCID iD: https://orcid.org/0000-0001-8530-2582



Mari Sulg is a third year PhD student at the Department of Energy Technology at Tallinn University of Technology. Her doctoral research investigates the use of additives in a biomass gasification in order to upgrade the local biomass and study gasification related problems. She holds a master's degree in applied chemistry and biotechnology. Her master's theses focused on biomass pretreatment with ionic liquids and lignin separation.
E-mail: mari.sulg@taltech.ee



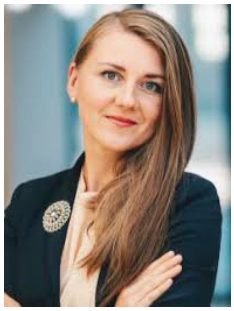
Pau Cascante Cirici ing., is an electrical and industrial engineer working as a MEP & FP engineer at PGI Engineering in Barcelona. He has experience in the computerization of the electrical distribution network and in the development of installation projects for industry and public construction. In 2019 he defended his Master Thesis "Biomass and Oil Shale Co-pyrolysis" at Tallinn University of Technology. The goals of the thesis were to study the Estonian biomass and oil shale co-pyrolysis at different temperatures, study the mass losses obtained from the experiments and make a characterization of the non-condensable gases obtained in the pyrolysis process.



Meelis Eldermann is a PhD student at the Department of Energy Technology at Tallinn University of Technology. His focus of research is Integrated Greenhouse Gas Emissions Analysis of Energy Production Processes from Estonian Oil Shale. Meelis is Vice Chairman of the Board and Technical Director of Viru Keemia Grupp, which is a private Estonian large-scale industrial enterprise. The key products in VKG's portfolio are various shale fuel oils and highly refined fine chemicals based on shale fuel oils.
E-mail: meelis.eldermann@taltech.ee



Alar Konist is a Professor and the head of the research group of Sustainable Energy and Fuels at the Department of Energy Technology of Tallinn University of Technology.
His interests include thermal energy processes that can offer pure CO_2 streams for sequestration and effects of activation conditions on preparation of porous carbon from oil shale. Prof. Konist's current R&D pursuits are strongly focused on oxy-fired CFBC technology, activation of oil shale and co-pyrolysis/co-gasification of biomass and oil shale. He is executive committee member at the International Energy Agency (IEA) Technology Collaboration Programme (TCP). Especially in the field of Fluidized Bed Conversion (FBC) of fuels applied to clean energy production provides a framework for international collaboration on energy technology development and deployment. He has been responsible for designing and building of new research laboratory for combustion processes. The most unique and self-designed device is 60 kWth CFB combustor.
https://orcid.org/0000-0001-5492-248X



Julija Gusca Dr. sc. ing., is a professor at the Institute of Energy Systems and Environment at the Riga Technical University. In 2011 she defended her PhD thesis "Research on Development of Latvian Energy Sector. Impact Assessment of Carbon Dioxide Capture and Storage Processes". Her research focuses on energy modelling, climate technologies and life cycle analysis. She also provides lectures on waste management to university students and is actively involved in development and implementation of projects related to environmental protection and sustainable energy management. Dr. sc. ing. J. Gusca is active in the Latvian Environmental Science and Education Council and the nongovernmental environmental organization "Nature Concerthall"
E-mail: julija.gusca@rtu.lv



Andres Siirde is Professor and the head of the Department of Energy Technology at Tallinn University of Technology (former TUT now TalTech). He received a PhD in Thermal Engineering at TUT in 1984, licenced engineer (1980). He has worked as a Senior Specialist in Eesti Energia Ltd (1998-2001). His current research is focused on combustion processes, and heat and power co-generation. He has gained experience in organising conferences and seminars, he is a member of several national and international committees. He has supervised 9 PhD dissertations, currently is supervising 3 PhD dissertations. He has participated in more than 50 R&D projects supported by public institutions and companies, majority of as principal investigator. He has 123 publications, which include 44 (ISI) indexed papers, 1 international book chapter, and 1 utility model.
E-mail: andres.siirde@taltec.ee
https://orcid.org/0000-0002-2352-6983

Publication II

Sulg, M., Konist, A., & Järvik, O. (2021). **Characterization of different wood species as potential feedstocks for gasification**. *Agronomy Research*, *19*(1), 276–299. https://doi.org/10.1016/j.biortech.2023.130086

Agronomy Research **19**(1), 276–299, 2021
https://doi.org/10.15159/AR.21.005

Characterization of different wood species as potential feedstocks for gasification

M. Sulg*, A. Konist and O. Järvik

Tallinn University of Technology, Department of Energy Technology, Ehitajate tee 5, UU19086 Tallinn, Estonia
*Correspondence: mari.sulg@taltech.ee

Received: August 26th, 2020; Accepted: January 12th, 2021; Published: January 18th, 2021

Abstract. This paper provides an extended overview of the chemical characteristics of 19 different wood species originating from Estonia. The variation of chemical composition in wood and bark was investigated using a variety of analytical techniques including WD-XRF, ICP-MS, and elemental analysis. Principal component analysis (PCA) was used to observe clustering in the sample set. It revealed a clear data clustering in terms of the wood and bark samples. Wood characteristics exhibit quite narrow ranges, on the other hand the composition of wood bark samples is significantly different and more distributed. The correlations and associations among 27 chemical parameters, including 16 ash-forming elements, were studied. Several significant positive correlations between Cr-Ni-Fe, Ca-Sr, Al-Na-Si-Ti, K-Mg-P, Fe-Zn-Cr-Ni-Cu, Ash-Ca, N-S-P and O-volatile matter were found. Most of the metallic components are negatively correlated with volatile matter, C, H, O and heating value and are positively related to each other, or no significant correlation was identified. Results are compared to literature data and technical quality standards for biomass. Biomass feedstocks availability and composition for gasification process was discussed. Wood samples had higher volatiles content than in bark which is an indication that higher conversion rate and lower gasification temperature can be used. Spruce, pine and black alder barks have higher fixed carbon content than other common species that may increase biochar yield. Commonly available woods like Scots pine, Norway spruce, aspen, birch, black alder and grey alder may considered as suitable feedstocks for gasification because of their low N, S, Cl, and ash content together with high volatile matter, however, relatively high total heavy metals content were found from birch and grey alder barks compared to other hardwoods.

Key words: biomass, biomass ash, chemical composition.

INTRODUCTION

In order to reduce the share of oil shale in the Estonian energy sector, renewable fuels like woody biomass are increasingly becoming a prospective alternative to produce energy and reduce environmental impacts like greenhouse gas (GHG) emissions and the amount of ash in landfills (Konist et al., 2013). Moreover, renewable energy directive sets targets for EU Member States to raise the share of renewable sources to at least 32% by 2030 (Official Journal of the European Union, 2009; Amanatidis, 2019). There is a huge perspective for increasing natural biomass use and for co-gasification with solid

fossil fuels in the energy sector (Vassilev et al., 2013). Via gasification, biomass can be converted to synthesis gas (syngas) which is a platform for heat and power production and an intermediate to produce chemicals. The co-gasification of many biomass/coal combinations were investigated by Koppejan & van Loo (2016), Thengane et al. (2019), Ma et al. (2019), Mallick et al. (2020). For Estonian, biomass co-combustion with oil shale would be a great alternative and offers near-term solutions to cut down CO_2 emissions.

Biomass is considered a highly reactive fuel (Koppejan & van Loo, 2016) and is easy to ignite at relatively low temperatures (García et al., 2012), however in industrial plants fuel feeding requires special measures (Caillat & Vakkilainen, 2013). From previous work of our research group (Maaten et al., 2019), biomass co-combustion with oil shale was found to be technologically promising. However, the characteristics of woody biomass and the possible effects of its composition on gasification were not included in the previous work.

Biomass composition is highly variable and depends on many factors, like the type of biomass, plant species and part of the plant; growth, transport and deposition conditions; geographic location; harvesting time and technique; pick-up of extraneous material (dust, dirt, soil) etc (Vassilev et al., 2010). A lot of different data about biomass composition are available, especially about major species in Nordic countries (Eriksson et al., 2004; Antero, 2006; Werkelin et al., 2010, 2011; Pesonen et al., 2014), but there is a lack of information involving Estonian biomass characteristics that may influence thermochemical biomass conversion processes like gasification. In order to estimate the Estonian renewable energy potential, it is necessary to investigate and map biomass characteristics that are related to regional biomass including all major species in Estonia. Furthermore, the present work includes also trace elements in local wood species which is important because Estonia is one of the major wood pellets exporters (Kaup, 2018).

A direct link exists between the chemical composition of biomass and the gas obtained by gasification. For example, the calorific value of syngas depends on the heating value and moisture content of the fuel (Kirsanovs & Žandeckis, 2015). Gil et al. (2019) statistically analysed biomass properties that influence gasification and found that carbon and hydrogen contents and the heating value of the biomass promote gas production. Also, important constituents that should be considered in gasifier selection are silica, chlorine, sulphur and alkali metals, which can cause slagging, fouling, hazardous emissions and high-temperature corrosion.

The gasification process is strongly influenced or controlled by the catalyst, which leads to high selectivity towards desired products. Catalysts can be expensive and rapidly deactivated when in direct contact with biomass, and therefore, are not in common use in industrial biorefineries. Using biomass with a suitable mineral composition that acts as a catalyst may improve the syngas composition. It is reported that alkali and alkaline earth metals are the best catalysts for promoting char gasification (Nzihou et al., 2013). K and Ca in feedstocks may exhibit a catalytic effect, enhancing the char gasification reactivity and leading to a higher carbon conversion rate. Early work on the importance of alkali catalysts was done by Elliott et al. (1984), who claimed the optimum concentration of catalyst to be 3×10^{-4}–1.5×10^{-3} mol of alkali per gram of biomass. Sueyasu et al. (2012) soaked feed biomass in a K solution before gasification to minimize tar emissions. Also, transition metals can participate as catalysts: Fe accelerates gasification and Ni prevents carbon deposition, which helps in conditioning biomass-derived syngas. Many studies have reported Ca to be a promising catalyst for increasing the gasification

rate of the char (Nzihou et al., 2013; Perander et al., 2015; Link et al., 2018). On the other hand, high alkali contents are considered a serious problem in biomass gasification due to contamination of equipment and increase maintenance costs (Ren et al., 2019).

The aim of this study was to analyse different types of wood species harvested from Estonia and analyse their suitability as gasification feedstock based on their characteristics and chemical composition. The selection of wood species was based on the principle that all dominant species harvested in Estonia should be covered in this study. Dominant wood species in Estonia are Scots pine (36%), silver birch (25.6%), Norway spruce (19.7%), aspen (7.0%), grey alder (6.8%) and black alder (3.8%) (Raudsaar et al., 2018). Additional tree species like common laburnum, hawthorn, European crab apple, blackthorn, common lilac, European ash, Norway maple, common plum, rowan, white willow, bird cherry, wych elm and common juniper were also selected for the current study. These generally have a small volume (1.2%) of the total growing stock compared to the dominant species. However, the wider selection of wood species gives a more detailed overview of biofuel characteristics and their relationships.

It is known that physicochemical properties of bark and wood differ (Olanders & Steenari, 1995; Frandsen et al., 2007; Vassilev et al., 2010; Werkelin et al., 2010; Johansson et al., 2016; Koppejan & van Loo, 2016); therefore, a comparison between bark and wood was made. Most studies have focused only on common wood species or analysed whole tree parts that contains both wood and bark and limited information on the separate components. Wood species were characterized by proximate and ultimate analysis, like ash content, heating value, volatile matter, C, H, N, S, Cl content and concentration of microelements/trace components. The data were compared to literature sources where possible. The results are compared with the data of Technical Specification (ISO 17225), which defines the biomass requirements and typical values and ranges for coniferous and broad-leaf wood and bark (results are obtained from a combination of research from Sweden, Finland, Denmark, Netherland and Germany). This study enhances our understanding of biomass composition as feedstock for gasification and will be beneficial to developing energy efficient processes.

MATERIALS AND METHODS

In total, 19 different wood species were investigated. These include 16 broad-leaf species: common laburnum (*Laburnum Anagyroides),* hawthorn (*Crataegus),* European crab apple (*Malus sylvestris*), blackthorn (*Prunus spinosa*), common lilac *(Syringa vulgaris),* European ash *(Fraxinus excelsior),* Norway maple *(Acer platanoides),* common plum *(Prunus domestica),* rowan (*Sorbus aucuparia),* white willow *(Salix alba),* bird cherry *(Prunus padus),* wych elm *(Ulmus glabra),* grey alder *(Alnus incana),* silver birch *(Betula pendula),* aspen *(Populus tremula),* black alder *(Alnus glutinosa).* 3 coniferous wood species were also included: common juniper *(Juniperus communis),* Scots pine *(Pinus Sylvestris),* Norway spruce *(Picea abies).* Samples originated from northern and southern Estonia in order to represent a wider population of tree species.

Wood samples were provided as air-dried logs. Wood and bark were separated mechanically before further analyses. The wood and bark ratios were determined gravimetrically after drying. Samples were grinded with a cutting mill and homogenized according to ISO 14780 solid biofuel sample preparation standard.

Wood samples were dried at 105 °C to a constant weight (ISO 18134-3). Ash content was determined at 550 °C (ISO 18122). Volatile matter was determined by burning the sample in a muffle furnace at 900 °C, following the procedure described in ISO 18123. Fixed carbon is the mass remaining after volatilization, excluding ash and moisture component. It can be calculated as subtracting from 100% the sum of the volatile matter and ash in percentage (Telmo et al., 2010).

Gross calorific value at constant volume ($q_{V,gr}$) was measured with IKA C2000 and IKA C5000 bomb calorimeters (ISO 18125). Gross calorific value on a dry basis ($q_{V,gr,d}$) includes the condensation enthalpy of water. Net calorific value, also called the lower heating value ($q_{p,net,d}$), is obtained when the condensation enthalpy of water is not included.

A Vario MACRO CHNS Elementar Analyser System was used to measure the C, H and N contents of the dry matter (ISO 16948). Oxygen content was calculated from the C, H, N, S, Cl and ash. Cl and S contents were measured with a Dionex 1000 ion chromatograph (ISO 16994). A Rigaku WD-XRF and Thermo Scientific iCAP Qc ICP-MS were used to determine ash forming elements and trace components in the biomass (ISO/TS 16996, ISO 16968).

Analysis results are presented according to the requirements of ISO standards. Uncertainties for every method is determined by the Nordtest (Magnusson et al., 2017) or ISO GUM method (Joint Committee For Guides In Metrology, 2008) or the relative standard deviation is given. Uncertainty estimations according to (a) the Nordtest approach (Uc, k = 2): HV – 3.9%; Ash – 43.0%; S – 3.2%, Cl – 4.2%, Volatiles – 4.6%; C – 1.10%; H – 4.1%; N – 19.1%; Mg – 9.4%; Fe – 9,1%; Mn – 5.4%; Zn – 11.4%; Cr – 14.8%; Ni – 16.4%; Sr – 6.6%; Ti – 11.3%; Cu – 7.4%; Pb – 8.1%; K – 19.8%; Na – 75.5% (b) ISO GUM approach (Uc, k = 2): O – 3.0%, FC – 27.7% and (c) RSD (rel%): Ca – 1.1%; Al – 29.2%; P – 2.2%; Si – 14.8%.

PCA was carried out with the aim of highlighting possible clusters of wood types characterized by similar properties. PCA is a chemometric technique for analysing the structure of the observations (wood and bark samples) and the variables (proximate, ultimate and trace metal analyses). PCA finds lines, planes and hyperplanes in the K-dimensional space that approximate the data as well as possible (Jackson, 1991; Jollife & Cadima, 2016). PCA was conducted via XLSTAT Statistical Software for MS Excel.

Chemical correlations between variables were determined in order to understand some of the fundamental relationships and trends. Data from the analysed woody biomass were subjected to the Pearson's correlation test (Plata, 2006) to calculate correlation coefficient values between 26 characteristics. The calculated correlation coefficient values include the statistically significant as well as statistically insignificant R^2 relationships, at a 95% confidence level.

RESULTS AND DISCUSSION

Proximate, ultimate analysis and heating value results are presented in Table 1. Minor and trace elements are shown in Table 2. Overall, 26 different parameters were measured for every sample. For better understanding, results are grouped as common and all wood species. Scots pine, silver birch, Norway spruce, aspen, grey alder and black alder are largely the most available resource in Estonia (Raudsaar et al., 2018), and therefore, some special attention is given to them.

Table 1. Proximate and ultimate analysis and heating value of different wood species. Literature data is included and refer to the wood type in the row above. (A – ash; VM – volatile matter; FC – fixed carbon; C – carbon; H – hydrogen; N – nitrogen; S – sulfur; O – oxygen; Cl – chlorine; HHV – higher heating value; LHV – lower heating value, wt% db – weight percent of dry basis)

Feedstock **Wood**	Content of wood or bark, %	Proximate analysis (wt% db)			Ultimate analysis (wt% db)						Heating value (MJ kg^{-1})	
		A	VM	FC	C	H	N	S	O	Cl	HHV	LHV
1. Broad-leaf wood (BLW)												
Aspen	87.2	0.4	87.0	12.6	50.2	6.2	0.1	0.01	43.1	< 0.01	20.07	18.72
Pesonen et al. (2014)		0.8			47.8	5.9	-				20.04	18.76
Bird cherry	90.1	0.5	86.4	13.1	48.1	6.5	0.1	< 0.01	44.8	0.01	19.11	17.69
Black alder	86.9	0.4	86.1	13.5	50.6	6.2	0.2	0.03	41.8	< 0.01	19.79	18.45
Blackthorn	81.9	0.6	84.4	15.0	48.4	6.3	0.2	< 0.01	44.5	0.01	19.24	17.86
Common laburnum	90.1	0.5	81.2	18.3	47.8	6.6	0.3	0.07	44.6	0.02	19.59	18.15
Common lilac	89.4	0.5	85.0	14.5	48.7	6.5	0.2	< 0.01	44.2	0.01	19.55	18.14
Common plum	57.9	0.5	83.2	16.3	49.5	6.4	0.2	< 0.01	43.4	0.01	19.65	18.26
European ash	94.9	0.4	84.9	14.7	49.1	6.5	0.1	< 0.01	43.8	0.01	19.44	18.03
European crab apple	96.3	0.8	83.5	15.8	47.0	6.5	0.1	0.02	45.6	0.01	19.22	17.81
Grey alder	90.8	0.4	85.7	13.9	49.9	6.6	0.2	< 0.01	43.0	< 0.01	19.95	18.52
Pesonen et al. (2014)		0.33			48.5	6.1	0.2				20.44	19.11
Hawthorn	92.9	1.6	81.6	16.8	48.1	6.5	0.2	0.05	43.6	0.01	19.82	18.40
Norway maple	92.7	0.6	86.2	13.3	48.7	6.5	0.1	< 0.01	44.1	0.01	19.36	17.95
Rowan	92.4	0.8	85.0	14.2	48.5	6.5	0.1	< 0.01	44.1	< 0.01	19.07	17.65
Silver birch	87.3	0.3	86.9	12.8	49.3	6.6	0.1	< 0.01	43.7	0.01	19.94	18.10
Pesonen et al. (2014)		0.4			48.2	6.1	-				19.80	18.46
White willow	92.7	0.5	85.2	14.3	48.4	6.5	0.1	< 0.01	44.5	< 0.01	19.72	18.31
Wych elm	89.8	1.8	79.9	18.4	49.6	6.5	0.2	< 0.01	42.1	0.01	19.69	18.29
Common BLW												
Mean	88.0	0.4	86.4	13.2	50.0	6.4	0.2	0.02	43.1	< 0.01	19.94	18.45
Minimum	86.9	0.3	85.7	12.6	49.3	6.2	0.1	0.01	42.6	< 0.01	19.79	18.10
Maximum	90.8	0.4	87.0	13.9	50.6	6.6	0.2	0.03	43.7	0.01	20.07	18.72
All BLW												
Mean	87.8	0.7	84.5	14.8	48.9	6.5	0.2	0.01	43.9	0.01	19.58	18.15
Minimum	57.9	0.3	79.9	12.6	47.0	6.2	0.1	0.01	42.1	< 0.01	19.07	17.65
Maximum	96.3	1.8	87.0	18.4	50.6	6.6	0.3	0.03	45.6	0.01	20.07	18.72

Table 1 (continued)

Feedstock	Content of wood or bark, %	Proximate analysis (wt% db)			Ultimate analysis (wt% db)						Heating value (MJ kg^{-1})	
		A	VM	FC	C	H	N	S	O	Cl	HHV	LHV
2. Coniferous wood (CW)												
Common juniper	86.2	1.2	82.3	16.6	48.8	6.8	0.2	< 0.01	43.1	0.01	20.65	19.16
Norway spruce	92.2	0.3	85.5	14.2	50.3	6.6	0.1	< 0.01	42.7	0.01	19.79	18.35
Scots pine	89.3	0.3	85.2	14.5	50.1	6.6	0.2	< 0.01	42.8	0.01	20.04	18.61
Mason et al. (2015)		2.0	82.5	17.5	47.4	5.3	1.3		45.9		18.6	
Common CW												
Mean	90.7	0.3	85.4	14.3	50.2	6.6	0.1	0.01	42.7	0.01	19.92	18.48
All CW												
Mean	89.2	0.6	84.3	15.1	49.8	6.7	0.1	0.01	42.8	0.01	20.16	18.71
Minimum	86.2	0.3	82.3	14.2	48.8	6.6	0.1	0.01	42.7	0.01	19.79	18.35
Maximum	92.2	1.2	85.5	16.6	50.3	6.8	0.2	0.01	43.1	0.01	20.65	19.16
Bark												
Broad-leaf wood (BLW)												
Aspen	12.9	3.5	79.8	16.7	53.4	6.4	0.9	0.07	35.8	< 0.01	21.37	19.99
Bird cherry	9.9	4.9	72.8	22.4	48.6	5.9	1.0	0.06	39.7	0.01	19.36	18.07
Black alder	13.1	3.2	71.3	25.5	55.1	5.9	1.3	0.05	34.4	0.02	21,97	20,69
Blackthorn	18.2	6.8	76.3	16.9	52.6	6.7	0.9	0.06	33.0	0.03	22.77	21.32
Common laburnum	9.9	2.7	77.0	20.3	49.2	6.4	2.5	0.10	39.0	0.02	21.02	19.62
Common lilac	10.6	3.2	76.3	20.5	48.6	6.1	0.9	0.07	41.1	0.01	19.85	18.52
Common plum	42.1	5.9	67.5	26.6	48.6	5.5	1.0	0.05	38.9	0.01	19.58	18.37
European ash	5.1	9.3	74.8	15.9	45.0	5.5	0.6	0.06	39.6	0.01	17.86	16.66
Zajac et al. (2018)		9.14										
European crab apple	3.7	16.9	69.2	13.9	44.1	5.2	1.0	0.07	32.8	0.01	16.47	15.34
Grey alder	9.2	2.7	74.0	23.4	53.5	6.5	1.1	0.05	36.2	< 0.01	22.27	20.86
Hawthorn	7.1	13.7	68.8	17.5	47.9	5.7	0.9	0.11	31.6	0.03	19.46	18.22
Norway maple	7.3	10.4	74.0	15.6	43.9	5.5	0.8	0.03	39.4	0.01	17.14	15.94
Bryers, (1996)		4	76.6	19.4	52	6.2	0.4	0.11	41.3			
Rowan	7.6	4.1	77.9	18.0	49.4	6.5	0.6	0.04	39.4	0.01	20.63	19.22

Table 1 (continued)

Feedstock	Content of wood or bark, %	Proximate analysis (wt% db)			Ultimate analysis (wt% db)						Heating value (MJ kg^{-1})	
		A	VM	FC	C	H	N	S	O	Cl	HHV	LHV
Silver birch	12.7	1.4	80.1	18.5	56.3	7.0	0.4	0.02	34.8	0.02	24.18	22.66
Bryers, (1996)		2.1	78.5	19.4	57.0	6.7	0.5	0.10	35.7			
White willow	7.3	9.0	69.6	21.4	45.8	5.4	0.6	0.08	39.1	0.01	18.48	17.30
Wych elm	10.2	13.4	72.0	14.6	44.8	5.5	0.9	0.07	35.4	0.01	17.31	16.12
Bryers, (1996)		8.1	73.1	18.8	50.9	5.8	0.7	0.11	42.5			
Common BLW												
Mean	12.0	2.7	76.3	21.0	54.6	6.4	0.9	0.05	35.3	0.01	22.45	21.05
Minimum	9.2	1.8	71.3	16.7	53.4	5.9	0.4	0.02	34.4	< 0.01	21.37	19.99
Maximum	13.1	3.5	80.1	25.5	56.3	7.0	1.3	0.07	36.3	0.02	24.18	22.66
All BLW												
Mean	11.5	6.8	73.5	19.8	49.3	6.0	0.9	0.06	37.0	0.01	19.97	18.68
Minimum	3.7	1.4	67.5	13.9	43.9	5.2	0.4	0.02	31.7	< 0.01	16.47	15.34
Maximum	42.1	16.9	80.1	26.6	56.3	7.0	2.5	0.11	41.2	0.03	24.18	22.66
Coniferous wood (CW)												
Common juniper	13.8	7.2	73.0	19.8	49.2	6.0	0.6	0.07	37.0	0.03	19.66	18.35
Norway spruce	7.9	7.9	71.1	21.0	48.4	5.6	0.6	0.02	37.6	0.01	18.72	17.50
Frandsen et al. (2007)		4.9			49.9	5.8	0.5	0.04		0.02		
Antero (2006)		2.3	77	23	51.1	6	0.4	0.03			20.3	19.0
Brunner et al. (2013)		4.8			49.8	5.7	0.34	0.03	40.8	0.01		
Scots pine	10.7	3.1	70.1	26.9	52.8	6.1	1.2	0.05	36.9	0.01	21.40	20.08
Jerzak, (2020)		1.56	67.98		55.95	5.29	0.05	0.03	37.03	0.012		
Antero (2006)		2.3	74.3	25.7	53.4	5.8	0.4	0.03			21.3	20.0
Vassilev et al. (2010)		1.9	73.7	24.4	53.8	5.9	0.3	0.07	39.9	0.01		
Common CW												
Mean	9.3	5.5	70.6	24.0	50.6	5.8	0.9	0.04	37.2	0.01	20.06	18.79
All CW												
Mean	10.8	6.0	71.4	22.6	50.1	5.9	0.8	0.05	37.2	0.01	19.93	18.64
Minimum	7.9	3.1	70.1	19.8	48.4	5.6	0.6	0.03	36.9	0.01	18.72	17.50
Maximum	13.8	7.9	73.0	26.9	52.8	6.1	1.2	0.07	37.6	0.03	21.40	20.08

Table 2. Minor and trace elements (ppm, db)

Feedstock	Al	K	Na	Ca	Si	Mg	Fe	P	Mn	Zn	Cr	Ni	Sr	Ti	Cu	Pb
Wood																
Broad-leaf wood (BLW)																
Aspen	51	479	20	890	51	648	47	100	3	6	-	0.2	2.3	-	0.9	< 0.1
Werkelin et al. (2010)	6	1,370	15	998	63	286	5		49							
Bird cherry	22	547	17	1,482	68	280	46	98	9	5	1.5	0.2	2.3	2.7	0.4	0.1
Black alder	17	354	6	1,171	35	354	43	104	10	6	-	0.1	2.9	-	1.5	-
Blackthorn	23	779	29	1,920	55	415	40	96	1	2	1.1	0.1	7.6	0.5	0.4	-
Common laburnum	29	766	32	1,146	95	338	41	139	2	3	0.4	0.1	4.8	-	0.6	-
Common lilac	24	693	34	1,127	61	388	41	194	2	15	0.1	-	3.3	-	0.1	-
Common plum	23	699	31	1,060	66	297	43	143	1	3	0.2	0.1	3.4	1.9	1.8	-
European ash	17	597	114	891	46	360	40	81	0.2	2	0.1	0.4	3.0	-	1.5	-
European crab apple	29	869	41	2,551	58	365	42	124	1	5	0.2	0.1	10.1	2.4	0.8	-
Grey alder	19	496	12	1,091	35	268	41	137	8	8	0.4	0.1	2.2	-	0.9	0.3
Hawthorn	40	1,124	232	5,522	100	394	45	372	2	12	0.5	0.2	6.9	0.9	2.9	-
Norway maple	20	769	22	1,316	48	417	40	162	13	2	0.2	0.2	1.4	0.1	0.4	-
Rowan	17	1,093	40	1,692	38	513	41	79	114	7	1.3	1.0	3.1	1.1	0.4	0.4
Silver birch	14	473	12	1,036	21	421	39	51	44	14	0.3	0.3	2.5	2.1	0.2	0.5
Werkelin et al. (2010)	2	315	4	636	77	92	6		102							
White willow	28	1,192	31	975	51	333	43	288	2	17	0.1	0.1	2.2	2.4	1.0	-
Wych elm	21	4,847	47	3,371	175	391	43	172	1	2	0.2	0.0	10.4	0.3	2.0	-
Common BLW																
Mean	25	451	13	1,047	36	423	43	98	16	8	0.2	0.2	2.5	0.5	0.9	0.2
Minimum	14	354	6	890	21	268	39	51	3	6	0.0	0.1	2.2	0.0	0.2	0.0
Maximum	51	496	20	1,171	51	648	47	137	44	14	0.4	0.3	2.9	2.1	1.5	0.5
All BLW																
Mean	25	986	45	1,703	63	386	42	146	13	7	0.4	0.2	4.3	0.9	1.0	0.1
Minimum	14	354	6	890	21	268	39	51	0	2	0.0	0.0	1.4	0.0	0.1	0.0
Maximum	51	4,847	232	5,522	175	648	47	372	114	17	1.5	1.0	10.4	2.7	2.9	0.5

Table 2 (continued)

Feedstock	Al	K	Na	Ca	Si	Mg	Fe	P	Mn	Zn	Cr	Ni	Sr	Ti	Cu	Pb
Coniferous wood (CW)																
Common juniper	30	591	43	5,817	49	371	42	181	5	5	0.4	0.2	3.0	1.7	0.9	-
Norway spruce	14	246	13	1,118	26	233	38	17	11	5	0.3	0.2	8.9	1.2	0.3	1.4
Werkelin et al. (2010)	3	235	7	752	93	99	5		100							
Scots pine	16	530	16	718	28	241	41	103	6	6	0.3	0.1	1.4	-	1.0	0.1
Werkelin et al. (2010)	4	407	15	641	123	189	8		81							
Common CW																
Mean	15	388	15	918	27	237	40	60	9	5	0.3	0.1	5.2	0.6	0.7	0.7
All CW																
Mean	20	456	24	2,551	34	282	40	100	7	5	0.3	0.2	4.5	1.0	0.7	0.5
Minimum	14	246	13	718	26	233	38	17	5	5	0.3	0.1	1.4	0.0	0.3	0.0
Maximum	30	591	43	5,817	49	371	42	181	11	6	0.4	0.2	8.9	1.7	1.0	1.4
Bark																
Broad-leaf wood (BLW)																
Aspen	70	4,727	86	9,527	164	1,618	55	812	25	123	-	0.1	14.1	0.3	2.1	-
Bird cherry	316	1,787	142	22,762	616	645	391	589	215	108	254.7	128.5	27.8	14.5	36.3	3.5
Blackthorn	84	1,959	125	26,708	222	1,268	65	615	11	13	1.4	0.9	87.4	3.5	6.2	0.2
Black alder	85	122	66	13,191	255	470	60	195	75	27	1.0	0.5	26.8	1.6	9.5	1.2
Common laburnum	154	5,468	73	6,479	431	1,451	115	1381	11	52	3.7	0.8	22.1	6.0	3.9	0.4
Common lilac	209	3,972	197	10,259	659	1,154	167	757	21	119	1.5	37.6	24.0	9.2	3.4	0.6
Common plum	209	2,968	120	29,078	492	934	261	490	18	38	78.7	44.6	66.3	14.5	20.8	1.2
European ash	605	1,503	359	34,067	2,930	962	1377	300	103	960	407	236.7	64.1	37.5	41.6	2.7
European crab apple	393	4,039	297	63,910	1,379	1,434	125	985	28	135	9.9	1.7	189.6	31.6	6.7	1.8
Grey alder	393	1,414	63	8,715	247	476	494	404	62	109	191.7	92.3	14.3	7.1	26.7	4.5
Hawthorn	2,810	2,432	1,204	38,453	9,487	946	581	777	61	139	8.2	2.0	48.4	160	14.8	4.6
Norway maple	343	3,817	181	43,797	3,068	1,198	154	619	233	99	3.3	1.9	29.3	9.4	6.1	0.8
Rowan	117	3,131	123	15,863	345	1,246	120	505	833	139	6.9	2.7	21.7	2.8	9.6	0.8
Silver birch	102	606	38	4,489	163	703	184	195	201	157	59.9	31.0	10.5	2.4	5.2	0.4

Table 2 (continued)

Feedstock	Al	K	Na	Ca	Si	Mg	Fe	P	Mn	Zn	Cr	Ni	Sr	Ti	Cu	Pb
Werkelin et al. (2010)	19	1,710	14	7,860	114	323	24		534							
White willow	146	5,741	289	33,966	910	1,481	71	800	16	332	0.3	0.2	24.2	2.6	4.6	0.1
Wych elm	153	5,067	149	49,587	4,140	1,102	73	870	11	13	1.8	1.2	138.3	8.7	8.6	0.6
Common BLW																
Mean	163	1,717	63	8,981	207	817	198	402	91	104	84.2	31.0	16.4	2.9	10.8	1.5
Minimum	70	122	38	4,489	163	470	55	195	25	27	1.0	0.1	10.5	0.3	2.1	0.0
Maximum	393	4,727	86	13,191	255	1,618	494	812	201	157	191.7	92.3	26.8	7.1	26.7	4.5
All BLW																
Mean	356	2,800	207	25,421	1,416	995	250	598	116	152	70.7	37.9	54.1	17.7	12.6	1.4
Minimum	70	122	38	4,489	163	470	55	195	11	13	0.3	0.1	10.5	0.3	2.1	0.0
Maximum	2,810	5,741	1,204	63,910	9,487	1,618	1,377	1,381	833	960	407.2	236.7	189.6	160	41.6	4.6
Coniferous wood (CW)																
Common juniper	405	1,574	302	27,033	1,094	566	151	424	41	39	5.3	1.2	15.4	18.5	4.0	3.1
Norway spruce	79	786	86	32,175	193	795	114	333	193	231	98.5	45.3	188.9	2.8	14.3	0.7
Frandsen et al. (2007)	616	2,493	103	13,196	3,866	781	377	361	428							
Werkelin et al. (2011)	98	2,030	26	8,350	171	865	39	452	714							
Antero (2006)		3,003	89													
Brunner et al. (2013)		1,825	79	13,450	1,810	822		338		85						
Scots pine	87	2,095	29	12,947	102	459	186	310	48	50	138.2	91.4	15.7	3.5	14.4	0.2
Ragland et al. (1991)	2,149	1,333	280	5,282	5,278	1,137	609									
Werkelin et al. (2010)	908	3,180	22	6,350	60	874	52		343							
Common CW																
Mean	83	1,441	58	22,561	148	627	150	322	120	141	118.4	68.3	102.3	3.2	14.3	0.4
All CW																
Mean	190	1,485	139	24,052	463	607	150	356	94	107	80.7	45.9	73.3	8.3	10.9	1.3
Minimum	79	786	29	12,947	102	459	114	310	41	39	5.3	1.2	15.4	2.8	4.0	0.2
Maximum	405	2,095	302	32,175	1,094	795	186	424	193	231	138.2	91.4	188.9	18.5	14.4	3.1

It is noticeable that in most of the species bark is less than 10% of the overall stem wood (Table 1). However, there are some exceptions like common plum where the bark ratio reached over 42%. This result may be explained by the factors that affect bark thickness: wood species, the age and growing conditions (Sonmez et al., 2007; Koman & Feher 2015). It should be considered that wood chips are generally produced from whole trees; therefore, the prominent component is wood and bark makes only a small contribution to the average. However, bark is a main source of ash, different extractives and elements that may affect the biomass gasification process and need careful consideration.

Ash yield

Ash content is an important quality parameter of biomass. A high content of ash is undesirable in most conversion processes as it causes problems related to utilization and process design, reduces the heating value (Elbersen et al., 2017) and affects dust emission (Koppejan & van Loo, 2016). Biomass with an ash content over 10% is considered to have a high risk of slag formation (Ren et al., 2019). However, there is no evidence that the ash content in a gasification process directly influences gas composition, although ash can cause a variety of problems like slagging, which is influenced by the presence of alkaline metals in biomass.

Results show that the wood part of most of the species has a relatively low ash content ranging between 0.3 to 1.8%. Only hawthorn and wych elm have a higher ash content, 1.56% and 1.75%, respectively, compared to typical broad-leaf wood values (0.2–1.0%). The ash content of pine and spruce (0.2–0.3%) matches standardized values of 0.1–1.0% according to ISO 17225. However, common juniper has a higher ash content than other softwoods. Mason et al. (2015) report much higher ash values for pine and willow, 1.9% and 2.0%, respectively. On the other hand, the alder ash content is similar to that from Pesonen et al. (2014). It is stated that the ash content in untreated wood of different species is 0.1% to 0.6% and in bark 3% to 5% (Ragland et al., 1991), but it can reach up to 20% for some biomasses (Caillat & Vakkilainen, 2013). In gasification mostly a mixture of bark and wood is used; therefore, ash content is primary dependent on the bark content of the feedstock. Results show that broad-leaf trees have higher ash contents that coniferous wood, which is similar to earlier findings (Alakangas et al., 2016).

The ash content of bark (1.4–16.9%) was significantly higher than that of stem wood (0.3–1.8%). Silver birch, alder and common laburnum have the lowest ash contents in the bark: 1.4%, 2.7% and 2.7%, respectively. These values lie between the typical broad-leaf wood bark ash content values of 0.8–3.0% according to ISO 17225. The bark ash content of birch and European ash, 1.4 and 9.3%, respectively, are similar to the values of 2.1% (Bryers, 1996) and 9.14% (Zając et al., 2018) reported in previous studies. However, most of the analysed Estonian hardwood barks have higher ash values than typical hardwood. The wood species with the highest bark ash content are European apple tree 16.9%, hawthorn 13.7%, wych elm 13.4% and Norway maple 10.4%. High ash content may be due to mossy bark. Contaminants from soil can lead to severe problems like fouling and slagging (Caillat & Vakkilainen, 2013). The ash content of 3.1% for pine bark was within the typical range of values for softwood bark (< 1.0–3.0%) and comparable to the value reported by Antero (2006) (2.3%). Norway spruce and common juniper have higher ash contents of 7.9 and 7.2%, respectively.

A high ash content is normally undesirable since it complicates the operational process. Moreover, it is stated that higher ash content promotes the growth of CO and H_2 concentration in the syngas and the decrease of CH_4 content (Kirsanovs & Žandeckis, 2015). On the other hand, it is possible to use biomass with a suitable ash composition that may act as a natural catalyst for char gasification and tar removal. Therefore, ash yield alone is not a sufficient parameter for estimating the suitability of different woody samples. The chemical composition, especially alkali and alkali-earth metals concentrations, should additionally be considered (discussed in the following paragraphs).

Heating value

Heating value (HV) is an expression of the energy content released when burnt in air (McKendry, 2002). HV is not highly variable from one tree species to another (Table 1). The HHV of wood lays between 19.07 and 20.65 MJ kg^{-1}. These results are similar to earlier findings, where no significant differences in HVs of different wood species and barks were found (Pesonen et al., 2014). On contrary, HHV of bark is much more distributed and values range between 16.47 and 24.18 MJ kg^{-1}. Moreover, silver birch bark has the highest HV of 24.18 MJ kg^{-1} exceeding a typical hardwood bark HV of 20.0 MJ kg^{-1} (according to ISO 17225). This result may be explained by the fact that birch bark is rich in extractives and suberin (Pinto et al., 2009) that may contribute to higher HV. Also, it is reported that lignin content has strong positive correlation to HV (Demirbaş, 2001). However, Pesonen et al. (2014) states that the HV of silver birch wood HV is much lower, 18.46 MJ kg^{-1}, but aspen and alder have very similar results to current results. The lowest HV determined was for European crab apple bark, 16.47 MJ kg^{-1}, where a negative correlation is seen between ash content (16.91%) and HV. The HV of the pine bark analysed is similar to those reported by Antero (2006), McKendry (2002) and Phyllis2 Database. In contrast, spruce bark has a lower HV than reported by Antero (2006) and the Phyllis2 Database, but still lies between values that are typical for softwood barks. Overall, the mean HVs of hardwood and softwood are very similar, although softwood samples tend to have a slightly higher HV, as supported by previous findings (Ragland et al., 1991; Nurmi, 2000).

The HHV of the biomass along with C and H content were found to promote the concentrations of CO and combustible gas, the calorific value of the product gas and the gasification conversion (Gil et al., 2019). Therefore, bark samples that have much higher HHV than wood samples may appear to be more suitable feedstocks for gasification.

Volatile matter

Data for the volatile matter (VM) of the biomass samples indicates that there is no significant difference between broad-leaf and coniferous wood. The same trend is seen in bark samples. Wood samples have higher VMs compared to barks (79.9–86.6% versus 67.5–80.1%). According to the literature, VM in woody biomass lies between 70.20 and 93.99% (Miles et al., 1996; Koziński & Saade, 1998; McKendry, 2002; Cuiping et al., 2004; Demirbas, 2004; Eriksson et al., 2004; Grammelis et al., 2006; Saidur et al., 2011; García et al., 2012; Miccio et al., 2012; Rizvi et al., 2015; Lu et al., 2018). The VM of willow and pine wood is similar to that result reported by Mason et al. (2015). Silver birch bark had the highest VM among all barks, similar to results obtained by Bryers (1996). The VM content of Norway spruce coincides with the content reported by Antero (2006).

According to the literature, a higher volatile matter increases the biomass conversion rate in comparison to biomasses with higher fixed carbon content (Roldan, 2018). Therefore, the conversion rate of wood samples in thermochemical processes should be much higher than bark samples. Kurkela (1996) found that a lower volatiles content decreases the reactivity of pine bark compared to wood, and therefore, pine bark gasification needs an extra 100 °C increase in the temperature. These findings suggest that samples with higher VM matter, like wood samples, are preferred for gasification when a lower gasification temperature is required.

Fixed carbon

Fixed carbon (FC) is the carbon found in the material that remains after volatile materials are emitted. FC content is linked to the biochar yield which is reported to be higher for biomasses with high FC (Roldan, 2018). FC in wood and bark samples varies between 12.6–18.4% and 13.9–26.9%, respectively. It is possible to hypothesise that gasification of bark samples yields more biochar. Biochar may be a valuable by-product that can be used as a soil amendment or in carbon sequestration applications (Hansen et al., 2015). Therefore, from the analysed data set the most suitable samples for a high biochar yield would be spruce and black alder bark that have by far the highest FC, low ash content and belong to prevalent wood species in Estonia.

Carbon

The typical range of carbon (C) content in softwood is between 47–54% and in hardwood 48–52%, on a dry basis, according to ISO 17225. The present study shows that there is no significant difference in C content between hardwood and softwood wood, as in hardwood it varies between 47.0 to 49.9% and in softwoods from 48.8 to 50.3%. On the other hand, bark samples have a much higher variation between different species – 43.9 to 56.3%. Silver birch bark stands out as having the highest C content of 56.3%, which is similar to results reported in the literature (Bryers, 1996). Wych elm, white willow, European ash, European crab apple and Norway maple have C content below the typical hardwood bark range of 47 to 55% (ISO 17225). Norway spruce, however, has a lower C content than Scots pine, 48.4% and 52.8%, respectively. In the literature the same pattern is apparent between pine and spruce bark (Antero, 2006; Frandsen et al., 2007; Vassilev et al., 2010; Brunner et al., 2013; Jerzak, 2020).

Hydrogen

Hydrogen (H) is one of the parameters that has a higher influence on the heating value along with carbon, oxygen and sulfur (Telmo et al., 2010). According to the results, most of the species have higher H content in the wood than the bark with a few exceptions like silver birch, blackthorn, rowan and aspen. The H content of the analysed samples in broad-leaf wood is slightly higher than reported in the literature (Pesonen et al., 2014; Mason et al., 2015) lying between 6.3 and 6.6%. Hardwood wood, on the other hand, have a wide distribution in H content, varying between 5.2–7.0%. The H content of softwood bark is similar that reported in the literature (Antero, 2006; Vassilev et al., 2010; Brunner et al., 2013; Phyllis2 Database).

A higher H content is preferred in biomass as it results in a higher concentration of H_2 and a higher H_2/CO ratio in the gasification outlet gas according to hierarchical cluster and principal component analyses conducted by Gil et al., (2019).

Oxygen

Lignocellulosic fuel has a comparatively high oxygen (O) content that contributes to low heating values. Oxygen content is one of the most significant parameters along with gasification temperature, that determine the chemical efficiency of the gasification (Schuster et al., 2001). O content is very similar in all woods and ranges between 42.1 to 45.6%, but in bark samples it lies between 31.6 and 41.3%. O content in the literature is reported mostly on the basis of the whole wood and the content varies between 40.6 and 44.6% among different wood species (Miles et al., 1996; Koziński & Saade, 1998; Cuiping et al., 2004; Demirbas, 2004; Eriksson et al., 2004; Saidur et al., 2011; García et al., 2012; Miccio et al., 2012; Brunner et al., 2013; Lu et al., 2018; Phyllis2 Database). Kirsanovs & Žandeckis (2015) point out that lower O content in the feedstock necessitates a higher amount of air to be injected into the gasifier in order to achieve the required equivalent ratio. In addition, a higher C/O mass ratio in the fuel increases the heating value of the syngas. Therefore, common hardwood barks like grey alder, black alder, silver birch and aspen that have higher C/O mass ratios, ranging between 1.43 to 1.62, may be a more suitable feedstock when the highest HV of syngas is required.

Nitrogen

Results show that nitrogen (N) content in bark is remarkably higher than in wood, varied from 0.1 to 0.3% and 0.4 to 2.5%, respectively. Typical N content in hardwood and softwood lays between < 0.01 to 0.5% (ISO 17225). Common laburnum bark differs greatly from other species and the N content reaches 2.5%. A relatively high N content (1.2%) was also found in Scots pine bark. On the one hand, this is similar to the result for pine wood, which has a N content of 1.3%, as reported by Mason et al. (2015). However, Brunner et al. (2013), Frandsen et al. (2007), Antero (2006) report much lower N contents in softwood bark ranging between 0.05–0.5%. N is an important characteristic that should be considered in gasification and design of gas cleaning section. N is converted into N_2, NH_3 and HCN during gasification. The N_2 content in the syngas decreases the calorific value of the syngas produced. Ammonia can be eliminated from product gas by increasing the gasification temperature so it decomposes to nitrogen (Devi et al., 2003). Also, NH_3 can be separated from the gas flow by adding H_2SO_4 (Zisopoulos et al., 2018), where the product ammonium sulphate can be further used as fertilizer. Samples that have a higher N value should be avoided if possible, e.g. common laburnum, black alder and Scot's pine bark.

Sulphur and chlorine

The advantage of untreated woody biomass is the low content of sulphur (S) and chlorine (Cl). The presence of Cl and S in the feedstock often leads to the formation of sulphates and facilitates fouling (Miles et al., 1996). The problem is that HCl formation and condensation can occur on the cooler parts of equipment, often on heat exchangers, which will lead to corrosion of the metal surface. In gasification, S is transformed to H_2S or COS, but as the concentrations are low, the issue is not very common in biomass gasification. It is seen that most of the sulphur originates from the bark as a majority of wood samples have an S content below 0.01%. Common laburnurm, hawthorn and European crab apple stand out as they have relatively high S contents both in wood and bark compared to other tree species, and in order to avoid S and Cl related problems, these samples can be excluded from the selection of possible feedstocks for gasification.

The S content of fuel increases when the bark content is higher. Cl content in barks is slightly higher compared to woods, ≤ 0.01% and 0.01–0.03%, respectively. Higher Cl contents can be found when woody biomass contains needles or leaves (Alakangas et al., 2016), however these parts of the tree were out of the scope of this study.

Minor and trace elements

According to Zevenhoven & Kilpinen (2001), the elements can be classified as follows: major (> 1.0%), minor (0.1–1.0%) and trace (< 0.1%) elements. The present results show that elemental classification is slightly different and changeable in the case of wood and bark. Major elements in both are C, H, N, O, but also Ca can be classified as a major component in bark where its concentration may exceed 6%. However, in stem wood Ca is a dominant minor element and all other determined elements: Al, Na, Si, Mg, Fe, P, Cu, Mn, Ni, Zn, Sr, Cr, Ti, Pb, belong to the trace elements range. K is found as either a minor or trace element depending on the wood type. In the bark samples, there is variation between different species and K, Mg, Si can be classified as minor elements. All in all, the major and minor elements in biomass, in decreasing order of abundance, are C > O > H > N > Ca > K > Mg > P > S > Cl > Si > Na > Fe > Al > Mn > Zn > Sr > Cr > Ni > Ti > Cu > Pb.

Many of the tested wood and bark samples contain high concentrations of Ca, K, Mg and Na that, according to different studies, improve the gasification process (Elliott et al., 1984; Sueyasu et al., 2012; Perander et al., 2015; Ren et al., 2019). These results support earlier findings that the majority of ash forming elements are found within the bark (Kleinhans et al., 2018). Also, Werkelin et al. (2011) investigated the chemical composition of different parts of Norway spruce and reported lower Al, K, Si and Mn in wood than in the present work and much higher values of Mn and K in bark. Scots pine and silver birch, on the other hand, show small amounts of Al, Na and Si. Generally, common wood species stand out as having relatively low contents of ash-forming elements compared to all analysed species.

Ca is the dominate ash forming element in biomass, especially in bark samples where concentrations were up to twelve times higher than those of the wood samples. Similar findings have been reported by Kleinhans et al. (2018). The Ca content of the wood species ranged within rather wide limits, 718–63,910 ppm, depending on the wood type. The highest Ca content of 63,910 and 49,587 ppm was found from the European crab apple and wych elm bark samples, respectively. The lowest Ca content was observed in Scots pine, aspen and European ash wood samples: 718, 890 and 891 ppm, respectively. A higher Ca content in the feedstock is advantageous. In some cases, limestone as a source of calcium is added because it acts as a sulphur capture technique and prevents agglomeration (Miles et al., 1996). Koppejan & van Loo (2016) indicate that ashes of agricultural crops with low concentrations of Ca and high concentrations of potassium (K) start to sinter and melt at significantly lower temperatures than woody biomass. In this study, the Ca content of most of the samples outweigh K content, but there are two exceptions: willow and wych elm wood – these samples have a much higher probability to cause lower ash melting behaviour.

K is the second most abundant alkali element in biomass. K is stated as one of the elements that in high concentrations together with the high silica and chlorine content, is known to create ash deposit problems (Kurkela, 1996). K is detected as KCl, K_2SO_4, K_2CO_3, K_3PO_4 in biomass ash (Mlonka-Mędrala et al., 2020). Results show that broad-leaf

wood species tend to have higher K contents than softwood. On the other hand, K is reported as an effective catalyst in gasification and it enhances tar reforming (Sueyasu et al., 2012; Nzihou et al., 2013). Gil et al. (2019) also found that a high H_2 content and high H_2/CO ratio in the gas product are related to the higher H/O ratio and K_2O in biomass. Therefore, samples that have a higher K content may be favoured instead, when a low content of tar in the syngas is required, although sintering problem should be considered.

It has been found that the Si content in hardwood bark may reach up to 2% and in case of softwood up to 0.5% (ISO 17225). Interestingly, all analysed samples had lower Si content than typical values, from 0.002 to 0.41% (except hawthorn bark with 0.9% Si). Although, a similar pattern exists where bark has majority of Si content compared to the whole wood. These results seem to be consistent with other research which found that the silica content of clean bark is higher than that of wood (Ragland et al., 1991). The high silica content in bark or wood originates from soil components and sand.

Iron (Fe) content varied between 38 ppm and 1,377 ppm. It is stated that the typical Fe content in woods lies between 0–100 ppm and in bark it may reach up to 800 ppm (ISO 17225). European ash wood was enriched in Fe (1,377 ppm), but all other samples are comparable to typical values.

Al content in most of the woods and barks are in accordance to technical standard, that propose values of < 10 to 1,200 ppm (ISO 17225). Smallest amount of Al is found from common species (< 393 ppm). On the other hand, hardwood barks show higher concentrations than recommended values in standard, from 70 to 2,810 ppm. Na content in woods and barks are below 200 ppm and 1,200 ppm, respectively and are in accordance to typical values.

Woody biomass has higher amounts of heavy metals than annually harvested crops because wood has a longer rotation period for accumulation of heavy metals (Koppejan & van Loo, 2016). Barks of hawthorn, European ash, bird cherry, and rowan stand out as they have relatively high amount of Mn, Zn, Cr, Ni, Sr, Ti, Cu and Pb. Silver birch and grey alder have higher concentration of heavy metals than other common hardwoods. In addition, Norway spruce bark has twice as high of a heavy metals concentration as Scots pine bark.

Correlations between characteristics

The Pearson correlation coefficient was used to assess linear associations between biomass parameters in order to elucidate which feedstock features have an impact on each other (Table 3). The strength of the correlation is described using the guide that Evans (1996) suggests for the absolute value of r: 0.40–0.59 as 'moderate'; 0.60–0.79 as 'strong'; 0.80–1.0 as 'very strong'. Knowing correlations between variables gives the opportunity to predict biomass composition without a need to carry out a full set of analyses.

The present data show very strong positive correlations ($r \geq 0.8$) between the following characteristics: Cr-Ni-Fe, Ca-Sr, HV-C, Al-Na-Si-Ti, K-Mg-P, Fe-Zn-Cr-Ni-Cu, Ash-Ca, N-S-P and O-VM. Most of the ash forming elements like Si, Ca, K, P, Al, Mg, Fe, S, Sr, Na and Ti have moderate to very strong correlations with ash. Also, Mn is classified as an ash-forming element according to Werkelin et al., (2011). Cr and Ni together with Ca, Fe and Cu are non-volatile metals that are found to exit principally in equal concentrations in the bottom ash and the fly ash (Nzihou & Stanmore, 2013). However, this was not supported in the present study where no significant relationships between ash yield and Mn, Cr and Ni were determined.

Table 3. Pearson's correlation matrix between any two variables ($P \leq 0.05$)

	Ash	VM	FC	C	H	N	S	O	Cl	HHV	Al	K	Na	Ca	Si	Mg	Fe	P	Mn	Zn	Cr	Ni	Sr	Ti	Cu	Pb	
Ash	1.0	-0.8	0.2	-0.5	-0.8	0.5	0.7	-0.7	0.5	-0.5	0.6	0.6	0.7	1.0	0.7	0.7	0.4	0.7	0.1	0.4	0.2	0.2	0.8	0.6	0.4	0.5	+1
VM	-0.8	1.0	-0.7	0.1	0.8	-0.7	-0.8	0.8	-0.5	0.1	-0.5	-0.6	-0.5	-0.8	-0.5	-0.6	-0.4	-0.7	-0.2	-0.4	-0.4	-0.4	-0.6	-0.4	-0.6	-0.5	
FC	0.2	-0.7	1.0	0.3	-0.3	0.6	0.4	-0.5	0.3	0.3	0.1	0.2	0.1	0.3	0.0	0.2	0.2	0.3	0.2	0.2	0.3	0.3	0.3	0.1	0.5	0.3	
C	-0.5	0.1	0.3	1.0	0.5	0.1	-0.1	-0.2	0.1	0.9	-0.2	-0.3	-0.3	-0.5	-0.4	-0.2	-0.2	-0.3	0.0	-0.3	0.0	0.0	-0.4	-0.2	-0.1	0.0	
H	-0.8	0.8	-0.3	0.5	1.0	-0.4	-0.6	0.5	-0.1	0.6	-0.4	-0.5	-0.5	-0.8	-0.5	-0.5	-0.4	-0.5	0.0	-0.5	-0.3	-0.3	-0.7	-0.4	-0.5	-0.4	
N	0.5	-0.7	0.6	0.1	-0.4	1.0	0.8	-0.7	0.4	0.2	0.3	0.6	0.3	0.5	0.3	0.6	0.3	0.8	0.1	0.2	0.2	0.2	0.4	0.2	0.4	0.4	
S	0.7	-0.8	0.4	-0.1	-0.6	0.8	1.0	-0.8	0.5	-0.1	0.6	0.7	0.6	0.7	0.6	0.8	0.4	0.9	0.1	0.4	0.2	0.2	0.4	0.5	0.4	0.5	
O	-0.7	0.8	-0.5	-0.2	0.5	-0.7	-0.8	1.0	-0.6	-0.2	-0.5	-0.4	-0.5	-0.7	-0.5	-0.6	-0.3	-0.6	-0.2	-0.3	-0.2	-0.2	-0.6	-0.5	-0.4	-0.5	
Cl	0.5	-0.5	0.3	0.1	-0.1	0.4	0.5	-0.6	1.0	0.2	0.5	0.1	0.6	0.4	0.5	0.3	0.2	0.4	0.0	0.1	0.0	0.0	0.3	0.5	0.1	0.4	
HHV	-0.5	0.1	0.3	0.9	0.6	0.2	-0.1	-0.2	0.2	1.0	-0.1	-0.2	-0.2	-0.5	-0.3	-0.1	-0.1	-0.1	0.1	-0.2	0.0	0.0	-0.4	-0.2	-0.1	0.0	
Al	0.6	-0.5	0.1	-0.2	-0.4	0.3	0.6	-0.5	0.5	-0.1	1.0	0.2	1.0	0.4	0.9	0.2	0.5	0.3	0.1	0.3	0.2	0.2	0.2	1.0	0.4	0.7	
K	0.6	-0.6	0.2	-0.3	-0.5	0.6	0.7	-0.4	0.1	-0.2	0.2	1.0	0.3	0.5	0.3	0.8	0.1	0.8	0.1	0.2	0.0	0.0	0.3	0.1	0.1	0.1	
Na	0.7	-0.5	0.1	-0.3	-0.5	0.3	0.6	-0.5	0.6	-0.2	1.0	0.3	1.0	0.6	0.9	0.4	0.5	0.4	0.1	0.3	0.1	0.1	0.3	1.0	0.3	0.6	
Ca	1.0	-0.8	0.3	-0.5	-0.8	0.5	0.7	-0.7	0.4	-0.5	0.4	0.5	0.6	1.0	0.6	0.7	0.4	0.6	0.2	0.4	0.3	0.2	0.8	0.5	0.5	0.5	
Si	0.7	-0.5	0.0	-0.4	-0.5	0.3	0.6	-0.5	0.5	-0.3	0.9	0.3	0.9	0.6	1.0	0.3	0.5	0.4	0.1	0.3	0.1	0.1	0.3	0.9	0.3	0.6	
Mg	0.7	-0.6	0.2	-0.2	-0.5	0.6	0.8	-0.6	0.3	-0.1	0.2	0.8	0.4	0.7	0.3	1.0	0.2	0.9	0.3	0.4	0.1	0.1	0.5	0.2	0.2	0.1	
Fe	0.4	-0.4	0.2	-0.2	-0.4	0.3	0.4	-0.3	0.2	-0.1	0.5	0.1	0.5	0.4	0.5	0.2	1.0	0.2	0.1	0.9	0.9	0.9	0.2	0.5	0.8	0.7	
P	0.7	-0.7	0.3	-0.3	-0.5	0.8	0.9	-0.6	0.4	-0.1	0.3	0.8	0.4	0.6	0.4	0.9	0.2	1.0	0.1	0.2	0.0	0.0	0.5	0.3	0.2	0.3	
Mn	0.1	-0.2	0.2	0.0	0.0	0.1	0.1	-0.2	0.0	0.1	0.1	0.1	0.1	0.2	0.1	0.3	0.1	0.1	1.0	0.2	0.2	0.1	0.1	0.0	0.3	0.2	
Zn	0.4	-0.4	0.2	-0.3	-0.5	0.2	0.4	-0.3	0.1	-0.2	0.3	0.2	0.3	0.4	0.3	0.4	0.9	0.2	0.2	1.0	0.7	0.8	0.3	0.3	0.7	0.4	
Cr	0.2	-0.4	0.3	0.0	-0.3	0.2	0.2	-0.2	0.0	0.0	0.2	0.0	0.1	0.3	0.1	0.1	0.9	0.0	0.2	0.7	1.0	1.0	0.2	0.1	0.9	0.5	
Ni	0.2	-0.4	0.3	0.0	-0.3	0.2	0.2	-0.2	0.0	0.0	0.2	0.0	0.1	0.2	0.1	0.1	0.9	0.0	0.1	0.8	1.0	1.0	0.2	0.1	0.9	0.5	
Sr	0.8	-0.6	0.3	-0.4	-0.7	0.4	0.4	-0.6	0.3	-0.4	0.2	0.3	0.3	0.8	0.3	0.5	0.2	0.5	0.1	0.3	0.2	0.2	1.0	0.2	0.3	0.2	
Ti	0.6	-0.4	0.1	-0.2	-0.4	0.2	0.5	-0.5	0.5	-0.2	1.0	0.1	1.0	0.5	0.9	0.2	0.5	0.3	0.0	0.3	0.1	0.1	0.2	1.0	0.3	0.7	
Cu	0.4	-0.6	0.5	-0.1	-0.5	0.4	0.4	-0.4	0.1	-0.1	0.4	0.1	0.3	0.5	0.3	0.2	0.8	0.2	0.3	0.7	0.9	0.9	0.3	0.3	1.0	0.7	
Pb	0.5	-0.5	0.3	0.0	-0.4	0.4	0.5	-0.5	0.4	0.0	0.7	0.1	0.6	0.5	0.6	0.1	0.7	0.3	0.2	0.4	0.5	0.5	0.2	0.7	0.7	1.0	-1

Strong positive correlations ($0.60 \leq r \leq 0.79$) occurred also between Ash-Na-Si-Mg-P-Sr-Ti, VM-H, N-Mg, S-Ash-K-Na-Ca-Si-Mg, HV-H, K-P-Pb, Ca-Si-Mg-P. Compared to previous studies there were similar findings, for example strong positive correlation for Al-Ti-Si, N-S-P and K-Mg-P (Vassilev et al., 2010), S-N-Cl (Jenkins et al., 1998), Ash-Ca-Na-Si, K-P-Mg, Ca-S-P (Monti et al., 2008).

Very strong negative relationships occur between Ash-VM, Ash-H, VM-Ca and Ca-H. Strong negative correlations are mainly associated with VM, C, H, O and HV which are mostly negatively correlated with trace elements. VM has a negative correlation with most of the parameters, except with O, H, C and heating value. Same pattern is seen with O, where a positive correlation is only observed with volatiles and a moderate correlation with H. This finding was also reported by Vassilev et al. (2010) who stated there is a strong negative relationship between ash-O, O-N, O-S, O-P. In contrast to earlier findings, however, no evidence of negative correlations between trace elements (e.g. Si-Ca, Si-Mg, Si-K, Si-Mn, Ca-K, Ca-Al, K-Al, Ca-Al, Fe-Ca) was detected. In this study, several strong correlations between metallic elements were found, for example Al-Na-Si-Ti, Ca-Sr, Ca-Si, Ca-Mg, Si-Pb, Fe-Pb, Zn-Cr-Ni, Cu-Pb. According to Vassilev et al. (2012) the Si-Al-Fe-Na-Ti association is related mostly as detrital silicates and oxyhydroxides, excluding authigenic opal and Ca-Mg-Mn is commonly related to authigenic oxalates and carbonates.

VM correlates with H content in the data set, which is in agreement with the conclusion of Caillat & Vakkilainen (2013) that a higher VM content is due to a high hydrogen content and depends on the nature of the material and thermochemical process conditions. It has also been suggested that a high VM and fixed carbon content increase the heating value (Saidur et al., 2011). This does not appear to be the case and no correlation between VM and HV was detected in the current study.

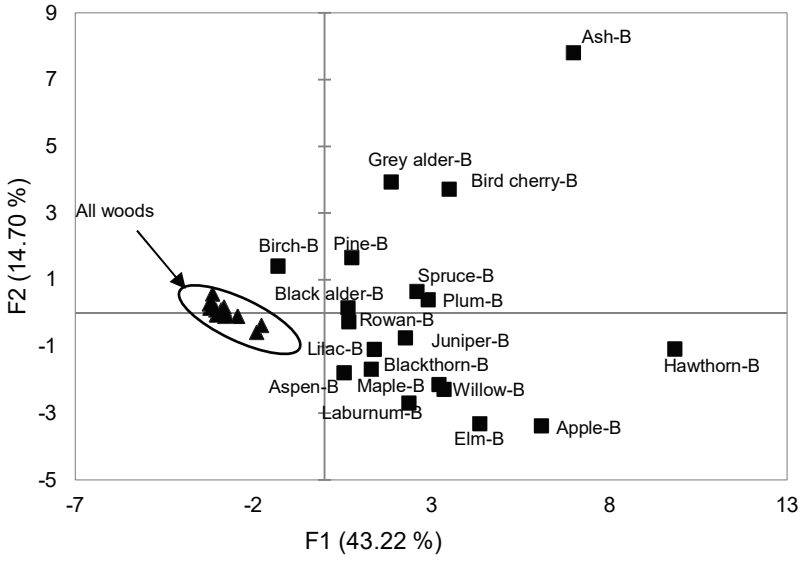


Figure 1. Graphical dispersion based on the PCA obtained from 26 variables (autoscaled): B – bark; W – wood.

A principal component analysis (PCA) was conducted on the variables studied in order to observe possible groupings and/or separation among wood species. PCA scatter plot (Fig. 1) revealed a clear data clustering in terms of the sample type using the scores of the first two principal components with a total variance of 57.9%. Generally, a total variance of 70% is considered as satisfactory in PC analysis. In this case, a lower total variance was accepted as satisfactory because descriptive purpose was desired, and it gave sufficient interpretation and scattering of the samples. Wood samples form a relative compact cluster that is characterized by high O, H, VM and HHV and low ash, while the bark samples are much more diverse and distributed over a wider range that is characterized by high ash and ash-forming element concentration. This suggests that different woods have similar compositions and there is no significant difference between species. It is possible, therefore, that the grouped biomass samples will show similar behaviours even if they are namely different. This means that if the process conditions are similar, the same behaviour can be expected among wood samples. However, the layout of bark samples reflects their variability and differences in composition. Interestingly, birch bark belongs to the wood cluster. This can be explained by the very high heating value (24.18 MJ kg^{-1}), volatiles content (80.1%) and carbon content (56.34%), makes it similar to wood samples. Results show that there are some significant differences and exceptions between wood species. For instance, hawthorn bark had remarkably high Al, Na, Ca and Si content compared to others.

The loading plot (Fig. 2) illustrates the connections of the variables to each other and gives an impression about correlations between features. The loading unravel the magnitude (large or small correlations) and in which way (positive or negative correlation) the variables contribute to the scores (Jackson, 1991; Jollife & Cadima, 2016). Sample distributions follow the loading values that wood samples spread in horizontal direction due to contents of volatiles, hydrogen, oxygen, Al, Ti, Na, Si, Ca, S and ash, and in the vertical direction due to mainly Cr, Ni, K content. It reveals that VM, H and O exhibit negative loadings in the negative side of the first principal component (F1). On the other hand, Al, Ti, Na, Ca, S and ash show significant positive loading contributions to the first principal component (F1).

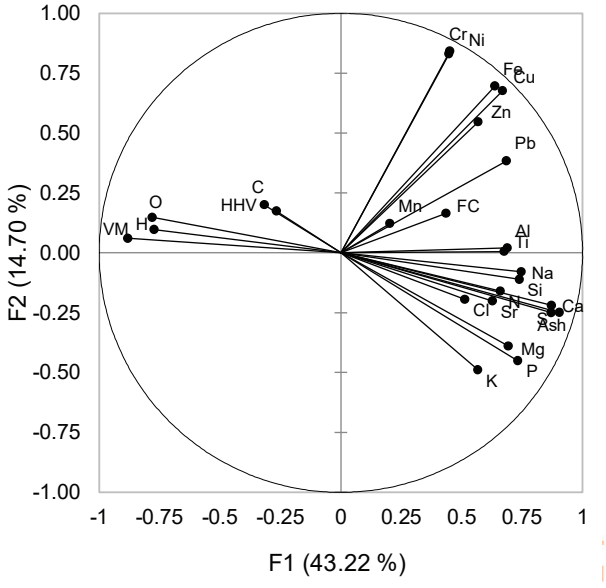


Figure 2. Correlations between variables according to PCA.

CONCLUSIONS

Based on results obtained experimentally and information available in the literature, this paper gives an overview of the characteristics of different Estonian wood species.

Statistical analysis supports the knowledge that woody biomass is heterogenous and its composition depends on its origin, growing environment and wood-specific mineral uptake.

Some conclusions based on complete proximate, ultimate and ash analyses of 19 different wood and bark samples can be made:

1) Wood samples have a relatively predictable composition where parameters vary in a narrow range. On the other hand, wood bark composition is more diverse and depends on the wood species.

2) Birch bark composition is more similar to wood samples than other bark samples, mainly due to its very high heating value, high content of C, H and volatiles and low ash content.

3) Main parameters that cause wood and bark samples clustering are volatiles, hydrogen, oxygen, ash, Al, Ti, Na, Si and Ca.

4) Very strong positive correlations were found, namely: Cr-Ni-Fe, Ca-Sr, HV-C, Al-Na-Si-Ti, K-Mg-P, Fe-Zn-Cr-Ni-Cu, Ash-Ca, N-S-P and O-VM.

5) Strong positive correlations occurred between Ash-Na-Si-Mg-P-Sr-Ti, VM-H, N-Mg, S-Ash-K-Na-Ca-Si-Mg, HV-H, K-P-Pb, Ca-Si-Mg-P.

6) Most of the ash forming elements have moderate to very strong correlation with ash, except Mn, Cr, Ni.

7) Very strong negative relationships occur between Ash-VM, Ash-H, VM-Ca and Ca-H.

8) Results show that not all wood species coincide with typical wood or bark. Most of the analysed hardwood barks have higher ash yields compared to a typical hardwood.

9) Gasification feedstock should be chosen considering the aim of gasification. To increase the yield of biochar, bark should be used because of the high content of fixed carbon. When a high reactivity and conversion rate is required, the wood part should be used because of its high volatile matter content.

10) Common wood species (Scots pine, Norway spruce, aspen, birch, grey alder and black alder) are perspective feedstock for gasification because of the low S, N, Cl, and ash content and high volatile matter.

11) Hardwood species have higher heavy metal contents (Mn, Zn, Cr, Ni, Sr, Ti, Cu, Pb) than softwoods. Of the common species, birch and grey alder have over three times higher total heavy metal content than other common hardwoods. In addition, spruce bark has more than two times higher total heavy metals content than pine bark.

ACKNOWLEDGEMENT. European Regional Development Fund.

REFERENCES

Alakangas, E., Hurskainen, M., Laatikainen-Luntama, J. & Korhonen, J. 2016. P*roperties of Indigenous Fuels in Finland*. Technical Research Centre of Finland, VTT Technology No. 272, Espoo, Finland, pp. 222.

Amanatidis, G. 2019. European Policies on Climate and Energy towards 2020, 2030 and 2050. European Parliament

Moilanen, A. 2006. *Thermogravimetric Characterisations of Biomass and Waste for Gasification Processes*. PhD Thesis, Åbo Akademi University, Espoo, Finland. VTT Publications 607, pp. 103 and 97.

Brunner, T., Biedermann, F., Kanzian, W., Evic, N. & Obernberger, I. 2013. Advanced Biomass Fuel Characterization Based on Tests with a Specially Designed Lab-Scale Reactor. *Energy and Fuels* **27**(10), 5691–5698. doi: 10.1021/ef400559j

Bryers, R.W. 1996. Fireside Slagging, Fouling, and High-Temperature Corrosion of Heat-Transfer Surface Due to Impurities in Steam-Raising Fuels. *Progress in Energy and Combustion Science* **22**(1), 29–120. doi: 10.1016/0360-1285(95)00012-7

Caillat, S. & Vakkilainen, E. 2013. Large-Scale Biomass Combustion Plants: An Overview. *Biomass Combustion Science, Technology and Engineering*, 189–224. Elsevier Inc. doi: 10.1533/9780857097439.3.189

Cuiping, L., Chuangzhi, W., Yanyongjie & Haitao, H. 2004. Chemical Elemental Characteristics of Biomass Fuels in China. *Biomass and Bioenergy* **27**(2), 119–130. doi: 10.1016/j.biombioe.2004.01.002

Demirbaş, A. 2001. Relationships between Lignin Contents and Heating Values of Biomass. *Energy Conversion and Management* **42**(2), 183–188. doi: 10.1016/S0196-8904(00)00050-9

Demirbas, A. 2004. Combustion Characteristics of Different Biomass Fuels. *Progress in Energy and Combustion Science* **30**(2), 219–230. doi: 10.1016/j.pecs.2003.10.004

Devi, L., Ptasinski, K.J. & Janssen, F.J.J.G. 2003. A Review of the Primary Measures for Tar Elimination in Biomass Gasification Processes. *Biomass and Bioenergy* **24**(2), 125–140. doi: 10.1016/S0961-9534(02)00102-2

Elbersen, W., Lammens, T.M., Alakangas, E.A., Annevelink, B., Harmsen, P. & Elbersen, B. 2017. *Lignocellulosic Biomass Quality: Matching Characteristics With Biomass Conversion Requirements*. Modeling and Optimization of Biomass Supply Chains: Top-Down and Bottom-up Assessment for Agricultural, Forest and Waste Feedstock, pp. 55–78. doi: 10.1016/B978-0-12-812303-4.00003-3

Elliott, D.C., Hallen, R.T. & Sealock, L.J. 1984. Alkali Catalysis in Biomass Gasification. *Journal of Analytical and Applied Pyrolysis* **6**(3), 299–316. doi: 10.1016/0165-2370(84)80024-8

Eriksson, G., Kjellström, B., Lundqvist, B. & Paulrud, S. 2004. Combustion of Wood Hydrolysis Residue in a 150 KW Powder Burner. *Fuel* **83**(11–12), 1635–1641. doi: 10.1016/j.fuel.2004.02.012

Evans, J.D. 1996. *Straightforward Statistics for the Behavioral Sciences*. Brooks/Cole Publishing, University of California, pp. 600.

EVS-EN ISO 17225-1. 2014. 'Solid biofuels - Fuel specifications and classes - Part 1: General requirements'. Estonia centre for standardization, Tallinn, Estonia & European Commmitee for Standardization

Frandsen, F.J., van Lith, S.C., Korbee, R., Yrjas, P., Backman, R., Obernberger, I., Brunner, T. & Jöller, M. 2007. Quantification of the Release of Inorganic Elements from Biofuels. *Fuel Processing Technology* **88**(11–12), 1118–28. doi: 10.1016/j.fuproc.2007.06.012

García, R., Pizarro, C., Lavín, A.G. & Bueno, J.L. 2012. Characterization of Spanish Biomass Wastes for Energy Use. *Bioresource Technology* **103**(1), 249–58. doi: 10.1016/j.biortech.2011.10.004

Gil, M.V., González-Vázquez, M.P., García, R., Rubiera, F. & Pevida, C. 2019. Assessing the Influence of Biomass Properties on the Gasification Process Using Multivariate Data Analysis. *Energy Conversion and Management* **184**, 649–60. doi: 10.1016/j.enconman.2019.01.093

Grammelis, P., Skodras, G. & Kakaras, E. 2006. Effects of Biomass Co-Firing with Coal on Ash Properties. Part I: Characterisation and PSD. *Fuel* **85**(16 SPEC. ISS.), 2310–2315. doi: 10.1016/j.fuel.2006.01.036

Hansen, V., Müller-Stöver, D., Ahrenfeldt, J., Holm, J.K., Henriksen, U.B. & Hauggaard-Nielsen, H. 2015. Gasification Biochar as a Valuable By-Product for Carbon Sequestration and Soil Amendment. *Biomass and Bioenergy* **72**(1), 300–308. doi: 10.1016/j.biombioe.2014.10.013

Jackson, J.E. 1991. *A User's Guide to Principal Components*. *A User's Guide to Principal Components*. United States of America, pp. 592.

Jenkins, B.M., Bexter, L.L., Miles, T.R.Jr. & Miles, T.R. 1998. Combustion Properties of Biomass. *Fuel Processing Technology* **54**(1–3), 17–46.

Jerzak, W. 2020. Effect of Pine Bark Combustion Temperature on Content of Major, Minor, and Trace Elements in Ashes: Experimental Study and Thermodynamic Equilibrium Calculations. *Journal of Energy Engineering* **146**(1), 04019031-1-9. doi: 10.1061/(ASCE)EY.1943-7897.0000632

Johansson, A.C., Wiinikka, H., Sandström, L., Marklund, M., Öhrman, O.G.W. & Narvesjö, J. 2016. Characterization of Pyrolysis Products Produced from Different Nordic Biomass Types in a Cyclone Pilot Plant. *Fuel Processing Technology* **146**, 9–19. doi: 10.1016/j.fuproc.2016.02.006

Joint Committee For Guides In Metrology. 2008. 'Evaluation of Measurement Data – Guide to the Expression of Uncertainty in Measurement'. *International Organization for Standardization Geneva ISBN* 50, pp. 134.

Jollife, I.T. & Cadima, J. 2016. Principal Component Analysis: A Review and Recent Developments. *Phil. Trans. R. Soc. A* **374**, 1–16. doi: 10.1098/rsta.2015.0202

Kaup, M. 2018. *International Competitiveness of Estonian Pellet Industry*. Master's Thesis, University of Tartu, Tartu, Estonia, 113 pp. (in Estonian).

Kirsanovs, V. & Žandeckis, A. 2015. Investigation of Fuel Effect on Biomass Gasification Process Using Equilibrium Model. *Agronomy Research* **13**(2), 500–510.

Kleinhans, U., Wieland, C., Frandsen, F.J. & Spliethoff, H. 2018. Ash Formation and Deposition in Coal and Biomass Fired Combustion Systems: Progress and Challenges in the Field of Ash Particle Sticking and Rebound Behavior. *Progress in Energy and Combustion Science* **68**, 65–168. doi: 10.1016/j.pecs.2018.02.001

Koman, S. & Feher, S. 2015. Basic Density of Hardwoods Depending on Age and Site. *Wood Research* **60**(6), 907–912.

Konist, A., Pihu, T., Neshumayev, D. & Külaots, I. 2013. Low Grade Fuel - Oil Shale and Biomass Co-Combustion in CFB Boiler. *Oil Shale* **30**(2 SUPPL.), 294–304. doi: 10.3176/oil.2013.2S.09

Koppejan, J. & van Loo, S. 2016. Handbook of Biomass Combustion and Cofiring: Prepared by Task 32 of the Implementing Agreement on Bioenergy, Twente University Press, Enschede, the Netherlands, pp. 23–67.

Koziński, J.A. & Saade, R. 1998. Effect of Biomass Burning on the Formation of Soot Particles and Heavy Hydrocarbons. An Experimental Study. *Fuel* **77**(4), 225–37. doi: 10.1016/S0016-2361(97)00201-9

Kurkela, E. 1996. Formation and Removal of Biomass-Derived Contaminants in Fluidized-Bed Gasification Processes. Technical Research Centre of Finland, *VTT Publications* 287, 47 p. + app.87 p.

Link, S., Tran, K-Q., Bach, Q-V., Yrjas, P., Lindberg, D., Arvelakis, S. & Rosin, A. 2018. Catalytic Effect of Oil Shale Ash on CO2 Gasification of Leached Wheat Straw and Reed Chars. *Energy* **152**, 906–13. doi: 10.1016/j.energy.2018.04.013

Lu, G., Zhang, K. & Cheng, F. 2018. The Fusion Characteristics of Ashes from Anthracite and Biomass Blends. *Journal of the Energy Institute* **91**(5), 797–804. doi: 10.1016/j.joei.2017.05.001

Ma, X., Zhao, X., Gu, J. & Shi, J. 2019. Co-Gasification of Coal and Biomass Blends Using Dolomite and Olivine as Catalysts. *Renewable Energy* **132**, 509–14. doi: 10.1016/j.renene.2018.07.077

Maaten, B., Konist, A. & Siirde, A. 2019. High-Speed Thermogravimetric Analysis of the Combustion of Wood and Ca-Rich Fuel. *Journal of Thermal Analysis and Calorimetry* **138**(4), 2807–2811. doi: 10.1007/s10973-019-08785-6

Magnusson, B., Näykki, T., Hovind, H., Krysell, M. & Sahlin, E. 2017. Handbook for Calculation of Measurement Uncertainty in Environmental Laboratories, Nordtest Report TR 537 (Ed.4). Taastrup, Denmark, pp. 51.

Mallick, D., Mahanta, P. & Moholkar, V.S. 2020. Co–Gasification of Coal/Biomass Blends in 50 KWe Circulating Fluidized Bed Gasifier. *Journal of the Energy Institute* **93**(1), 99–111. doi: 10.1016/j.joei.2019.04.005

Mason, P.E., Darvell, L.I., Jones, J.M, Pourkashanian, M. & Williams, A. 2015. Single Particle Flame-Combustion Studies on Solid Biomass Fuels. *Fuel* **151**, 21–30. doi: 10.1016/j.fuel.2014.11.088

McKendry, P. 2002. Energy Production from Biomass (Part 1): Overview of Biomass. *Bioresource Technology* **83**(1), 37–46. doi: 10.1016/S0960-8524(01)00118-3

Miccio, F., Ruoppolo, G., Kalisz, S., Andersen, L., Morgan, T.J. & Baxter, D. 2012. Combined Gasification of Coal and Biomass in Internal Circulating Fluidized Bed. *Fuel Processing Technology* **95**, 45–54. doi: 10.1016/j.fuproc.2011.11.008

Miles, T.R., Baxter, L.L., Bryers, R.W., Jenkins, B.M. & Oden, L.L. 1996. Alkali Deposits Found in Biomass Power Plants: Vol. 1. National Renewable Energy Laboratory, NREL/TP-433-8142

Mlonka-Mędrala, A., Magdziarz, A., Gajek, M., Nowińska, K. & Nowak, W. 2020. Alkali Metals Association in Biomass and Their Impact on Ash Melting Behaviour. *Fuel* **261.** doi: 10.1016/j.fuel.2019.116421

Monti, A., Virgilio, N.D. & Venturi, G. 2008. Mineral Composition and Ash Content of Six Major Energy Crops. *Biomass and Bioenergy* **32**(3), 216–223. doi: 10.1016/j.biombioe.2007.09.012

Nurmi, J. 2000. *Characteristics and Storage of Whole-Tree Biomass for Energy*. *Doctoral Dissertation. The Finnish Forest Research Institute Research Papers* **758**, 1–42.

Nzihou, A. & Stanmore, B. 2013. The Fate of Heavy Metals during Combustion and Gasification of Contaminated Biomass-A Brief Review. *Journal of Hazardous Materials* **256**, 56–66. doi: 10.1016/j.jhazmat.2013.02.050

Nzihou, A., Stanmore, B. & Sharrock, P. 2013. A Review of Catalysts for the Gasification of Biomass Char, with Some Reference to Coal. *Energy* **58**, 305–17. doi: 10.1016/j.energy.2013.05.057

Official Journal of the European Union. 2009. 'Directive 2009/28/EC of the European Parliament and of the Council of 23 April 2009 on the Promotion of the Use of Energy from Renewable Sources and Amending and Subsequently Repealing Directives 2001/77/EC and 2003/30/EC'.

Olanders, B. & Steenari, B.M. 1995. Characterization of Ashes from Wood and Straw. *Biomass and Bioenergy* **8**(2), 105–15. doi: 10.1016/0961-9534(95)00004-Q

Perander, M., DeMartini, N., Brink, A., Kramb, J., Karlström, O., Hemming, J., Moilanen, A., Konttinen, J. & Hupa, M. 2015. Catalytic Effect of Ca and K on CO2 Gasification of Spruce Wood Char. *Fuel* **150**, 464–72. doi: 10.1016/j.fuel.2015.02.062

Pesonen, J., Kuokkanen, T., Kaipiainen, E., Koskela, J., Jerkku, I., Pappinen, A. & Villa, A. 2014. Chemical and Physical Properties of Short Rotation Tree Species. *European Journal of Wood and Wood Products* **72**(6), 769–77. doi: 10.1007/s00107-014-0841-5

Phyllis2, 'Database for the Physico-Chemical Composition of (Treated) Lignocellulosic Biomass, Micro- and Macroalgae, Various Feedstocks for Biogas Production and Biochar'. Available at https://phyllis.nl/

Pinto, P.C.R.O., Sousa, A.F., Silvestre, A.J.D., Neto, C.P., Gandini, A., Eckerman, C. & Holmbom, B. 2009. Quercus Suber and Betula Pendula Outer Barks as Renewable Sources of Oleochemicals: A Comparative Study. *Industrial Crops and Products* **29**(1), 126–32. doi: 10.1016/j.indcrop.2008.04.015

Plata, S. 2006. A Note on Fisher's Correlation Coefficient. *Applied Mathematics Letters* **19**(6), 499–502. doi: 10.1016/j.aml.2005.02.036

Ragland, K.W., Aerts, D.J. & Baker, A.J. 1991. Properties of Wood for Combustion Analysis Pre-Exponential Factor for Hydrocarbons Pre-Exponential Factor for Pyrolysis. *Bioresource Technology* **37**, 161–68. doi: 10.1016/0960-8524(91)90205-X

Raudsaar, M., Sims, A., Timmusk, T., Pärt, E. & Nikopensius, M. 2018. *Forest Resources, Yearbook Forest 2017*. Estonian Environment Agency, 75 pp. (in Estonian).

Ren, J., Cao, J.P., Zhao, X.Y., Yang, F.L. & Wei, X.Y. 2019. Recent Advances in Syngas Production from Biomass Catalytic Gasification: A Critical Review on Reactors, Catalysts, Catalytic Mechanisms and Mathematical Models. *Renewable and Sustainable Energy Reviews* **116**. doi: 10.1016/j.rser.2019.109426

Rizvi, T., Xing, P., Pourkashanian, M., Darvell, L.I., Jones, J.M. & Nimmo, W. 2015. Prediction of Biomass Ash Fusion Behaviour by the Use of Detailed Characterisation Methods Coupled with Thermodynamic Analysis. *Fuel* **141,** 275–84. doi: 10.1016/j.fuel.2014.10.021

Roldan, R. 2018. Report of the Laboratory Tests for Pyrolysis of Forestry Residues. AgroCycle www.AgroCycle.eu.

Saidur, R., Abdelaziz, E.A., Demirbas, A., Hossain, M.S. & Mekhilef, S. 2011. A Review on Biomass as a Fuel for Boilers. *Renewable and Sustainable Energy Reviews* **15**(5), 2262–2289. doi: 10.1016/j.rser.2011.02.015

Schuster, G., Löffler, G., Weigl, K. & Hofbauer, H. 2001. Biomass Steam Gasification - An Extensive Parametric Modeling Study. *Bioresource Technology* **77**(1), 71–79. doi: 10.1016/S0960-8524(00)00115-2

Sonmez, T., Keles, S. & Tilki, F. 2007. Effect of Aspect, Tree Age and Tree Diameter on Bark Thickness of Picea Orientalis. *Scandinavian Journal of Forest Research* **22**(3), 193–97. doi: 10.1080/02827580701314716

Sueyasu, T., Oike, T., Mori, A., Kudo, S., Norinaga, K. & Hayashi, J.I. 2012. Simultaneous Steam Reforming of Tar and Steam Gasification of Char from the Pyrolysis of Potassium-Loaded Woody Biomass. *Energy and Fuels* **26**(1), 199–208. doi: 10.1021/ef201166a

Telmo, C., Lousada, J. & Moreira, N. 2010. Proximate Analysis, Backwards Stepwise Regression between Gross Calorific Value, Ultimate and Chemical Analysis of Wood. *Bioresource Technology* **101**(11), 3808–3815. doi: 10.1016/j.biortech.2010.01.021

Thengane, S.K., Gupta, A. & Mahajani, S.M. 2019. Co-Gasification of High Ash Biomass and High Ash Coal in Downdraft Gasifier. *Bioresource Technology* **273**, 159–68. doi: 10.1016/j.biortech.2018.11.007

Vassilev, S.V., Baxter, D., Andersen, L.K. & Vassileva, C.G. 2010. An Overview of the Chemical Composition of Biomass. *Fuel* **89**, 913–933. doi: 10.1016/j.fuel.2009.10.022

Vassilev, S.V., Baxter, D., Andersen, L.K. & Vassileva, C.G. 2013. An Overview of the Composition and Application of Biomass Ash. Part 1. Phase-Mineral and Chemical Composition and Classification. *Fuel* **105**, 40–76. doi: 10.1016/j.fuel.2012.09.041

Vassilev, S.V., Baxter, D., Andersen, L.K., Vassileva, C.G. & Morgan, T.J. 2012. An Overview of the Organic and Inorganic Phase Composition of Biomass. *Fuel* **94**, 1–33. doi: 10.1016/j.fuel.2011.09.030

Werkelin, J., Lindberg, D.l, Boström, D., Skrifvars, B.J. & Hupa, M. 2011. Ash-Forming Elements in Four Scandinavian Wood Species Part 3: Combustion of Five Spruce Samples. *Biomass and Bioenergy* **35**(1), 725–33. doi: 10.1016/j.biombioe.2010.10.010

Werkelin, J., Skrifvars, B.J., Zevenhoven, M., Holmbom, B. & Hupa, M. 2010. Chemical Forms of Ash-Forming Elements in Woody Biomass Fuels. *Fuel* **89**(2), 481–93. doi: 10.1016/j.fuel.2009.09.005

Zając, G., Szyszlak-Bargłowicz, J., Gołębiowski, W. & Szczepanik, M. 2018. Chemical Characteristics of Biomass Ashes. *Energies* **11**(11), 1–15. doi: 10.3390/en11112885

Zevenhoven, R. & Kilpinen, P. 2001. Control of Pollutants in Flue Gases and Fuel Gases, Chap. 8 Trace Elements, Alkali Metals. Espoo, Finland. pp. 1–30.

Zisopoulos, F.K., van der Goot, A.J. & Boom, R.M. 2018. Exergy Destruction in Ammonia Scrubbers. *Resources, Conservation and Recycling* **136**, 153–65. doi: 10.1016/j.resconrec.2018.04.014

Publication III

Sinisalu, M., Järvik, O., Mets, B., & Konist, A. (2024). **Co-gasification of biomass and oil shale under CO2 atmosphere: Comparative analysis of fixed-bed reactor, gas chromatography and thermogravimetric analysis coupled with mass spectroscopy (TGA–MS)**. *Bioresource Technology*, *393*. https://doi.org/10.1016/j.biortech.2023.130086

Bioresource Technology 393 (2024) 130086



Contents lists available at ScienceDirect

Bioresource Technology

journal homepage: www.elsevier.com/locate/biortech





Co-gasification of biomass and oil shale under CO_2 atmosphere: Comparative analysis of fixed-bed reactor, gas chromatography and thermogravimetric analysis coupled with mass spectroscopy (TGA-MS)

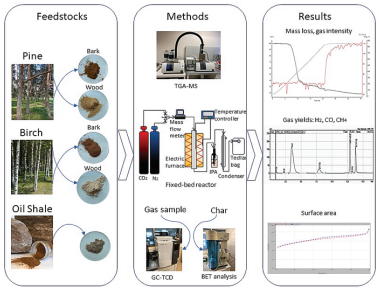
Mari Sinisalu *, Oliver Järvik, Birgit Mets, Alar Konist

Department of Energy Technology, Tallinn University of Technology, 19086 Tallinn, Estonia

HIGHLIGHTS

- Co-gasification of biomass-oil shale mixtures in CO_2 at 850 °C was conducted.
- Comparative analysis of fixed-bed reactor, gas chromatography and TGA-MS data.
- Catalytic effect on CO and CH_4 concentration was observed.
- Pine bark blend containing 10% oil shale exhibited the highest gas concentration.
- Oil shale impact on H_2 concentration was either inhibitory or not determined.

GRAPHICAL ABSTRACT



ARTICLE INFO

Keywords:
Co-gasification
Biomass
Oil shale
Synergetic effect

ABSTRACT

Co-gasification of biomass with oil shale offers potential for integrating renewable and fossil energy sources, reducing reliance on fossil fuels. Biomass (pine and birch wood and bark) and oil shale blends (10–30 wt%) were gasified under CO_2 conditions using thermogravimetric analysis coupled with mass spectrometry (TGA-MS), fixed-bed reactor, and gas chromatography. Results revealed an interaction between oil shale and biomass, enhancing CO and CH_4 concentrations in the producer gas. Bark samples demonstrated higher CO concentrations compared to wood samples, particularly in pine, with 16.1 vol% and 5.4 vol%, respectively. While birch wood showed increased H_2 evaporation in TGA-MS experiments, oil shale's impact on H_2 concentration was inhibitive, as shown by quantitative analysis. Pine bark, with a threefold catalytic index compared to other biomass samples, demonstrated the highest total gas concentrations (19.2 vol%). Interestingly, pine bark char blends exhibited the lowest surface areas (up to 434 m^2/g) among the tested samples.

1. Introduction

Gasification is a thermochemical process that involves the initial pyrolysis of the raw materials, followed by the conversion of resulting pyrolysis char into combustible gas through the introduction of a gasifying agent under high temperatures (Yang et al., 2019). The gas

* Corresponding author at: Ehitajate tee 5, 19086 Tallinn, Estonia.
E-mail address: mari.sinisalu@taltech.ee (M. Sinisalu).

https://doi.org/10.1016/j.biortech.2023.130086
Received 11 September 2023; Received in revised form 16 November 2023; Accepted 19 November 2023
Available online 21 November 2023
0960-8524/© 2023 Elsevier Ltd. All rights reserved.

mixture produced is mainly composed of CO, CO_2, H_2 and CH_4, with the specific composition being directly dependent on the gasifying agent (O_2, air, steam, or CO_2) and the type of feedstock (Mariyam et al., 2022). Advanced gasification techniques separate the pyrolysis and the gasification stages into single controlled stages, which are then integrated into a multi-stage gasification process. This approach is employed to enhance gas purity with minimal tar production, increase char conversion rates, and improve overall process efficiency. In other words, the gasification of biomass can be divided into two stages: 1) pyrolysis and 2) the conversion of the remaining char (Duman et al., 2014).

Reviews that specifically examine the production of CO-rich syngas through gasification technology, particularly in the context of CO_2-assisted gasification, have been receiving increased research attention in recent times (Chan et al., 2021). Most of the researchers are primarily investigating the co-gasification of biomass and coal reactivity in the presence of either CO_2 or steam. This is because Boudouard/steam gasification reactions are dominating during biomass co-gasification, which can maximize the production of low molecular weight gases (Wei et al., 2021). CO_2 gasification offers a mutually beneficial solution, in which CO_2 is converted to CO, achieving carbon emission mitigation. It can also improve thermal efficiency, promote dehydrogenation, and enhance tar cracking (Lee et al., 2017). Furthermore, CO_2 is a preferred gasification agent when a higher specific surface area of the char is desired (Chan et al., 2021). However, having a high concentration of CO_2 in the producer gas is undesirable (Gao et al., 2021). Therefore, the use of different additives or agents must be investigated to obtain a high-quality product with the desired properties.

Biomass is an energy source that is considered carbon–neutral, and as a result, it has gained growing interest as a low-carbon energy solution. Raw biomass is characterized by high moisture content, low calorific value and high molar ratios of O/C and H/C, making it a good source of hydrogen. However, the high oxygen content and volatile matter of biomass are not ideal for gasification, as they cause a higher proportion of CO_2 and tar in the produced gas (Tong et al., 2021). To obtain high-quality syngas, it is necessary to reduce the volatile matter and oxygen content of biomass prior to co-gasification (Chan et al., 2021; Tong et al., 2021). Additionally, the composition of the producer gas is highly influenced by the specific type and characteristics of the biomass being used. According to the multivariate statistical study by Gil et al. (2019), the key biomass characteristics that significantly influence gas production, the calorific value of the producer gas, gasification conversion, and energy efficiency, are the carbon and hydrogen contents, as well as the higher heating value of the biomass. The elevated concentration of H_2 and the molar ratio of H_2/CO in the producer gas can be attributed to the higher hydrogen-to-oxygen (H/O) ratio and the presence of K_2O in the ash content of the biomass. Gil et al. (2019) also found that a higher content of volatile matter and oxygen resulted in a decrease in the H_2 content in the producer gas. In contrast to previous findings, it is proposed that the increased concentration of volatiles and fixed carbon could potentially explain the observed increase in H_2 yield (Li et al., 2017). Therefore, previous research findings on the influence of biomass properties on gasification outcomes are inconclusive and highly dependent on the material used.

Biomass and oil shale exhibit large differences in their properties. Estonian oil shale is a well-investigated fossil fuel used for power and shale oil production (Konist et al., 2019) that contains organic matter called kerogen (up to 40 % (Altun et al., 2006)) and complex mineral matter, including calcite, dolomite, quartz, pyrite, feldspar and illite (Koel, 1999). Oil shale contains carbonate minerals, for example, $CaCO_3$, that, at high temperatures (above 700 °C), begin to decompose into CaO (a small amount of CaO already forming at around 500 °C during the decomposition of dolomite) and therefore it can be used as calcium precursor. It suggests that co-gasification of biomass with oil shale could be a promising approach and could potentially result in the production of higher-value products, such as syngas, which can be further converted into fuels, chemicals, and other valuable products. To fully understand the catalytic properties of oil shale as a CaO-based catalyst, it is crucial to investigate and elucidate the potential synergistic effects between impurities, minerals, and CaO. These impurities can vary in composition and quantity and may have a notable influence on the final product, as highlighted by previous studies conducted by Li et al. (2021a).

Due to the development of the biomass gasification process, the selection of appropriate catalysts has become increasingly crucial. The most desirable catalysts possess specific characteristics that increase the product yield, facilitate regeneration and frequency of use, reduce tar production, and are cost-effective. In general, three types of catalysts are used to increase the gasification yield: mineral catalysts (e.g., dolomite, limestone, magnesite), alkali and alkaline earth metals (e.g., Al, Fe, and K), and transition metals (e.g., Ni) (Shahbaz et al., 2020). Calcium oxide (CaO) based materials have been acknowledged as catalysts producing hydrogen-rich gas due to their high capacity of in-situ CO_2 capture and have gained broad attention due to their abundance and low cost (Gao et al., 2021; Li et al., 2021a). CaO is a desirable and effective catalyst for solid fuel gasification and is employed for tar reforming and methane reformation (Jeremiáš et al., 2018; Li et al., 2021a; Shahbaz et al., 2017). Gasification technology has been extensively studied and commercialized. However, catalytic co-gasification has mainly been investigated at the laboratory and bench-scale levels (Shahbaz et al., 2020).

Gasification of single-source feedstock has both advantages and disadvantages. Numerous studies have been conducted over the years, and they have concluded that obtaining producer gas in the proper state and with minimum environmental impact is a challenging task (Qudaih et al., 2013). For instance, thermal conversion of oil shale is more complex than that of coal due to its high ash content and the release of undesirable gases like H_2S, SO_x and NO_x (Yang et al., 2019). On the other hand, biomass gasification has many technical obstacles such as handling residues of tarry components and ash. Co-gasification has received growing attention as a process where mixing different types of fuels can potentially produce a catalytic effect. To achieve improved synergy, co-gasification often involves selecting feedstocks that possess distinct and significantly different characteristics and properties. Researchers have been investigating the impact of biomass and coal ratio on the yields of H_2 and CH_4 production through catalytic co-gasification (Shahbaz et al., 2020). Moreover, it has been demonstrated that mixing coal with biomass can significantly reduce the yields of SO_2, NOx, and tar while increasing gas yields (Mariyam et al., 2022). Co-gasification gives an opportunity to control the composition of produced gas by varying the ratio of feedstock (Shahbaz et al., 2020) and consequently offset the disadvantages of biomass, and improve the gasification product yield and purity (Yang et al., 2019).

Recent research has mainly focused on the synergistic effects of biomass co-gasification with feedstocks such as coal (Abdalazeez et al., 2021; He et al., 2021; Shahabuddin and Bhattacharya, 2021; Tong et al., 2021; Wei et al., 2021), municipal waste (Cai et al., 2021; Hameed et al., 2021; Zaini et al., 2020) and plastics (Burra and Gupta, 2018; Li et al., 2021b; Zheng et al., 2018). Studies have found that the mineral matter in biomass favors the efficiency of coal gasification due to the high concentration of alkali and alkaline earth metals, making co-gasification of biomass and coal a promising application (Wei et al., 2021). Once synergistic interactions have been found in the previously mentioned feedstocks, the scope of application can be expanded to other fossil fuels, such as oil shale. However, results regarding synergistic effects can be conflicting, which is often the case when studying coals of different origins. Jeong et al. (2014) observed a reactive synergy during co-gasification of coal and pine sawdust, which was attributed to the catalytic effects of alkaline metals, such as potassium. Satyam Naidu et al. (2016) demonstrated the synergistic behavior of a coal-biomass mixture in a CO_2 environment. However, the coal-biomass interaction mechanism during co-gasification remained unclear (Wei et al., 2021). Conversely, some studies claim that there is no synergistic effect

between different fuels. Collot et al. (1999) conducted several co-gasification tests but found no evidence of synergy in the CO_2 co-gasification of coal and biomass. Similarly, Kajitani et al. (2010) did not observe synergistic or inhibitive effects on the gasification reactivity of cedar bark and coal blend during CO_2 gasification. Also, Yang et al. (2021) found almost no interaction between cotton stalk and high-ash coal in co-pyrolysis/gasification, but the catalytic effect of alkali metals and alkaline earth metals was noticed to exist and was enhanced by the addition of steam. Furthermore, the CO_2 co-gasification of sub-bituminous coal with biomass imposed an inhibitory effect on the gasification reaction (Lahijani et al., 2015).

While there have been studies on the co-pyrolysis of oil shale and biomass (Chen et al., 2020; Jarvik et al., 2020; Mariyam et al., 2022), there has been limited research on the use of oil shale as an additive in biomass gasification. Therefore, this study aimed to contribute to the fields of solid fuel gasification research of the gasification of oil shale and biomass blends. To accomplish this, a fixed-bed gasifier and a thermogravimetric analyzer were used to gain a better understanding of the gasification process and assess the potential impact of oil shale as an additive in biomass co-gasification. Furthermore, the surface areas of chars were evaluated, as the presence of inorganic constituents is known to have an important impact on char's reactivity through their catalytic effects.

2. Materials and methods

2.1. Materials

The feedstocks used in this study were Estonian oil shale (OS) with a high ash content, along with biomass (BM) samples such as pine and birch wood (W) and bark (B), respectively PineW, PineB, BirchW, BirchB. Proximate, ultimate and elemental analyses were performed according to the standardized methods, with the details of the measurement methods and results provided in a prior study (Sulg et al., 2021). Results are presented in Table 1 and Table 2. The biomass and oil shale samples were ground to analytical size. Different combinations of feedstocks were prepared, with biomass mixed with oil shale at weight percentages of 10 %, 20 % and 30 %. For example, in the case of pine bark, the sample labeled as OS-PineB_10 consists of 90 % pine bark and 10 % oil shale.

2.2. Design of experiment

The number of experimental units corresponds to the total number of combinations of the levels of the factors being tested. In this experiment, there are 2 levels for biomass type (wood and bark), 2 levels for wood species (pine and birch), and 4 levels for oil shale content (0 %, 10 %, 20 %, and 30 %), as well as the pure oil shale tests. Therefore, the total number of experimental units is [2 (biomass type) x 2 (wood species) x 4 (oil shale content)] + 1 [number of pure oil shale tests]. It results in 17 experimental units, each representing a unique combination of factor levels.

The variables analyzed in this experiment include: H_2, CO and CH_4 concentration, residues from fixed-bed reactor and thermogravimetric analysis, H_2 intensity and specific surface area.

This experimental design allows for the investigation of the effects of biomass type, wood species, and oil shale content on the variables of interest.

2.3. Experimental reactor and methods

2.3.1. Experimental reactor

A cylindrical fixed-bed reactor (Fig. 1) was used for the gasification experiments, as this reactor type is commonly used for the co-gasification of different materials. The fixed-bed reactor has a bed of solid fuel particles that react with gasifying agent. A sample holder made of steel mesh containing approximately 1 g of blended mixtures of biomass with oil shale was loaded into the reactor. Prior to starting the experiment, the reactor was purged with nitrogen for 10 min, with a flow rate of 200 ml_{STP}/min to ensure an inert atmosphere. The sample was then heated in a nitrogen atmosphere from room temperature to 850 °C using a constant heating rate of 50 °C/min. During the co-pyrolysis phase, volatile matter is released, and the fuel is converted into char. CO_2 was introduced to the reactor once the furnace had reached the target temperature. The gasification regime was maintained at this condition for 17 min, with flow rates of 100 ml_{STP}/min for N_2 and CO_2. The gas product was passed through an isopropanol wash bottle to remove tars, and then cooled in a condenser and collected in Tedlar bags during the reaction, while the char was collected and weighed at the end of the run.

2.3.2. Thermogravimetric analyzer

Thermogravimetric analysis (TGA) was employed to establish the relationship between the weight change of the samples and the temperature. The thermal behavior was studied using a NETZSCH STA 449 F3 Jupiter® apparatus coupled with a NETZSCH QMS Aëolos® mass spectrometer. A flow of N_2 (purity 99.998 %) was used for the heating process, with the heating rate of 50 °C/min, until the temperature reached 850 °C. After reaching the set temperature, the isothermal gasification reaction of the pyrolyzed char sample was initiated by switching to a flow of CO_2 (purity > 99.995 %) (90 % CO_2 and 10 % N_2) for 15 min. The heating program used in the fixed-bed reactor was comparable, except that the gas flow was increased to ensure the transportation of all relevant gases and vapors from the sample zone to the ion source of the mass spectrometer for precise analysis. The sample mass used was approximately 5 mg.

2.3.3. Gas chromatography

Gas analysis was performed using a Shimadzu GC-2014 gas chromatograph with a valve system capable of determining H_2, CO, O_2, N_2, CO_2 and CH_4 in a single run. Thermal conductivity detector (TCD) and a packed column (SDC-200 Shimalite 60/80 mesh; 3.2 mm OD, 2.1 mm

Table 1
Physical and chemical properties of samples.

Samples	Ultimate analysis (% db)						Moisture content	Ash content (% db)	Volatile matter (% db)	Fixed carbon[a] (% db)	HHV (MJ/kg)
	C	TIC	H	N	S	O[a]					
PineB	52.79	N/A	6.08	1.19	0.05	36.89	4.8	3.1	71.1	21.0	21.40
PineW	50.12	N/A	6.59	0.19	0.01	42.77	8.5	0.3	85.2	14.5	20.04
BirchB	56.34	N/A	7.00	0.44	0.02	34.83	3.7	1.4	80.1	18.5	24.18
BirchW	49.31	N/A	6.62	0.08	0.01	43.70	7.7	0.3	86.9	12.8	19.94
BM average	**52.14**		**6.57**	**0.48**	**0.02**	**39.55**	**6.2**	**1.3**	**80.8**	**16.7**	**21.39**
OS	27.49	5.99	2.75	0.06	1.47	16.80	0.5	51.4	47.7	0.9	9.60

% db – mass percent on dry basis; TIC – total inorganic carbon; N/A – not applicable.
[a] Calculated: O%= 100 - (C% + H% + N% + S% + ash%); fixed carbon%= 100 - (volatile matter% + ash%).

Table 2
Inorganic elements in the fuels (ppm db).

Sample	Ca	Mg	Al	K	Si	Fe	P	Mn	Cr	Ni	Catalytic index
PineB	12 947	459	87	2 095	102	186	310	48	138.2	91.4	83.0
PineW	718	241	16	530	28	41	103	6	0.3	0.1	34.8
BirchB	4 489	703	102	606	163	184	195	201	59.9	31.0	22.6
BirchW	1 036	421	14	473	21	39	51	44	0.3	0.3	56.3
OS	176 206	18 373	17 960	11 454	67 096	16 998	374	301	23	20	1.7

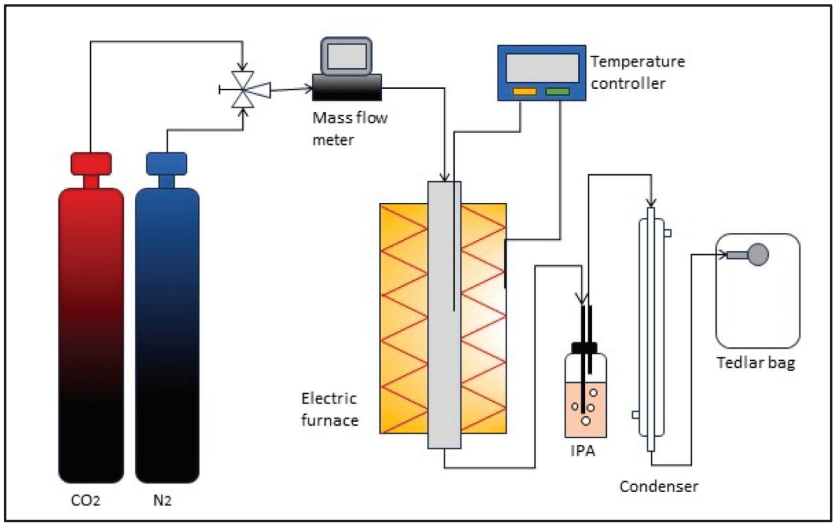


Fig. 1. Schematics of the used fixed-bed reactor.

ID, 9 m with PorapakN and MolSieve 5 Å 3 m, 2 mm ID) were used to measure the volume fraction of permanent gases. The initial oven temperature was set at 35 °C, and then it was increased to 120 °C at a rate of 20 °C/min, with helium (purity 99.996 %) as the carrier gas at a flow rate of 35 ml/min.

2.4. Char analysis

Surface area based on the Brunauer-Emmett-Teller (BET) theory was obtained using the Quantachrome Instruments Autosorb instrument through N_2 isotherms. Samples were subjected to a 20-hour degassing process in an outgassing apparatus at a temperature of 300 °C prior to analysis. This process aimed to remove any volatile components or residual gases present in the samples, ensuring the samples were in a stable and purified state for subsequent analysis.

2.5. Synergistic behavior investigation

In co-gasification, the observed weight losses would be greater or less than calculated from the weighted value of each feedstock. To assess the presence of synergy between OS and BM, theoretical weight loss values was calculated using Eq. (1) (Tong et al., 2021):

$$TG_{CAL} = x_{BM} TG_{BM} + x_{OS} TG_{OS} \quad (1)$$

where TG_{BM}, TG_{OS}, and TG_{CAL} refer to the weight loss of a BM, OS and their blends, respectively; and the x_{BM} and x_{OS} are the mass fractions of BM and OS in the blends.

The experimental and calculated gas concentrations were compared in the similar way to examine the potential catalytical effect between BM and OS. The calculation yield of the blends (Y_{CAL}) was obtained using Eq. (2) (Tong et al., 2021):

$$Y_{CAL} = x_{BM} Y_{BM} + x_{OS} Y_{OS} \quad (2)$$

where Y_{BM} and Y_{OS} are the gas concentrations of the individual BM and OS according to gas chromatography analysis, respectively.

3. Results and discussion

3.1. Feedstock characterization

Table 1 and Table 2 show the composition analysis of Estonian wood and oil shale samples. The proximate analysis of BM indicated that its moisture content, ash content, volatile matter, fixed carbon, and higher heating values were in the range of 3.7–8.5 %, 0.3–3.1 %, 71.1–86.9 %, 12.8–21 % and 19.94–24.18 MJ/kg, respectively. On the other hand, OS had an ash content of 51.4 %, volatile matter of only 47.7 %, and fixed carbon of 0.9 %, with a much lower heating value of 9.60 MJ/kg. Additionally, BM and OS varied significantly in ultimate analysis, as expected. The average C, H, N and O content in BM were much higher than in OS, at 52.14 % vs 27.49 %, 6.57 % vs 2.75 %, 0.48 % vs 0.06 % and 39.55 % vs 16.8 %, respectively, while the S content in OS was much higher than in BM, at 1.47 % vs 0.02 %, respectively. The analysis of other inorganic elements showed a wide range of values between BM samples, particularly between wood and bark samples (Table 2). It can be found that Ca contents of BM samples decrease in the order: PineB > BirchB > BirchW > PineW, especially the Ca content of PineB was much higher than that of pine wood. OS was shown to contain 17.6 wt% of Ca followed by 6.7 wt% Si, 1.8 wt% Mg and Al, while other elements such as Cr, Fe, P and Mn were less than 500 ppm. It was shown that Ca and K content in biomass play a significant catalytic role during gasification

process (Chan et al., 2021; Tong et al., 2021). Furthermore, a potential approach to evaluate the catalytic efficiency of minerals in the feedstocks involves comparing their catalytic indexes (He et al., 2022). In this study, catalytic index (CI) is calculated as the ratio of the combined catalytic inorganic elements (K, Ca, Mg, Na, Fe) to the combined inhibiting inorganic elements (Si, Al) (Bouraoui et al., 2015): $CI = (Fe+Ca+Mg+Na+K)/(Si+Al)$. The index of PineB was up to three times higher than that of other biomass types, with the following decreasing order: PineB < BirchW < PineW < BirchB < OS (Table 2). Higher catalytic index in biomass could potentially result in a stronger synergistic effect during the co-gasification process.

3.2. Mass loss and thermal behavior

The residual weights for the samples were compared using two methods: TGA and a fixed-bed reactor. The results presented in Fig. 2 show similar trend in the residual weights obtained from different wood samples. The final mass of the solid residue increased with the increase in the proportion of oil shale in the fuel blend. It is important to consider the mass gain during CO_2 due to the presence of CaO in the oil shale ash (Fig. 3). However, there were noticeable systematic differences in the residual weights obtained from fixed-bed reactor and TGA. One possible explanation for this discrepancy is the difference in the sample sizes used in the two methods, with the fixed-bed reactor requiring a sample size that is 200 times larger than that used in TG analysis. It may refer to a situation where gasification process in fixed-bed reactor is not fully completed, meaning that a portion of the material remains in solid instead of being converted into the producer gas.

To describe the thermal behavior of the fuels in specific and controlled environment, thermogravimetric analysis was used. The mass loss curves are provided in Fig. 3 and Fig. 4 a-d and they illustrate the mass loss range of the samples. First, the behavior of the oil shale and pure biomass samples were analyzed by TGA. The greatest mass loss for all birch and pine samples occurred within the temperature range of 200–400 °C. The degradation of bark samples was initiated at lower temperatures compared to wood samples, specifically around 210 °C for bark and 280 °C for wood. The mass loss of wood samples was more rapid and occurred within a narrower temperature range. At a temperature of 430 °C, the residual mass of wood samples dropped below 30 %, whereas for bark samples, it exceeded 40 %. This observed trend can be attributed to the higher cellulose content in wood, which leads to a degradation process resembling that of pure cellulose decomposition (Quan et al., 2016). Additionally, pine bark has a higher lignin content compared to birch (Quan et al., 2016). This is reflected in the measurement results, where the mass loss curve for pine follows a more gradual decline, mirroring the pattern seen in pure lignin.

Oil shale differs significantly from biomass in terms of mineral content. The mass loss of oil shale begins at a higher temperature than biomass and its decomposition can be divided into two stages. After gas exchange, an increase in sample mass is observed, indicating that CO_2 present in the environment is being captured through a reaction with CaO. CaO from oil shale ash is formed during the thermal decomposition of $CaCO_3$ and $CaMg(CO_3)_2$. The addition of oil shale results in a decrease in the mass loss of the samples (Fig. 4 a-d). This outcome is in line with expectations and can be attributed to the higher mineral content of the samples and the subsequent capture of CO_2 from the environment upon the addition of oil shale. According to Chen et al. (2019), the addition of CaO enhances the decomposition of biomass components, and the catalytic activity of CaO is correspondingly promoted when pyrolysis temperature is between 600 and 800 °C. Gao et al. (2021) found that the temperature of 800 °C exceeded the optimal range for the carbonation reaction of CaO. In accordance with Le Chatelier's principle, when the chemical reaction between CaO and CO_2 reaches equilibrium, an increase in temperature will cause a shift towards the reactants. On the other hand, results of this study demonstrate that a temperature of 850 °C is suitable for the reaction in case of oil shale and its blends, as evidenced by the increase in residual mass observed on the mass curves following the introduction of CO_2 into the process.

3.3. Product gas analysis and synergy quantification

The experimental weight loss curve was compared with the theoretical weight loss curve (Fig. 4 a-d). The theoretical mass curve is calculated using Eq. (1) and serves as an assessment of synergy presence. In line with a previous study by Tian et al. (2023), when the experimental weight loss curve is lower than the theoretical weight loss curve,

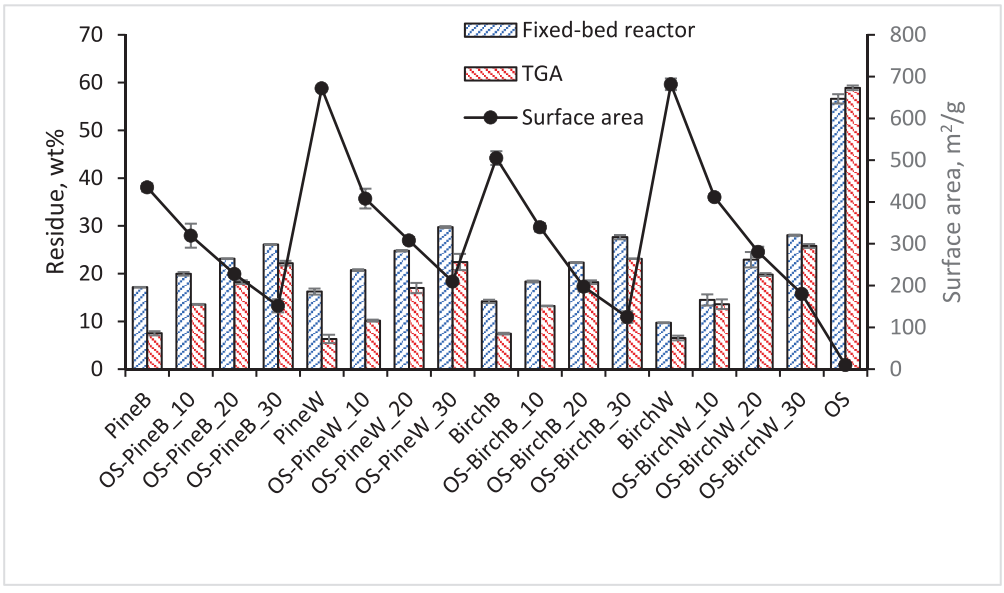


Fig. 2. Mass residues of gasification experiments in TGA and fixed-bed reactor and surface areas of char blends.

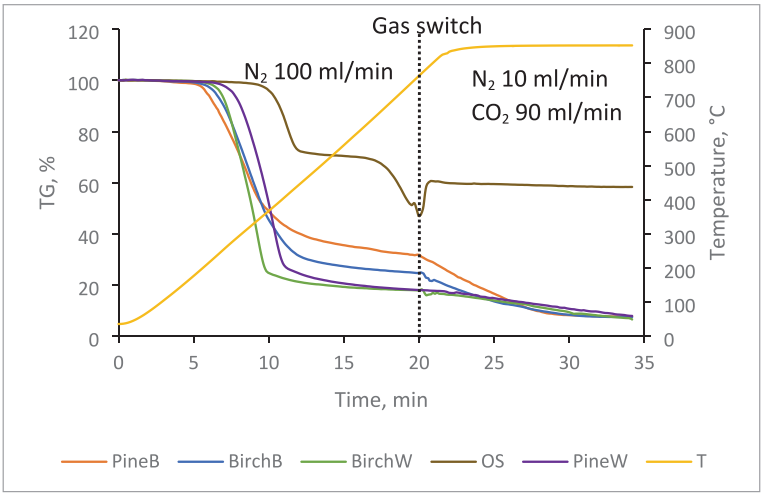


Fig. 3. Mass loss curves of natural feedstocks.

it signifies a higher actual volatile release and indicates a positive synergy during co-gasification. Conversely, if the calculated weight loss is higher than the experimental value, there is an inhibitory influence at present. For instance, in the case of PineB and OS 10 % and 20 % blends, a notable disparity between calculated and experimental results was observed during gasification stage. The calculated mass loss was lower and took place at a faster rate compared to the experimental mass loss. Therefore, it indicates inhibitory effect on co-gasification. BirchW exhibited the most significant differences between experimental and calculated values. The calculated results suggested that the mass loss should be lower than what was observed in the experiment, indicating an inhibitory effect. Conversely, PineW samples exhibited positive effect on co-gasification.

TGA tests were run with simultaneous MS to gather data about the evolving gases. Mass loss curves with the information about the released gaseous compounds were obtained (Fig. 5 a-d). The efficiency of gasification is evaluated in this study based on the trend of H_2 evolution, because the other main producer gas components such as CO and CH_4 were not possible to determine due to the overlapping in m/z values in N_2 and CO_2 environment.

Fig. 5 a-d illustrates the TGA-MS results describing the evolution of H_2 for biomass blends with oil shale. The release of hydrogen (m/z 2) occurred in two stages. The first stage started around the onset of mass loss of the bark at approximately 250 °C, and the second stage occurred after gas exchange. BirchW samples exhibit considerably higher hydrogen ion intensity compared to other biomass samples. In general, samples containing oil shale demonstrated a higher intensity of hydrogen release, especially in birch samples. This result confirms that oil shale as an additive in biomass gasification can increase H_2 yield in producer gas, presumably due to the high CaO content in ash and other mineral matter and depends on the biomass characteristics. However, the comparison of ion intensities is qualitative, therefore the results can only indicate the trends of release. Quantitative results obtained by gas chromatography are described in further sections.

The main gaseous products resulting from CO_2 gasification of oil shale and biomass were CO, H_2 and CH_4. Fig. 6 a-c present the comparison between the experimentally analyzed and calculated gas concentrations according to Eq. (2). If the experimental value exceeded the calculated value, it can be inferred that a catalytic effect was present. Calculated results were based on the individual results, revealing a disparity in gas concentrations between feedstocks. The variations can be attributed to the different composition of feedstocks, particularly in terms of volatiles, ash content and H/C ratio (Table 1 and Table 2).

For hydrogen, higher ratios of OS in the blend resulted in lower concentrations of H_2. The calculated and experimental results were relatively similar, although in most cases, the experimental values were lower than the theoretical values. This indicated either the absence or inhibitory effect of oil shale on biomass gasification. The previous findings support the observation that there is no apparent synergy between the mixed materials, as the gas concentration and the mixing ratio of biomass exhibited an almost linear relationship (Yang et al., 2021).

Fig. 6b shows a clear catalytic effect in the CO concentration in the PineB, PineW and BirchB blended samples. Additionally, bark samples demonstrated a higher CO concentration in comparison to wood samples. For example, CO concentration from PineB is more than three times higher than that of the wood sample, with values of 16.10 vol% and 5.35 vol%, respectively. PineB blend with 10 % oil shale increased the CO concentration to 16.71 vol% and was even higher than that of pure biomass sample. It could be inferred that the char produced from PineB was more reactive than other biomass chars during co-gasification (Char + CO_2 → 2CO). The higher CO concentration may be attributed to an increased carbon conversion rate as a result of co-gasification (Tong et al., 2021). It is also evident that the residue mass was lower for PineB with a 10 % oil shale content compared to other wood species blends. Furthermore, the elevated CO concentration could be attributed to the higher catalytic index of PineB.

For methane, a positive catalytic effect was observed in the case of PineW samples and BirchB samples (Fig. 6c). However, for other samples, the experimental results were in line with the calculated values, which means the catalytic effect was either expected or minimal. Yang et al. (2021) also found that the experimental concentrations of H_2, CO and CH_4 were almost equal to the calculated values during steam gasification. This suggests that the tar produced from biomass was predominantly converted into CO_2, as previously reported by Mallick et al. (2020).

The highest H_2 concentration (2.47 vol%) was obtained from the PineB. PineB differs significantly from other biomass samples in terms of its high Ca content, which can be up to 18 times higher compared to other samples (Table 2). This elevated Ca content in PineB may also contribute to its catalytic effect together with oil shale. Also, a higher potassium content may enhance its reactivity. Naturally occurring alkali and alkaline earth metal in the feedstock have been found to enhance the reactivity (Chan et al., 2021). Conversely, SiO_2 and Al_2O_3 have been found to have inhibitory effects on reactivity (Lahijani et al., 2015). Tian

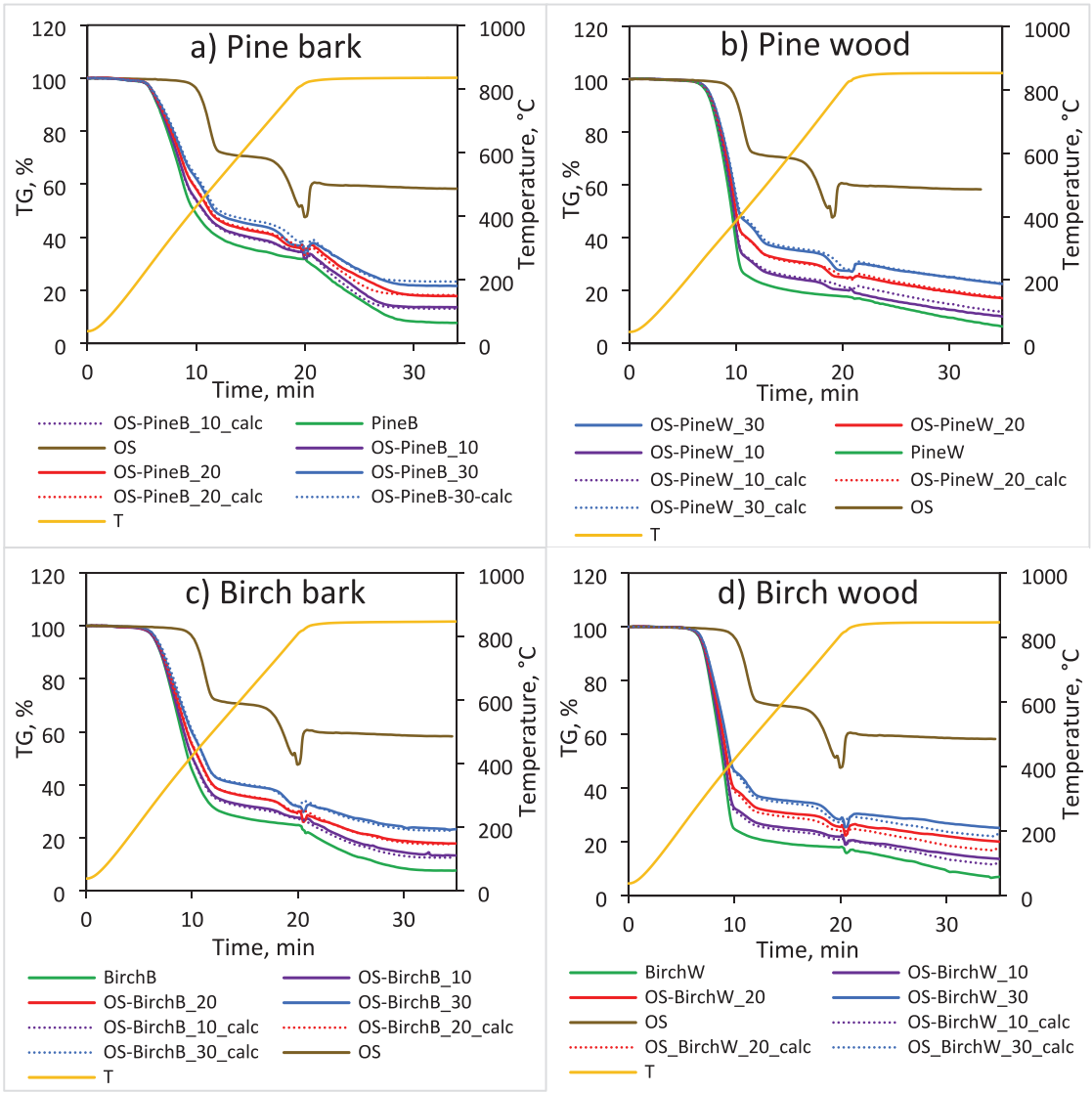


Fig. 4. Comparison of experiment and calculated values of TGA.

et al. (2017) suggested that biomass with a higher lignin content produced more H_2. Therefore, it can be assumed that PineB contains a higher amount of lignin, as well as resins. Furthermore, the production of H_2 could be attributed to the reforming reaction of the volatile components in biomass, while there was a limited thermal decomposition of methane ($CH_4 \rightarrow C + 2H_2$) and methane reforming ($CH_4 + CO_2 \rightarrow 2CO + 2H_2$) (Yang et al., 2021). In terms of achieving the highest concentrations of H_2, CO, and CH_4, the optimal blending ratio for co-gasification was found to be the PineB mixture with 10 % OS.

The obtained results do not provide a definitive conclusion regarding the most influential biomass properties on gas yields in co-gasification process, except for the concentration of Ca and K in biomass, which show an effect on gas concentrations. The correlation between gas concentrations and the characterized properties remains unclear. However, when comparing the properties of pure biomass and oil shale to their respective gas concentrations, it is evident that the gas concentration is significantly influenced by the feedstock properties, including carbon and hydrogen content, heating value, ash content, and volatile matter.

3.4. Characterization of biochar obtained from the gasification process

Apart from the gas products, chars were the important byproducts from biomass gasification. According to the International Union of Pure and Applied Chemistry (IUPAC) classification, the isotherms of all biomass chars exhibit type IV characteristics with an H4 hysteresis loop, which is indicative of the presence of slit-like pores (Tong et al., 2020). The type IV is a characteristic of mesoporous structure.

Results of the BET analysis for the char residues revealed significant differences in the surface area among the samples (Fig. 2). The char

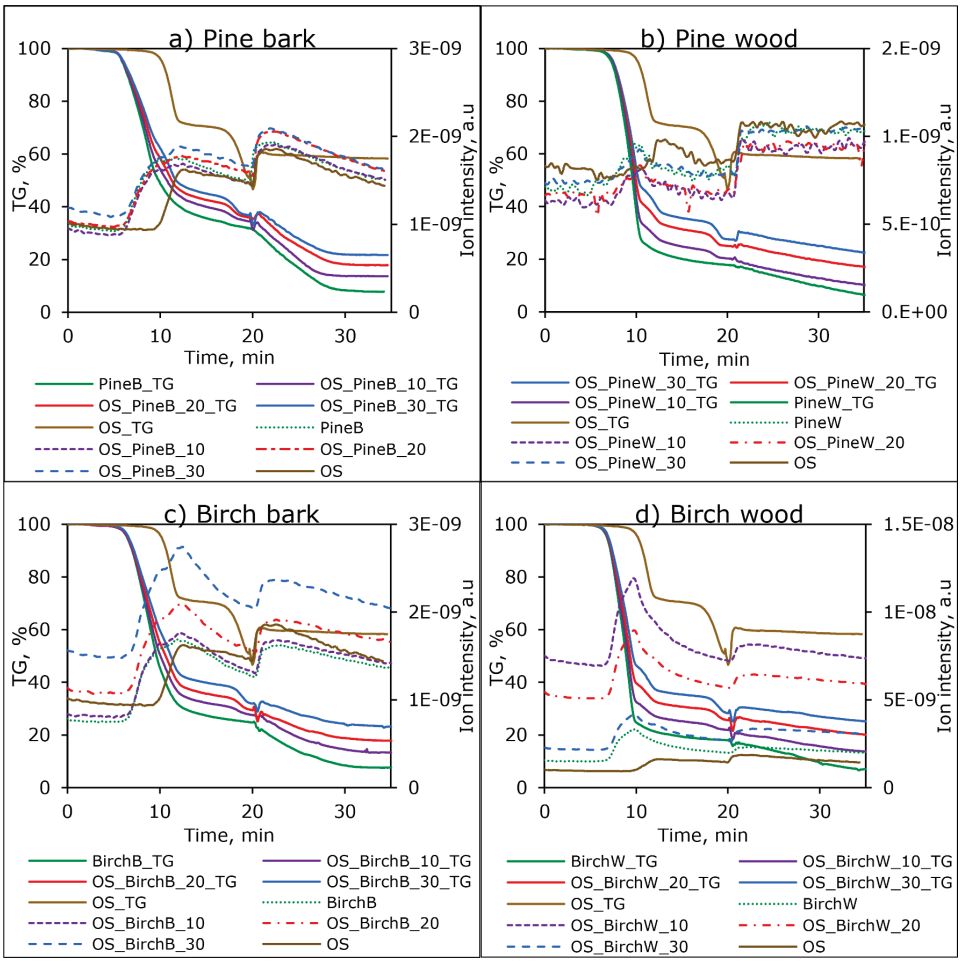


Fig. 5. Mass loss curves with the simultaneous evaporation of *m/z* 2 indicating the evaporation of H_2 in different BM blends.

residues from biomass exhibited higher surface areas compared to those from blended with oil shale samples. The surface areas of the chars of biomass and its blends were in the range of 124.62 – 681.69 m^2/g and the pure biomass char surface areas showed a decreasing trend in the order of BirchW char > PineW char > BirchB char > PineB char. The surface area of oil shale char was only 9.66 m^2/g. The presence of a higher concentration of inorganic compounds in fuel resulted in the formation of char with a reduced surface area due to the fusion of molten ash, which filled up the pores (Ronsse et al., 2013). It was observed that even pure woody samples with ash content ranging from 0.3 to 3.1 % exhibited a significant difference in surface areas (434–681 m^2/g), supporting the observation that the lower ash content in feedstock is associated with higher specific surface area. This indicates that the addition of OS had an adverse effect on the pore formation of the chars. Compared to previous studies, the surface area of pine char and pine dust exhibit a wide range, ranging from 220 m^2/g to 779.07 m^2/g (Duman et al., 2014; He et al., 2022; Liu et al., 2022; Zhang et al., 2023). The obtained results fall within the range of values, suggesting that the results are reliable.

The literature results are inconclusive regarding the overall effect of the char's surface area and pore volume on gasification reactivity (Roncancio and Gore, 2021). The BET surface areas of the biochars are typically associated with both their gasification activity and ash content (Duman et al., 2014). On the other hand, it has been reported that a large surface area has no influence on char reactivity (Wu et al., 2020). In a study conducted by He et al. (2022), the gasification performance of citrus peel and pine sawdust chars was compared. Interestingly, despite the citrus peel char having a surface area more than 10 times lower than that of pine sawdust (55.71 m^2/g and 599.31 m^2/g, respectively), the results revealed higher char reactivity and an enhanced concentration of H_2. Also, the present study suggests that higher surface area of residue char is not directly related to higher gas concentrations (H_2, CO, and CH_4). For instance, the current study showed that the gasification of PineB yielded the highest amounts of product gas, despite having the lowest surface area among the char residues of pure biomass samples. Drawing a parallel to the previous study conducted by He et al. (2022), it can be suggested that the higher reactivity observed in the biochar samples may be attributed to a greater reactivity index. Thus, based on the results presented in Table 2, it can be inferred that such a relationship holds true in this particular case, with PineB exhibiting a higher reactivity index. It can be concluded that the gas concentration was more influenced by ash composition rather than ash proportion in the mixture.

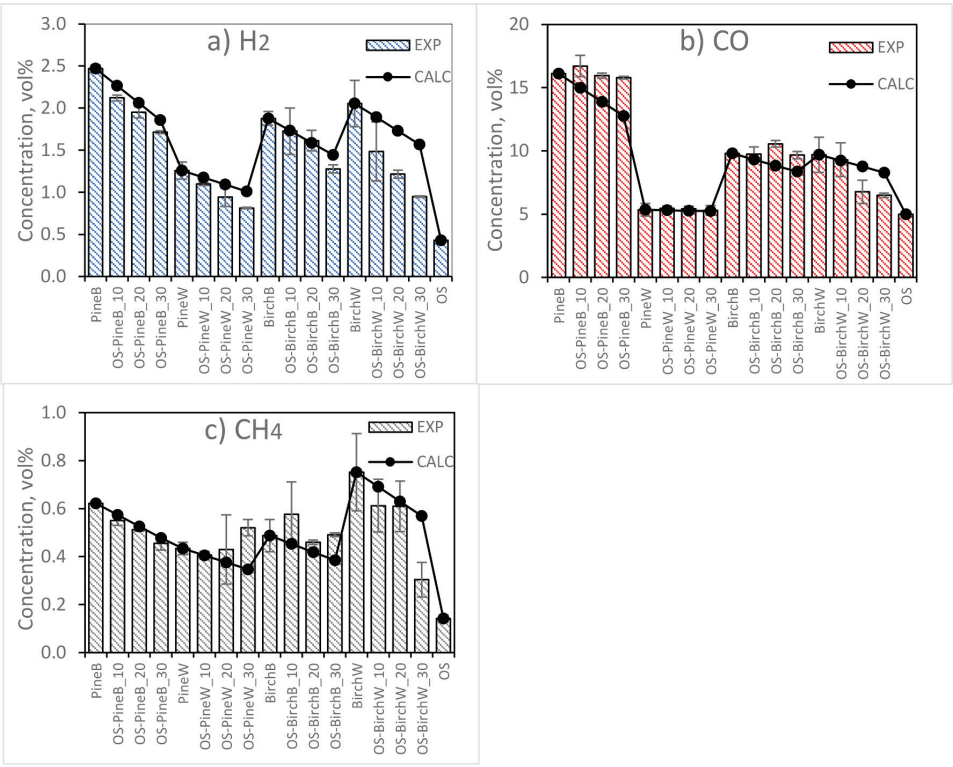


Fig. 6. Comparison of experimental and theoretical H_2, CO and CH_4 concentrations.

4. Conclusion

Gasification of pine and birch samples with oil shale additive were investigated under a CO_2 atmosphere. The increased H_2 evolution observed in the TG experiments indicated the catalytic effect of oil shale on biomass. The experiments conducted in a fixed-bed reactor, coupled with gas chromatography, demonstrated the catalytic effect on CO and CH_4 concentrations. The gas concentration exhibited a dependency on the biomass type and catalytic index. Particularly, PineB, with a catalytic index up to three times higher than other biomasses with a 10 % oil shale additive, yielded the highest gas concentration in the produced gas.

CRediT authorship contribution statement

Mari Sinisalu: Writing – original draft, Investigation, Methodology, Data curation. **Oliver Järvik:** Supervision, Validation, Resources. **Birgit Mets:** Methodology, Formal analysis. **Alar Konist:** Supervision, Funding acquisition.

Declaration of competing interest

The authors declare that they have no known competing financial interests or personal relationships that could have appeared to influence the work reported in this paper.

Data availability

Data will be made available on request.

Acknowledgments

Kristiina-Angela Kelder, Romi Viskar and Erik-Joel Petrov are acknowledged for their comprehensive assistance in conducting tests.

References

Abdalazeez, A., Li, T., Wang, W., Abuelgasim, S., 2021. A brief review of CO_2 utilization for alkali carbonate gasification and biomass/coal co-gasification: reactivity, products and process. J. CO2 Util. 43, 101370 https://doi.org/10.1016/j.jcou.2020.101370.

Altun, N.E., Hiçyilmaz, C., Hwang, J.Y., Bağci, A.S., Kök, M.V., 2006. Oil shales in the world and Turkey; reserves, current situation and future prospects: a review. Oil Shale 23, 211–227. https://doi.org/10.3176/oil.2006.3.02.

Bouraoui, Z., Jeguirim, M., Guizani, C., Limousy, L., Dupont, C., Gadiou, R., 2015. Thermogravimetric study on the influence of structural, textural and chemical properties of biomass chars on CO_2 gasification reactivity. Energy 88, 703–710. https://doi.org/10.1016/j.energy.2015.05.100.

Burra, K.G., Gupta, A.K., 2018. Synergistic effects in steam gasification of combined biomass and plastic waste mixtures. Appl. Energy 211, 230–236. https://doi.org/10.1016/j.apenergy.2017.10.130.

Cai, J., Zeng, R., Zheng, W., Wang, S., Han, J., Li, K., Luo, M., Tang, X., 2021. Synergistic effects of co-gasification of municipal solid waste and biomass in fixed-bed gasifier. Process Saf. Environ. Prot. 148, 1–12. https://doi.org/10.1016/j.psep.2020.09.063.

Chan, Y.H., Rahman, S.N.F.S.A., Lahuri, H.M., Khalid, A., 2021. Recent progress on CO-rich syngas production via CO_2 gasification of various wastes: a critical review on efficiency, challenges and outlook. Environ. Pollut. 278 https://doi.org/10.1016/J.ENVPOL.2021.116843.

Chen, B., Han, X., Tong, J., Mu, M., Jiang, X., Wang, S., Shen, J., Ye, X., 2020. Studies of fast co-pyrolysis of oil shale and wood in a bubbling fluidized bed. Energy Convers. Manag. 205, 112356 https://doi.org/10.1016/j.enconman.2019.112356.

Chen, X., Li, S., Liu, Z., Chen, Y., Yang, H., Wang, X., Che, Q., Chen, W., Chen, H., 2019. Pyrolysis characteristics of lignocellulosic biomass components in the presence of CaO. Bioresour. Technol. 287, 121493 https://doi.org/10.1016/j.biortech.2019.121493.

Collot, A.G., Zhuo, Y., Dugwell, D.R., Kandiyoti, R., 1999. Co-pyrolysis and co-gasification of coal and biomass in bench-scale fixed-bed and fluidized bed reactors. Fuel 78, 667–679. https://doi.org/10.1016/S0016-2361(98)00202-6.

Duman, G., Uddin, M.A., Yanik, J., 2014. The effect of char properties on gasification reactivity. Fuel Process. Technol. 118, 75–81. https://doi.org/10.1016/J.FUPROC.2013.08.006.

Gao, N., Śliz, M., Quan, C., Bieniek, A., Magdziarz, A., 2021. Biomass CO2 gasification with CaO looping for syngas production in a fixed-bed reactor. Renew. Energy 167, 652–661. https://doi.org/10.1016/j.renene.2020.11.134.

Gil, M.V., González-Vázquez, M.P., García, R., Rubiera, F., Pevida, C., 2019. Assessing the influence of biomass properties on the gasification process using multivariate data analysis. Energy Convers. Manag. 184, 649–660. https://doi.org/10.1016/j.enconman.2019.01.093.

Hameed, Z., Aslam, M., Khan, Z., Maqsood, K., Atabani, A.E., Ghauri, M., Khurram, M.S., Rehan, M., Nizami, A.S., 2021. Gasification of municipal solid waste blends with biomass for energy production and resources recovery: current status, hybrid technologies and innovative prospects. Renew. Sustain. Energy Rev. 136, 110375 https://doi.org/10.1016/j.rser.2020.110375.

He, Z., Sun, Y., Cheng, S., Jia, Z., Tu, R., Wu, Y., Shen, X., Zhang, F., Jiang, E., Xu, X., 2021. The enhanced rich H_2 from co-gasification of torrefied biomass and low rank coal: the comparison of dry/wet torrefaction, synergetic effect and prediction. Fuel 287, 119473. https://doi.org/10.1016/j.fuel.2020.119473.

He, J., Yang, Z., Guo, M., Gu, L., Zhang, L., Yan, Y., Ran, J., 2022. Experimental study on the key factors affecting the gasification performance between different biomass: compare citrus peel with pine sawdust. Int. J. Hydrogen Energy 47, 30428–30439. https://doi.org/10.1016/j.ijhydene.2022.07.004.

Jarvik, O., Sulg, M., Cascante Cirici, P., Eldermann, M., Konist, A., Gusca, J., Siirde, A., 2020. Co-pyrolysis and co-gasification of biomass and oil shale. Environ. Clim. Technol. 24, 624–637. https://doi.org/10.2478/rtuect-2020-0038.

Jeong, H.J., Park, S.S., Hwang, J., 2014. Co-gasification of coal–biomass blended char with CO_2 at temperatures of 900–1100 °C. Fuel 116, 465–470. https://doi.org/10.1016/J.FUEL.2013.08.015.

Jeremiáš, M., Pohořelý, M., Svoboda, K., Skoblia, S., Beňo, Z., Šyc, M., 2018. CO2 gasification of biomass: the effect of lime concentration in a fluidised bed. Appl. Energy 217, 361–368. https://doi.org/10.1016/j.apenergy.2018.02.151.

Kajitani, S., Zhang, Y., Umemoto, S., Ashizawa, M., Hara, S., 2010. Co-gasification reactivity of coal and woody biomass in high-temperature gasification, in: Energy and Fuels. American Chemical Society, pp. 145–151. doi: 10.1021/ef900526h.

Koel, M., 1999. Estonian oil shale [WWW Document]. URL https://www.kirj.ee/public/oilshale/Est-OS.htm (accessed 4.7.21).

Konist, A., Järvik, O., Pikkor, H., Neshumayev, D., Pihu, T., 2019. Utilization of pyrolytic wastewater in oil shale fired CFBC boiler. J. Clean. Prod. 234, 487–493. https://doi.org/10.1016/j.jclepro.2019.06.213.

Lahijani, P., Zainal, Z.A., Mohammadi, M., Mohamed, A.R., 2015. Conversion of the greenhouse gas CO_2 to the fuel gas CO via the Boudouard reaction: a review. Renew. Sustain. Energy Rev. 41, 615–632. https://doi.org/10.1016/J.RSER.2014.08.034.

Lee, J., Yang, X., Cho, S.H., Kim, J.K., Lee, S.S., Tsang, D.C.W., Ok, Y.S., Kwon, E.E., 2017. Pyrolysis process of agricultural waste using CO_2 for waste management, energy recovery, and biochar fabrication. Appl. Energy 185, 214–222. https://doi.org/10.1016/J.APENERGY.2016.10.092.

Li, J., Burra, K.R.G., Wang, Z., Liu, X., Gupta, A.K., 2021b. Co-gasification of high-density polyethylene and pretreated pine wood. Appl. Energy 285, 116472. https://doi.org/10.1016/j.apenergy.2021.116472.

Li, H., Wang, Y., Zhou, N., Dai, L., Deng, W., Liu, C., Cheng, Y., Liu, Y., Cobb, K., Chen, P., Ruan, R., 2021a. Applications of calcium oxide–based catalysts in biomass pyrolysis/gasification – a review. J. Clean. Prod. 291, 125826 https://doi.org/10.1016/j.jclepro.2021.125826.

Li, B., Yang, H., Wei, L., Shao, J., Wang, X., Chen, H., 2017. Hydrogen Production from Agricultural Biomass Wastes Gasification in a Fluidized Bed with Calcium Oxide Enhancing. https://doi.org/10.1016/j.ijhydene.2017.01.138.

Liu, S., Wu, G., Syed-Hassan, S.S.A., Li, B., Hu, X., Zhou, J., Huang, Y., Zhang, S., Zhang, H., 2022. Catalytic pyrolysis of pine wood over char-supported Fe: bio-oil upgrading and catalyst regeneration by CO_2/H_2O. Fuel 307, 121778. https://doi.org/10.1016/j.fuel.2021.121778.

Mallick, D., Mahanta, P., Moholkar, V.S., 2020. Co-gasification of biomass blends: performance evaluation in circulating fluidized bed gasifier. Energy 192. https://doi.org/10.1016/j.energy.2019.116682.

Mariyam, S., Shahbaz, M., Al-Ansari, T., Mackey, H.R., McKay, G., 2022. A critical review on co-gasification and co-pyrolysis for gas production. Renew. Sustain. Energy Rev. 161, 112349 https://doi.org/10.1016/J.RSER.2022.112349.

Quan, C., Gao, N., Song, Q., 2016. Pyrolysis of biomass components in a TGA and a fixed-bed reactor: thermochemical behaviors, kinetics, and product characterization. J. Anal. Appl. Pyrolysis 121, 84–92. https://doi.org/10.1016/J.JAAP.2016.07.005.

Qudaih, R., Talab, I., Syed, S., Janajreh, I., Hamdan, M., 2013. Material characterization and gasification of Jordanian oil shale. Energy, Environ. Econ. Res. Compend. 17–32.

Roncancio, R., Gore, J.P., 2021. CO_2 char gasification: a systematic review from 2014 to 2020. Energy Convers. Manag. X 10, 100060. https://doi.org/10.1016/j.ecmx.2020.100060.

Ronsse, F., van Hecke, S., Dickinson, D., Prins, W., 2013. Production and characterization of slow pyrolysis biochar: influence of feedstock type and pyrolysis conditions. GCB Bioenergy 5, 104–115. https://doi.org/10.1111/gcbb.12018.

Satyam Naidu, V., Aghalayam, P., Jayanti, S., 2016. Synergetic and inhibition effects in carbon dioxide gasification of blends of coals and biomass fuels of Indian origin. Bioresour. Technol. 209, 157–165. https://doi.org/10.1016/j.biortech.2016.02.137.

Shahabuddin, M., Bhattacharya, S., 2021. Enhancement of performance and emission characteristics by co-gasification of biomass and coal using an entrained flow gasifier. J. Energy Inst. 95, 166–178. https://doi.org/10.1016/j.joei.2021.01.012.

Shahbaz, M., Yusup, S., Inayat, A., Patrick, D.O., Ammar, M., 2017. The influence of catalysts in biomass steam gasification and catalytic potential of coal bottom ash in biomass steam gasification: a review. Renew. Sustain. Energy Rev. 73, 468–476. https://doi.org/10.1016/j.rser.2017.01.153.

Shahbaz, M., Al-Ansari, T., Inayat, M., Sulaiman, S.A., Parthasarathy, P., McKay, G., 2020. A critical review on the influence of process parameters in catalytic co-gasification: Current performance and challenges for a future prospectus. Sustain. Energy Rev Renew. https://doi.org/10.1016/j.rser.2020.110382.

Sulg, M., Konist, A., Järvik, O., 2021. Characterization of different wood species as potential feedstocks for gasification. Agron. Res. 19, 2021.

Tian, T., Li, Q., He, R., Tan, Z., Zhang, Y., 2017. Effects of biochemical composition on hydrogen production by biomass gasification. Int. J. Hydrogen Energy 42, 19723–19732. https://doi.org/10.1016/j.ijhydene.2017.06.174.

Tian, B., Wang, J., Qiao, Y., Huang, H., Xu, L., Tian, Y., 2023. Understanding the pyrolysis synergy of biomass and coal blends based on volatile release, kinetics and char structure. Biomass Bioenergy 168. https://doi.org/10.1016/J.BIOMBIOE.2022.106687.

Tong, W., Liu, Q., Yang, C., Cai, Z., Wu, H., Ren, S., 2020. Effect of pore structure on CO_2 gasification reactivity of biomass chars under high-temperature pyrolysis. J. Energy Inst. 93, 962–976. https://doi.org/10.1016/J.JOEI.2019.08.007.

Tong, S., Sun, Y., Li, X., Hu, Z., Worasuwannarak, N., Liu, H., Hu, H., Luo, G., Yao, H., 2021. Gas-pressurized torrefaction of biomass wastes: Co-gasification of gas-pressurized torrefied biomass with coal. Bioresour. Technol. 321, 124505 https://doi.org/10.1016/j.biortech.2020.124505.

Wei, J., Wang, M., Wang, F., Song, X., Yu, G., Liu, Y., Vuthaluru, H., Xu, J., Xu, Y., Zhang, H., Zhang, S., 2021. A review on reactivity characteristics and synergy behavior of biomass and coal Co-gasification. Int. J. Hydrogen Energy. https://doi.org/10.1016/j.ijhydene.2021.02.162.

Wu, R., Beutler, J., Price, C., Baxter, L.L., 2020. Biomass char particle surface area and porosity dynamics during gasification. Fuel 264, 116833. https://doi.org/10.1016/J.FUEL.2019.116833.

Yang, Z., Wu, Y., Zhang, Z., Li, H., Li, X., Egorov, R.I., Strizhak, P.A., Gao, X., 2019. Recent advances in co-thermochemical conversions of biomass with fossil fuels focusing on the synergistic effects. Sustain. Energy Rev Renew. https://doi.org/10.1016/j.rser.2018.12.047.

Yang, P., Zhao, S., Zhang, Q., Hu, J., Liu, R., Huang, Z., Gao, Y., 2021. Synergistic effect of the cotton stalk and high-ash coal on gas production during co-pyrolysis/gasification. Bioresour. Technol. 336, 125336 https://doi.org/10.1016/j.biortech.2021.125336.

Zaini, I.N., Gomez-Rueda, Y., García López, C., Ratnasari, D.K., Helsen, L., Pretz, T., Jönsson, P.G., Yang, W., 2020. Production of H_2-rich syngas from excavated landfill waste through steam co-gasification with biochar. Energy 207, 118208. https://doi.org/10.1016/j.energy.2020.118208.

Zhang, M., Fan, G., Liu, N., Yang, M., Li, X., Wu, Y., 2023. Tar removal in pine pyrolysis catalyzed by bio-char supported nickel catalyst. J. Anal. Appl. Pyrolysis 169, 105843. https://doi.org/10.1016/j.jaap.2022.105843.

Zheng, Y., Tao, L., Yang, X., Huang, Y., Liu, C., Zheng, Z., 2018. Study of the thermal behavior, kinetics, and product characterization of biomass and low-density polyethylene co-pyrolysis by thermogravimetric analysis and pyrolysis-GC/MS. J. Anal. Appl. Pyrolysis 133, 185–197. https://doi.org/10.1016/j.jaap.2018.04.001.

Appendix 2

Table A.1. Correlation coefficients between biomass compositional parameters and producer gas components

	C	H	N	S	O	A	VM	FC	HHV	Ca	Mg	Al	K	Si	Fe	P	Mn	Cr	Ni	SSA	H_2	CO	CH_4
C	1.00																						
H	0.36	1.00																					
N	0.42	-0.69	1.00																				
S	0.38	-0.72	1.00	1.00																			
O	-0.96	-0.09	-0.66	-0.62	1.00																		
A	0.51	-0.61	0.99	0.99	-0.73	1.00																	
VM	-0.52	0.60	-0.99	-0.98	0.74	-0.99	1.00																
FC	0.73	-0.37	0.93	0.90	-0.89	0.95	-0.96	1.00															
HHV	0.99	0.49	0.29	0.25	-0.91	0.40	-0.40	0.62	1.00														
Ca	0.42	-0.68	0.99	1.00	-0.66	0.99	-0.99	0.91	0.30	1.00													
Mg	0.87	0.46	0.24	0.24	-0.81	0.37	-0.33	0.50	0.91	0.29	1.00												
Al	0.94	0.03	0.70	0.67	-1.00	0.77	-0.77	0.90	0.89	0.71	0.81	1.00											
K	0.20	-0.84	0.97	0.98	-0.47	0.94	-0.94	0.81	0.07	0.97	0.06	0.52	1.00										
Si	0.99	0.27	0.51	0.47	-0.98	0.60	-0.60	0.78	0.97	0.51	0.88	0.97	0.30	1.00									
Fe	0.88	-0.11	0.79	0.77	-0.98	0.86	-0.85	0.95	0.81	0.80	0.75	0.99	0.64	0.92	1.00								
P	0.62	-0.51	0.97	0.95	-0.81	0.98	-0.99	0.99	0.50	0.95	0.39	0.83	0.89	0.68	0.90	1.00							
Mn	0.90	0.66	0.06	0.04	-0.77	0.19	-0.17	0.40	0.96	0.09	0.95	0.75	-0.15	0.88	0.66	0.26	1.00						
Cr	0.55	-0.57	0.98	0.98	-0.76	1.00	-0.99	0.96	0.43	0.99	0.41	0.80	0.93	0.63	0.88	0.98	0.23	1.00					
Ni	0.46	-0.65	0.99	1.00	-0.69	1.00	-0.99	0.93	0.34	1.00	0.32	0.74	0.96	0.55	0.82	0.97	0.13	1.00	1.00				
SSA	-0.76	0.33	-0.91	-0.89	0.91	-0.95	0.95	-0.99	-0.66	-0.91	-0.60	-0.93	-0.79	-0.82	-0.97	-0.97	-0.47	-0.96	-0.93	1.00			
H_2	0.24	-0.52	0.70	0.76	-0.43	0.76	-0.69	0.57	0.20	0.78	0.45	0.51	0.73	0.35	0.59	0.61	0.16	0.75	0.76	-0.67	1.00		
CO	0.32	-0.63	0.88	0.92	-0.55	0.91	-0.86	0.75	0.24	0.92	0.39	0.62	0.88	0.42	0.71	0.80	0.12	0.90	0.91	-0.81	0.96	1.00	
CH_4	-0.41	-0.34	0.03	0.13	0.31	0.07	0.03	-0.21	-0.37	0.13	0.03	-0.22	0.17	-0.32	-0.16	-0.15	-0.22	0.05	0.09	0.09	0.68	0.48	1.00

Color scale ranges from −1 (red) to +1 (blue), with white indicating no correlation.

Table A.2. Interpretation of the size of correlation coefficient [178]

Size of Correlation	Interpretation
0.90 to 1.00 (-0.90 to -1.00)	Very highly positive (negative correlation)
0.70 to 0.90 (-0.70 to -0.90)	Highly positive (negative) correlation
0.50 to 0.70 (-0.50 to -0.70)	Moderately positive (negative) correlation
0.30 to 0.50 (-0.30 to -0.50)	Low positive (negative correlation)
0.00 to 0.30 (0.00 to -0.30)	Negligible

Curriculum vitae

Personal data

Name:	Mari Sinisalu
Date of birth:	19.11.1991
Place of birth:	Estonia
Citizenship:	Estonian

Contact data

E-mail:	mari.sinisalu@taltech.ee

Education

2018–2026	Tallinn University of Technology, PhD
2015–2017	Tallinn University of Technology, Applied Chemistry and Biotechnology, MSC
2011–2015	Tallinn University of Technology, Material Science, BSC
2008–2011	Võru Kreutzwald Gymnasium, High school

Language competence

English	Fluent
Estonian	Native

Professional employment

2017–2021	Tallinn University of Technology, Business Development Specialist and Quality Assistant of Laboratory of Department of Energy Technology

Elulookirjeldus

Isikuandmed

Nimi:	Mari Sinisalu
Sünniaeg:	19.11.1991
Sünnikoht:	Eesti
Kodakondsus:	eestlane

Kontaktandmed

E-post:	mari.sinisalu@taltech.ee

Hariduskäik

2018–2026	Tallinna Tehnikaülikool, Mehhanotehnika, PhD
2015–2017	Tallinna Tehnikaülikool, Rakenduskeemia ja biotehnoloogia, MSC
2011–2015	Tallinna Tehnikaülikool, Materjalitehnoloogia, BSC
2008–2011	Võru Kreutzwaldi Gümnaasium, keskharidus

Keelteoskus

Inglise keel	kõrgtase
Eesti keel	emakeel

Teenistuskäik

2017–2021	Tallinna Tehnikaülikool, ettevõtlus- ja kvaliteedispetsialist Energiatehnoloogia instituudi teadus- ja katselabor

ISSN 2585-6901
ISBN 978-9916-80-588-6